Universidad de La Laguna

PROGRAMA DOCTORADO CIENCIAS DE LA SALUD
Verificado ANECA, Resol. 19-3-2014

Doctorado en Ciencias de la Salud

Tesis Doctoral

"Alterations of neuronal lipid rafts functionality following a Parkinson disease-like lesion associated with brain aging"

Ana Canerina Luis Amaro

Directores de Tesis
Dra. Raquel Marín Cruzado
Dr. Alfredo Giménez-Cassina Sendón

Universidad de La Laguna
Departamento de Ciencias Médicas Básicas

2020

Escuela de Doctorado y Estudios de Posgrado
Universidad de La Laguna

Universidad de La Laguna

PROGRAMA DOCTORADO CIENCIAS DE LA SALUD
Verificado ANECA, Resol. 19-3-2014

Dra. Dña. **Raquel Marín Cruzado**, Catedrática del Departamento de Ciencias Médicas Básicas de la Universidad de La Laguna.

Dr. D. **Alfredo Giménez-Cassina Sendón**, Investigador "Ramón y Cajal" del Centro de Biología molecular "Severo Ochoa" de la Universidad Autónoma de Madrid.

HACEN CONSTAR

Que Dña. **Ana Canerina Luis Amaro**, Licenciada en Biología, ha realizado bajo nuestra dirección el trabajo contenido en la memoria titulada **"Alterations of neuronal lipid rafts functionality following a Parkinson disease-like lesion associated with brain aging"**

Revisado el presente trabajo, consideramos que reúne los requisitos necesarios para su presentación y defensa ante el tribunal correspondiente con el fin de optar al grado de Doctor en Ciencias de la Salud por la Universidad de La Laguna.

Y para que así conste y surta los efectos oportunos, firmamos la presente en San Cristóbal de La Laguna a 02 de noviembre de 2020.

Fdo.: Raquel Marín Cruzado

Fdo.: Alfredo Giménez-Cassina Sendón

Escuela de Doctorado y Estudios de Posgrado
Universidad de La Laguna

FINANCIACIÓN

La realización del presente trabajo de investigación ha sido posible gracias a la concesión de un contrato predoctoral cofinanciado por la Agencia Canaria de Investigación, Innovación y Sociedad de la Información de la Consejería de Economía, Conocimiento y Empleo y por el Fondo Social Europeo (FSE) Programa Operativo Integrado de Canarias 2014-2020, Eje 3 Tema Prioritario 74 (85%) en la convocatoria 2015. Así mismo ha sido financiado por una beca de investigación de Obra Social La Caixa-Fundación CajaCanarias para Posgraduados de la Universidad de La Laguna, convocatoria 2014 y una beca de investigación Fundación CajaCanarias para Posgraduados en la convocatoria 2013.

Por su parte, Alfredo Giménez-Cassina Sendón es beneficiario de un contrato Ramón y Cajal (RYC2014-15792) del Ministerio de Economía y Competitividad /MINECO, convocatoria 2014.

Durante el desarrollo del presente trabajo se llevaron a cabo estancias internacionales financiadas por el Programa de Formación de Investigadores de la Universidad de La Laguna correspondiente al año 2015 (Universidad J.J. Strossmayer de Osijek), la Fundación IMFAHE y el "International Mentoring Programe, IMP" (Instituto Karolinska, 2016) y la Agencia Canaria de Investigación, Innovación y Sociedad de la Información de la Consejería de Economía, Conocimiento y Empleo y por el Fondo Social Europeo (FSE) (Instituto Karolinska, 2017).

Así mismo, este trabajo ha sido financiado por los siguientes proyectos de Investigación:

Gobierno de Canarias
Consejería de Economía, Industria, Comercio y Conocimiento
Agencia Canaria de Investigación, Innovación y Sociedad de la Información

FONDO SOCIAL EUROPEO
Canarias avanza con Europa

Unión Europea

"Papel de p73 como posible regulador de Reelin en la función cognitiva durante el envejecimiento y la patología tipo Alzheimer. Implicación de microdominios lipid raft" (SAF2017-84454-R). Investigadores principales: Dra. Raquel Marín Cruzado y Dra. Miriam González Gómez. Entidad financiadora: Ministerio de Ciencia e Innovación. Fecha: 2018 - 2020.

"Cambios asociados al envejecimiento en los microdominios de la membrana neuronal como factores seminales en procesos de neurodegeneracion" (SAF2014-52582-R). Investigadores principales: Dra. Raquel Marín Cruzado y Dr. Mario Díaz González. Entidad financiadora: Ministerio de Ciencia e Innovación. Fecha: 2015 - 2017.

"Alteraciones en la funcionalidad e interacciones de proteínas de señalización y constitutivas de lipid raft en enfermedades neurodegenerativas" (SAF2010-22114-C02-02). Investigadores principales: Dra. Raquel Marín Cruzado y Dr. Mario Díaz González. Entidad financiadora: Ministerio de Ciencia e Innovación. Fecha: 2011 - 2014.

"Nya sätt att reglera metabola vägar i hjärnan för behandling av barnepilepsi" (FO2015-0067). Investigador principal Dr. Alfredo Giménez-Cassina Sendón. Entidad financiadora: "Hjärnfonden". Fecha: 2015 - 2017.

"New strategies to treat pediatric epilepsy: Upregulation of ketone body metabolism in the brain" (M15-0096). Investigador principal Dr. Alfredo Giménez-Cassina Sendón. Entidad financiadora: "Åke Wibergs Stiftelse". Fecha: 2017.

Gobierno de Canarias
Consejería de Economía, Industria, Comercio y Conocimiento
Agencia Canaria de Investigación, Innovación y Sociedad de la Información

FONDO SOCIAL EUROPEO
Canarias avanza con Europa

Unión Europea

II

A mi familia

AGRADECIMIENTOS

Resumir más de seis años de trabajo y experiencias inolvidables no es una tarea fácil. Sobre todo cuando han sido tan intensos como estos que han pasado mientras recorría el camino que me ha traído hasta aquí. Me llevo un sinfín de vivencias maravillosas que no esperaba al empezar y que solo han sido posibles gracias a personas estupendas que de una u otra manera han puesto su granito de arena para que esta tesis hoy finalmente sea un proyecto realizado. Me gustaría dedicarles mi más sincero agradecimiento porque realmente lo merecen, aunque sea difícil mencionarles a todos.

En primer lugar me gustaría agradecer el enorme papel que Raquel, mi directora, ha jugado en este trabajo. Han sido innumerables las cosas que me has enseñado a lo largo de estos años sin las cuales no habría sido posible llegar hasta aquí. Desde el primer momento en que me acogiste en el laboratorio te esforzaste en enseñarme todo lo que iba a necesitar para desarrollar este trabajo. Durante este tiempo a tu lado no solo he aprendido de Ciencia y de Neurociencia, me has enseñado también a lidiar con las incontables dificultades que supone dedicarse a esta profesión en España. Agradezco especialmente que siempre has estado disponible para mí cuando lo he necesitado ¡y mira que debe ser difícil teniendo una agenda tan apretada como la tuya! No sé cómo lo consigues. Sabes que este trabajo es tan tuyo como mío. Gracias por todo.

Además, he tenido la suerte de también contar con Alfredo como director de este trabajo. Gracias por lo mucho que he podido aprender de ti. Las "chapas" (como tú las llamas) que me das son clases magistrales que valen oro y me han ayudado mucho, no solo a aclarar las ideas, sino también a continuar sintiendo la pasión por la Ciencia, a veces tan difícil de mantener. Aunque el tiempo que he estado trabajando a tu lado ha sido corto, ha resultado muy intenso en aprendizajes que estoy segura me valdrán, no solo en el ámbito de la investigación, sino en muchos otros.

En estos años que he pasado "entre pipetas" ha habido un grupo de personas que han hecho que el tiempo pase muy rápido y además me han ayudado con sus conocimientos, consejos y "trucos". Son todas las personas con las que he tenido la suerte de, en un momento u otro, compartir el día a día en el laboratorio: Patricia, David, Cecilia, Luis, Ricardo, Fátima, Dani, Lucas y Catalina. Los compañeros del Karolinska: Yuri, Mela y Renato. También otros profesores que han contribuido en mi formación científica como Miriam González y Mario Díaz. No puedo olvidar por supuesto las visitas que he realizado a los laboratorios de Marija Heffer y aunque breve, de Svjetlana Kalanj Bognar, así como los compañeros que allí conocí, sobre todo a Marta, Vedrana, Milorad y Ada.

Por último, pero no menos importante, a las personas que me han acompañado y apoyado en este proceso desde fuera del laboratorio, sobre todo mis amigas y mi familia. Son demasiadas personas y no puedo nombrarlas a todas. Sin embargo, no puedo pasar por alto a mi madre, el principal apoyo con el que siempre puedo contar. Quien cree en mí ciegamente y me anima a conseguir todo lo que me propongo y más. Gracias siempre por todo.

Contents

Table of contents

X

List of figures

List of tables

Abbreviations

Abbreviations

2-DG	2-Deoxy-D-glucose
AA	Arachidonic acid
AD	Alzheimer's disease
AMPA	Ionotropic glutamate receptor AMPA subtype
APS	(3-Aminopropyl)-triethoxysilane
ATP	Adenosine triphosphate
ATP-CR	ATP-Coupled respiration
BLOTTO	Bovine Lacto Transfer Technique Optimizer
BR	Basal respiration
Cho	Cholesterol
CTB-HRP	Cholera toxin B subunit-horseradish peroxidase
DA	Dopamine
DAB	3,3'-Diaminobenzidine
DAT	Dopamine transporter
DHA	Docosahexaenoic acid
DMEM	Dulbeco's Modified Eagle Medium
DPA	Docosapentaenoic acid
DTT	Dithiothreitol
EDTA	Ethylenediaminetetraacetic acid
ENS	Enteric nervous system
FA	Fatty acids
FCCP	Carbonyl cyanide 4-(trifluoromethoxy) phenylhydrazone
GAPDH	Glyceraldehyde 3-phosphate dehydrogenase
GPI	Glycosylphosphatidylinositol
HBSS	Hanks' Balanced Salt Solution
IAA	Iodoacetamide
IEF	Isoelectrofocusing
IHC	Immunohistochemistry
iPD	Incidental Parkinson Disease
Ld	Liquid disordered
Lo	Liquid ordered

Abbreviations

LR	Lipid rafts
M14	MPTP treated 14 month-old mice group
M6	MPTP treated 6 month-old mice group
MAO	Monoamine oxidase
mGluR1	Metabotropic glutamate receptor 1
mGluR5	Metabotropic glutamate receptor 5
MPP^+	1-Methyl-4-phenylpyridinium
MPTP	1-Methyl-4-phenyl-1,2,3,6-tetrahydropyridine hydrochloride
MR	Maximal respiration
Mw	Molecular weight
NMDAR2B	Ionotropic glutamate receptor NMDAR2B subtype
NR	Non-raft fractions
OCR	Oxygen Consumption Rate
PBS	Phosphate Buffered Saline
PBST	Phosphate Buffered Saline-Tween 20
PD	Parkinson disease
PFA	Paraformaldehyde
PI	Propidium Iodide
p*I*	Isoelectric point
PL	Proton Leak
PL	Polar lipids
PMSF	Phenylmethanesulfonyl fluoride
PrPc	Prion protein
PUFA	Polyunsaturated fatty acid
PVDF	Polyvinylidene difluoride
RT	Room Temperature
SDS-PAGE	Sodium dodecyl sulphate polyacrylamide gel electrophoresis
SEM	Standard error of the mean
SFA	Saturated fatty acids
SRC	Spare respiratory capacity
TBS	Tris Buffered Saline

Abbreviations

TBST	Tris Buffered Saline-Tween 20
TH	Tyrosine hydroxylase enzyme
UI	Unsaturation index
W14	Control 14 month-old mice group
W6	Control 6 month-old mice group
α-Syn	α-Synuclein

XX

Introduction

Parkinson disease overview

Parkinson disease (PD) is a complex and progressive neurodegenerative disorder characterized by both motor and non-motor symptoms. It represents the second most common neurodegenerative disease and affects mainly older persons, been a rare disease in those under 50 years. Prevalence varies among the different reports but there is certain consensus that set it between 1 and 2 per 10,000 in the general population. The prevalence in the group over 60 years is estimated around 1% and it increases with age, reaching 4% in the older group of age (Tysnes & Storstein, 2017).

Pathologically, PD is characterized by massive loss or degeneration of dopaminergic neurons in the *substantia nigra* of the midbrain and the presence of Lewy bodies and Lewy neurites which are intracellular inclusions of different proteins, mainly insoluble aggregates of α-synuclein.

The clinical features of PD include motor and non-motor symptoms such as cognitive impairment, behavioural or neuropsychiatry alterations and symptoms related to autonomic nervous system failures (Beitz, 2014) (Figure 1). There is strong evidence supporting the idea that many of the non-motor symptoms of PD may occur several years before the first motor signs appear, this stage is known as Prodromal Parkinson disease (Mahlknecht, et al., 2015). Regarding the motor dysfunction, there are four classic features that serve also as diagnosis criteria for PD: resting tremor, bradykinesia, muscular rigidity and postural instability. Resting tremor most commonly affects hands but it also can involve lips, chin, jaw and legs. It usually manifests unilaterally first and overtime it progress to bilateral. Bradykinesia or slowness of movement is considered the main feature of PD and traduces in difficulties with planning, initiating and executing movement and with performing sequential and simultaneous tasks. Difficulties performing tasks that require fine motor control, loss of spontaneous movement or facial expression, among other, can be produced as a consequence of bradykinesia. Muscular rigidity may affect proximally or distally and is associated with the "cogwheel"

phenomenon. Postural instability usually manifests later on the course of PD and produces an increased risk for fallings. Apart from the described classic motor symptoms, others such as freezing or postural deformities have been associated to PD (Jankovic, 2008). On the other hand, non-motor features of PD include a variety of symptoms that can be as disabling as the motor ones and frequently appear earlier than the motor symptoms. Cognitive decline appears in a high percentage of PD patients and specially manifests at the late stages of the disease. Neurobehavioral alterations associated with PD include depression, apathy, anxiety and hallucinations. Sleep disorders such as rapid eye movement sleep behaviour disorder both occur in PD patients and has been described as a risk factor for PD, thus it is now considered a pre-parkinsonian state. Olfactory dysfunction or hyposmia is diagnosed in a high percentage of PD patients and also has been reported as a risk factor for PD. The autonomic disorders manifest in a wide variety of alterations that may include orthostasis, constipation, dysphagia, urinary difficulties, sexual dysfunction, faecal incontinence and excessive salivation (Beitz, 2014; Jankovic, 2008). Additionally, gastrointestinal dysfunction and alterations in the microbiota have been associated as a key early event in the development of PD (Mukherjee et al., 2016).

Attending to the familiar history, PD cases may be considered as sporadic, when there are not first degree relatives affected, or familiar when those are present. Familiar cases represent around 15% of total and only 5% to 10% are linked to mutations in genes related to PD and present a Mendelian inheritance patterns. Sporadic PD with no genetic mutations associated represent the vast majority of cases (Bandres-Ciga et al., 2020).

More than 200 years after the first description of PD (Parkinson, 1817) no biomarkers are available for diagnosis and precise causes underlying the disorder remain elusive. Evidence available points to a multifactorial origin for PD, with genetic, environmental and behavioural factors that may increase the susceptibility to the disease or prevent it. However, aging remains as the main risk factor for the development of the disease (Figure 1). Familiar PD has been found associated to a

wide variety of mutations in a number of genes encoding proteins such as α-synuclein, LRRK2, PINK1, PARKIN, DJ-1, VPS35 and GBA1. Remarkably, around 50% of early onset PD cases were affected with any of these mutations, while genetic cases account for 2-3% of late development PD cases (Zeng et al., 2018). To a greater or lesser extent, the discovery of these mutations has improved the understanding of the molecular pathogenesis associated with them and so with the development of PD.

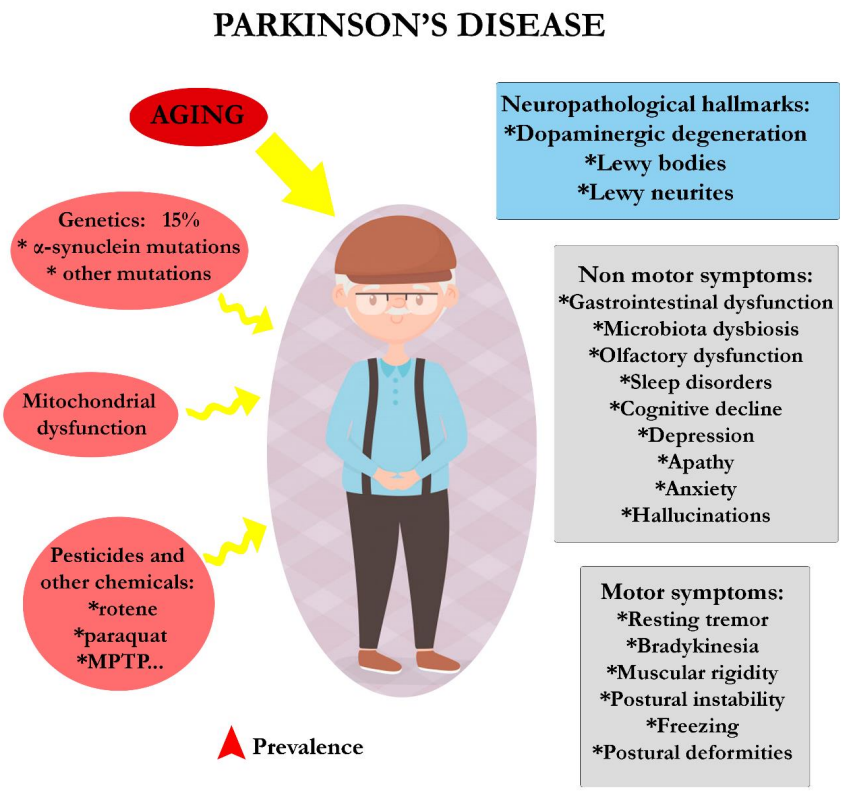

Figure 1. Illustration showing the main risk factors associated to Parkinson disease development and the most characteristic symptoms. A variety of genetic and environmental factors have been associated to increased risk of developing Parkinson disease, however aging remain as the main conditioning factor. Thus, as population ages the prevalence for PD increases. PD courses with a variety of symptoms that include motor and non-motor features.

Other risk factors have been associated with PD. Among those, exposure to pesticides shows a strong association with higher risk for PD. Brain injury history also shows a positive correlation with PD, however it is not clear whether it is a cause leading to increased risk or is a consequence of early stages of the disease. There are also many studies regarding the protective role of smoking and caffeine consumption. While the inverse relationship between smoking and PD remains controversial, strong evidence supports the decreased risk of PD related to caffeine intake (Elbaz et al., 2016).

The elevated prevalence observed in the older persons together with the progressive aging of population indicates that in the next 2 decades the number of PD cases may duplicate and reach 12 million as estimated by the Global Burden of disease Study (GBD 2016 Neurology Collaborators, 2019). This projection sets PD as an important cause of disability with a high burden for caregiving systems and patients. Therefore, a better understanding on the aetiology of the disorder that could lead to effective treatments or preventive strategies reveals urgent.

Alpha-synuclein in Parkinson disease

α-Synuclein (α-syn) is small protein that plays a central role in Parkinson disease. It is found as the main constituent of Lewy bodies and Lewy neurites and several mutations affecting the SNCA gene, which codifies for this protein, have been associated to familiar cases of PD. These two discoveries set the necessary implication of α-syn in the development of PD. Although the general consensus points to a neurotoxic role of α-syn aggregates, a clear picture of the mechanism by which this aggregates induce PD is still not available. Remarkably, aggregation of α-syn not only occurs in PD, but other neurodegenerative disorders such as dementia with Lewy bodies (DLB), multiple systems atrophy (MSA) or even Alzheimer's disease present aggregates of α-syn in different structures. This fact stress the relevance of α-syn in neuropathological processes.

Introduction

α-Synuclein is mainly found as a 14 kDa protein, composed by 140 amino acids encoded by the SNCA gene (Chen et al., 1995). Alternative splicing may generate shorter isoforms of the protein but the 14 kDa is the predominant form in neurons. The protein structure may be divided into three different domains. The N-terminus is a basic domain composed by amino acids 1-60 which present seven imperfect repeats containing the KTKEGV consensus sequence (Jakes et al., 1994). The central domain, known as the non-amyloidogenic component or NAC region, comprises the amino acids 61-95, is highly hydrophobic and is thought to be responsible of the aggregative properties of the protein (Ueda et al., 1993). Finally, an acidic C-terminal domain comprises the amino acids 96-140. This domain is frequent subject of post-translational modifications, a reason by which may be considered a relevant domain for the regulation of the protein conformation and function (Benskey et al., 2016; Oueslati et al., 2010; Surguchov, 2008). The monomeric protein is highly soluble and presents a natively unfolded structure that may progress to insoluble aggregated forms. In contact with membrane lipids, the N-terminus domain adopt an α-helix configuration that allows its interaction with the membrane (Shi et al., 2015).

α-Synuclein was firstly described localising in the presynaptic terminals in neurons, although it can be found at a lower frequency at the nucleus, cytosol and in the mitochondria-associated membrane in the endoplasmic reticulum (Guardia-Laguarta et al., 2014; Maroteaux et al., 1988). Apparently, α-syn preferentially binds to membranes with high curvature like those in the synaptic vesicles (Sulzer & Edwards, 2019). The physiological role of α-syn still is not completely clear, however, due to the predominant location in the presynaptic terminals it has been proposed to play a role in the endocytosis and exocytosis of the synaptic vesicles (Shi et al., 2015). Other physiological functions have been associated to α-syn such as calcium regulation, mitochondrial homeostasis, gene expression, protein phosphorylation or fatty acid binding. However the stronger evidence points to a role as a negative regulator of synaptic transmission, with special implication in dopamine (DA) release (Benskey et al., 2016; Sulzer & Edwards, 2019). This idea is

supported by findings in models producing overexpression of α-syn where a reduction in neurotransmitter release occurs and by evidence showing that mice lacking α-syn present decreased DA levels in the presynaptic terminal, increased DA release as well as decreased synaptic vesicle endocytosis (Abeliovich et al., 2000; Larsen et al., 2006; Vargas et al., 2014). Although initially α-syn was found to localize in the presynaptic terminal, more recently, it has been demonstrated that the protein exhibits a high mobility within this structure, presenting high concentrations in the synapsis in resting conditions and dispersing quickly in response to action potentials (Fortin et al., 2005). This mobility may explain the action mechanism of α-syn in down regulation of dopamine release. In resting conditions presence of α-syn in the presynaptic terminal exerts a series of interactions that overall reduce dopamine neurotransmission. This includes inhibition of DA synthesis and prevention of trafficking and docking of synaptic vesicles. In response to action potential α-syn disperses from the synaptic terminal and therefore its inhibitory role stops, allowing the release of neurotransmitters. Immediately after, α-syn returns to the previous location where it also contributes to enhanced DA recycling by endocytosis and packaging into vesicles (Benskey et al., 2016).

Several evidences point to the pathological character of aggregated α-syn. First, aggregates are found as major components of Lewy bodies and Lewy neurites, which represent the neuropathological hallmark of PD (Spillantini et al., 1997). Secondly, several mutations (A30P, E46K, H50Q, G51D or A53T) in the SNCA gene which are associated to early development of PD have been reported to promote the aggregation of the protein (Alam et al., 2019). Additionally, in PD, the progression of the disease have been reported to be accompanied by progression in the areas affected by aggregation of α-syn and such areas can be related to the symptomatology observed at the different stages (Braak et al., 2003). Finally, the pathological character of α-syn aggregates gets support from their involvement in other disorders, known collectively as synucleinopathies. Among these diseases, the locations affected by the deposits of aggregated α-syn differ and are correlated to the characteristics of the disorder (Brás et al., 2020). Altogether, this reinforces the

idea that aggregation of α-syn is at the base of PD development. However, the precise mechanism by which they produce the neurotoxic effect remains inconclusive. Two opposite hypothesis have been proposed to explain the toxicity produced by aggregated α-syn. On the one hand, a gain of toxic function mechanism, by which the aggregated forms will represent by itself a toxic species (D. van Rooijen et al., 2010). On the other hand, the hypothesis of a toxic loss of necessary function claims that α-syn in the non-aggregated forms plays a crucial role for the correct functioning of cell and that its aggregation will impede those functions (Benskey et al., 2016).

As previously mentioned, α-syn may occur in monomeric or aggregated forms, been the last the ones associated to neurotoxicity. However there are several configurations and aggregation states among these two forms and the toxicity level and pathological role of each form remains elusive. Also, the mechanism leading to aggregation of the protein is not clear although there are several factors and conditions that have been proved to promote α-syn aggregation. Some of those are point mutations or duplications and triplications in the SNCA gene, overexpression of α-syn, post-translational modifications, low pH or oxidative stress. Interestingly, the phosphorylation at serine 129 reveals of remarkable importance for aggregation since an elevated percentage of the α-syn found in LB and LN presents this post-translational modification (Fujiwara et al., 2002). The variety of forms in which α-syn may exist is wide, probably due to the multiple conformations that the unfolded nature of the protein confers, allowing to adopt different configurations depending on the previously mentioned conditions. To simplify these forms may classify into monomers, oligomers, proto-fibrils and mature fibrils. Even when the aggregation process is still not fully understood, it seem that oligomers and proto-fibrils may act as a seed in the aggregation process that would follow a feed-forward mechanism (Wood et al., 1999). Additionally, the pathological role of the different aggregated species (oligomers, proto-fibrils and fibrils) remains elusive. Evidence suggests that some oligomeric forms would prevent from further pathological aggregation. This "protective" forms would be an helically folded tetramer which would be less prone

to suffer aggregation than the monomeric forms (Bartels et al., 2011). On the contrary numerous evidence point to a toxic role of such oligomers (Ingelsson, 2016). The great variety of aggregated forms that rely on the term α-syn oligomers may explain the differences observed in the literature. Similarly, whether the oligomeric or fibrillary forms represent to most toxic species have been widely discussed. However, numerous evidence points to the toxic role of oligomers while fibrils may be mainly responsible for disease progression by propagation of aggregated forms (Alam et al., 2019; Benskey et al., 2016).

Despite the poor understanding of the pathological mechanisms exerted by the different forms of aggregated α-syn, it is clear that those forms correlate with the progression of PD. An interesting characteristic of those aggregates is that they are able to spread from cell to cell, invading different brain areas in what has been called a "prion-like" manner. This idea emerged from work showing that during the different stages of PD occurs a progression of the lesions that sequentially invades new brain structures (Braak et al., 2003). According to this, LB and LN appears in caudal brain during the first stages of the disease and progress to frontal cortex on the late stage. Additional support for this idea are findings that point to the possibility for α-syn segregation (Emmanouilidou et al., 2010) and internalization in neurons (Volpicelli-Daley et al., 2011). Further confirmation of the spreading process has been found in studies were injections of pathological α-syn in healthy mouse brains were easily able to reproduce the characteristic lesions found in PD (Luk et al., 2012). Moreover, inverse experiments in which healthy tissue was grafted into mouse brains overexpressing α-syn, and therefore prone to higher aggregation, demonstrated the transmission of aggregated α-syn (Hansen et al., 2011; Recasens & Dehay, 2014). More recently, it has been proposed that such spreading of α-synuclein may not only occur within the brain but even start in other nerve tissue and then propagate into the areas that are typically affected during the progression of Parkinson disease. According to this hypothesis the pathological aggregation of α-syn might start in the olfactory bulb or the enteric nervous system (ENS). From the ENS it would propagate retrogradely until it would reach the caudal part of the

central nervous system. From there the progression would occur as previously described in a caudal to rostral manner (Del Tredici & Braak, 2016).

Mitochondrial dysfunction in PD

An enormous body of evidence has found links between mitochondrial dysfunction and Parkinson disease. This evidence covers areas related to environmental factors involved in the development of PD, genetic mutations associated to familiar cases and even combined effects of genetic and environmental factors (Bose & Beal, 2016).

The role of mitochondrial dysfunction in PD started to be evaluated after the discovery of MPTP as a causative agent of several cases of parkinsonism among young patients (Langston et al., 1983). This neurotoxin produces the inhibition of Complex I of the mitochondrial electron respiratory chain and therefore impairs the mitochondrial activity and causes severe loss of dopaminergic neurons in the *substantia nigra*. After that, MPTP was successfully employed to generate animal models that reproduce Parkinson-like phenotype in non-human primates and mice, however not all the models reproduced the neuropathological hallmark of PD that represent the inclusions containing α-syn aggregates. Following this finding, other pesticides and chemicals like rotenone, paraquat, pyridaben, trichloroethylene and fenpyroximate were identified to produce a similar blockade of the mitochondria and an effect in the induction of dopaminergic degeneration in different animal models (Bose & Beal, 2016; Chaturvedi & Beal, 2008). Some of the animal models generated with these pesticides, for example mice and rats treated with rotenone, are also able to produce Lewy body-like inclusions and develop a robust PD phenotype (Betarbet et al., 2000; Grünewald et al., 2019; Jackson-Lewis et al., 2012).

Importantly, studies conducted with PD patient's samples, obtained either from post-mortem analysis of *substantia nigra* or from peripheral tissues (platelets and skeletal muscle), have found alterations in Complex I and IV consistent with a

decreased activity (Cardellach et al., 1993; Parker et al., 1989; Schapira et al., 1990). Related to this, links between elevated production of ROS has been found in PD brains also associated to α-syn aggregation (Bosco et al., 2006). In this line, it is very interesting that mouse models that overexpress α-synuclein show an increase in the neurotoxic effects observed after administration of MPTP. Meanwhile, α-syn KO mouse models are insensitive to this neurotoxic agent (Dauer et al., 2002).

A wide diversity of cellular and animal models has been used to evaluate the involvement of genes linked to PD in mitochondrial dysfunction. These models have incorporated some of the mutations that previously have been found in familiar cases of PD such as SNCA, Parkin, PTEN-induced kinase 1 (PINK1), DJ-1, LRRK2 and HtrA2. With these studies, numerous connections between these mutations and mitochondrial alterations, such as reduced activity of complex I and complex IV, decreased integrity of mitochondria, lower respiratory capacity, decreased ATP production and morphological alterations have been reported (Bose & Beal, 2016).

Remarkably, genes related to PD affected by mutations do not present always the same one, but on the contrary, for each gene a variety of mutations has been found. Therefore, it is not surprising the variety of pathological mechanisms proposed for the implication of such genes in the development of PD. In this sense, LRRK2 mutations associated to PD frequently increase its kinase activity leading to diverse alterations in a wide variety of cellular processes. The specific contribution of LRRRK2 mutations to mitochondrial dysfunction is not clear but several reports indicate that it may play a role in increasing oxidative stress, impairing mitochondria membrane potential and decreasing ATP production, damaging mitochondria DNA, inducing mitochondrial fragmentation and mitophagy (Singh et al., 2019). PINK1 and Parkin are involved in mitochondrial quality control by regulation of mitophagy, which is the removal of damaged mitochondria by autophagy. Thus mutations in either genes are associated to accumulation of dysfunctional mitochondria (Zeng et al., 2018). DJ-1 physiological functions appear to be related with a neuroprotective role against oxidative stress damage, taking this into account,

mutations in this gene occurring in PD patients will compromise neuronal response in such conditions (Biosa et al., 2017). In the SNCA gene, encoding for α-synuclein, the A53T mutation has been associated to mitochondrial fragmentation, elevated oxidative stress and mitochondrial dysfunction (Bido et al., 2017). The convergence of such a number genetic modifications associated to PD involved in mitochondrial functioning reinforces the role of mitochondria dysfunction as an important event in PD development.

Lipid rafts

Lipid rafts (LR) are membrane microdomains associated to signal transduction that present distinct composition and physicochemical properties. The concept was first established in 1997 as an explanation of the lateral heterogeneity widely observed in cell membranes (Simons & Ikonen, 1997). A consensual definition was adopted in the 2006 "Keystone Symposium on Lipid Rafts and Cell Function" establishing that "Membrane rafts are small (10-200 nm), heterogeneous, highly dynamic, sterol- and sphingolipid-enriched domains that compartmentalize cellular processes. Small rafts can sometimes be stabilized to form larger platforms through protein-protein and protein-lipid interactions" (Pike, 2006)

The distinct composition between LR and other non-raft membranes includes both their lipid and protein content. Rafts microdomains are enriched in cholesterol, sphingomyelin, gangliosides, sulphatides and cerebrosides, as well as saturated fatty acids (Fabelo et al., 2014) (Figure 2). Regarding the protein composition LR represent structures where certain proteins are enriched and others are excluded, in other words, LR present specific subsets of proteins. Caveolin, flotillin and GPI-linked proteins, are among those particularly frequent in these structures. However, not all lipid rafts present the same protein composition, this is, there are different types of LR regarding their protein content and related to their function (Pike, 2003). This distinct composition previously described leads to a

series of physicochemical properties such as lower density, less fluidity and insolubility in non-ionic detergents. The decreased fluidity of the membrane domain is also referred as a liquid-ordered phase (Lo) in contraposition with a liquid-disordered (Ld) phase with higher fluidity in the non-raft membranes. The insolubility in non-ionic detergents together with their lower density are key for the isolation of lipid rafts.

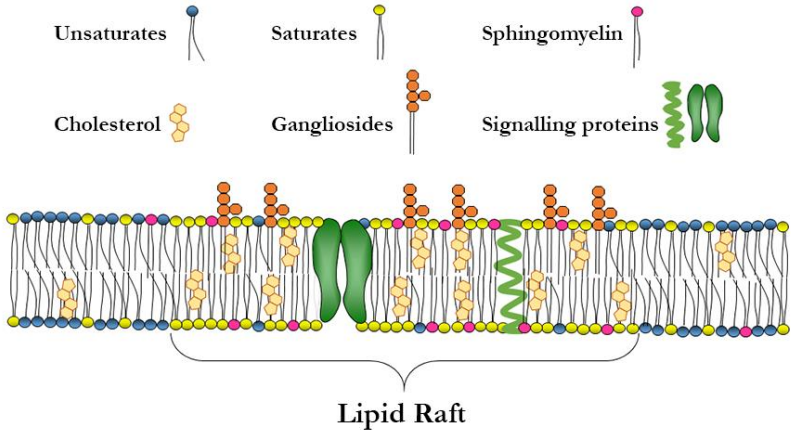

Figure 2. Schematic representation of lipid raft microdomains composition. Phospholipids with unsaturated fatty acids are represented with blue heads and those with saturated fatty acids with yellow heads. Lipid rafts are enriched in proteins involved in signalling pathways including transmembrane proteins or channels, among them.

The formation of LR structures have been explained in the basis of the self-aggregating properties of two of their main constituents, glycosphingolipids and cholesterol (Simons & Ikonen, 1997). Nonetheless, numerous explanations have been proposed for the selective distribution of proteins observed in LR. One of the most evident is the post-transcriptional lipid modifications, such as glycosylphosphatidylinositol (GPI) anchors and palmitoylation, that drive proteins into raft microdomains, while others like unsaturated, short and branched lipidic

moieties favours the non-raft localization (Levental et al., 2010). However, not all raft proteins hold this kind of post-transcriptional modifications. In this respect, other hypothesis such as the diffusion-driven, entropy and line tension-driven and affinity-driven lipid raft formation propose possible mechanisms for this sorting of proteins (Bieberich, 2018). It is noteworthy that certain proteins can be included or excluded from LR in response to a signalling cascade, remarking this fact the dynamic character of LR domains (Sonnino et al., 2015).

It is widely accepted that LR are involved in the regulation of signalling pathways. Since their first description, these membrane microdomains were thought to participate in signal transduction working as platforms where receptors localize and interact with ligands and effectors providing a sort of isolated platform from the rest of the membrane and therefore, avoiding inappropriate crosstalk between pathways. The proximity between receptors and ligands in LR would also improve their interaction accelerating the process (Simons & Ikonen, 1997). This idea has received support from the subsequent reports showing numerous signalling proteins that localize mainly in LR (Pike, 2003). LR are dynamic structures in which continuous lipid-lipid, lipid-protein and protein-protein interactions take place contributing to raft stabilization and activation of different signalling cascades (Marín, 2011).

Taking into account the elevated content in lipids in the brain, remarkably cholesterol and complex sphingolipids, is not surprising the abundance of LR in this tissue. Therefore, the role in signalling of LR gains special importance in brain cells, both neurons and glial cells. LR has been found involved in numerous and crucial functions and processes such as neuronal and glial survival (apoptosis and proliferation), differentiation, neurite outgrowth, synapse formation, synaptic transmission, neural cell adhesion (axon guidance, migration and neuron-glia interactions) and regulation of inflammation (Aureli et al., 2015).

Gangliosides

Gangliosides are important components of LR microdomains. This type of glycosphingolipid is present in the glycocalix of the majority of vertebrate cell types in a wide variety that can account for hundreds of different molecules. In the nervous system, gangliosides turn into the main component of the glycocalix and the variety among the structures represented sharply decreases. In the mammal brains only four complex gangliosides constitute the vast majority of this glycosphingolipids: GM1, GD1a, GD1b and GT1b. These gangliosides are synthetized stepwise by a series of enzymatic reactions that convert simpler gangliosides into more complex ones (Figure 3).

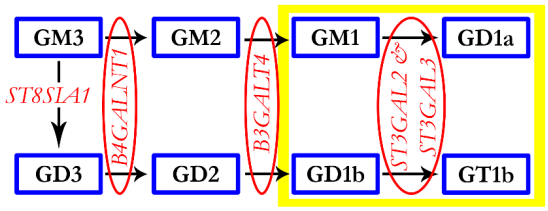

Figure 3. Schematic representation of the biosynthetic pathway of brain main gangliosides. Steps previous to the synthesis of GM3 have been omitted to simplify. Yellow box indicates the brain major gangliosides. Genes codifying for the enzymes that catalyse the different steps are indicated in red.

It is important to note that specific enzymes mediate the conversion at each step and that mutations occurring at any of them would truncate the biosynthetic pathway in the corresponding step leading to a different composition of gangliosides in the affected tissue. (Schnaar, 2016). For instance mouse models with deletion in the *B4galnt1* gene produce the depletion of all complex gangliosides that in WT mice are the major brain constituents (GM1, GD1a, GD1b and GT1b) which would be compensated by an increase in GM3 and GD3. The *ST8Sia1* KO express only GM1 and GD1a and the double KO *ST8Sia1/B4Galnt1* express GM3 as the main brain ganglioside (Schnaar et al., 2014).

As well as other sphingolipids, gangliosides present self-aggregating properties that have been associated to LR formation. Indeed, gangliosides and more specifically GM1, are considered as LR molecular markers, being the cholera toxin that specifically binds GM1 a frequent tool to identify these microdomains. In such structures, gangliosides not only play a structural role but also participate in the regulation of cellular functions. It has been proposed that gangliosides exert their regulative functions in two different ways. First, via lateral interactions with proteins on the same cell membrane and secondly by binding to proteins from different cells (Schnaar, 2016).

Understanding on the functions of gangliosides in the nervous system has been improved by the study of animal models in which ganglioside metabolism have been altered. Also, few cases on human subjects have identified mutations in genes involved in the gangliosides metabolism associated to severe motor and cognitive disabilities. Studies performed in mice lacking all complex brain gangliosides, completely (*B4galnt1*$^{-/-}$) or partially (*B4galnt1*$^{+/-}$), found the characteristic symptomatology of PD. These symptoms included motor impairment, loss of TH-positive neurons, depletion of striatal dopamine and detection of α-syn aggregates. Symptoms were more pronounced in the KO and, interestingly, were alleviated with the administration of L-dopa (G. Wu et al., 2012; G. Wu et al., 2011). Additional studies using this KO model reported that with aging the animals presented whole-body tremor and hyperactivity (Pan et al., 2005).

Lipid rafts in neurodegeneration

Considering the important role of lipid rafts as signalling platforms involved in crucial brain functions, it is reasonable to expect that alterations in the brain lipid composition that affect lipid raft formation may have profound effects in the signalling processes mediated by these microdomains (Sonnino et al., 2015). In fact, several studies have found connections between the main neurodegenerative

diseases such as Alzheimer's disease (AD) and Parkinson disease, amyotrophic lateral sclerosis (ALS), Huntington's and prion diseases and lipid raft disarrangements (Botto et al., 2014; Boussicault et al., 2018; Díaz et al., 2012; Fabelo et al., 2014, 2011; Martín et al., 2010; Zhai et al., 2009).

It is well known that aging is the main risk factor for neurodegenerative pathologies like AD or PD. Hence, analysis of the brain changes occurring during non-pathological aging may give some information that could help in the understanding of neurodegenerative diseases. Profound lipid changes have been widely observed in brain occurring parallel with aging. In the first instance a general reduction in total lipids content was observed (Svennerholm et al., 1994). Specifically, some lipid species such as cholesterol, gangliosides, sphingosine, ceramide, sphingomyelin, phosphoinositides and polyunsaturated fatty acids (PUFA) show characteristic alterations with aging (Ledesma et al., 2012). Some of the previously mentioned lipids have a significant role in the structure of LR and alterations of those would lead to disarrangements in LR maintenance. In this line, previous studies from our group have conducted to the hypothesis of "lipid raft aging" in which lipid rafts slowly suffer age-dependent modifications that compromise their integrity and affect their biophysical properties. Lipid raft aging has been found to be accelerated in a mouse model of Alzheimer's disease (AD) and correlated to changes observed in AD patients (Díaz et al., 2014, 2012; Fabelo et al., 2014, 2012).

The role of changes in ganglioside and cholesterol content in LR and its potential relation to neurodegeneration and dementia have been reviewed (Schengrund, 2010), finding that those alterations may lead in many cases to changes in cell function. More specifically, in PD association between certain forms of α-synuclein and GM1 has been found indicating a possible role of GM1-raft association with the regulation of α-syn toxicity. Related to this, some trials have found improvement in PD patients treated with GM1. In other line of evidence, it is worth to note that exposure to certain drugs such as alcohol or cocaine have been reported to induce marked changes in gangliosides composition in brain. Therefore

certain environmental factors such as exposure to drugs may induce alterations in LR that could be implicated in the development of neurodegenerative diseases. Taking into account that Parkinson disease aetiology has been related to numerous environmental factors, this evidence may support the role of LR alterations in the development of this pathology (Schengrund, 2010). Additionally to this, parkin, PINK1, α-synuclein and DJ-1 have been found located in LR microdomains. As previously mentioned, mutations in all these four proteins have been associated to genetic cases of PD (Grassi et al., 2020).

Analysis of LR from human frontal cortex have shown important alterations in the lipid composition of these structures related to PD (Fabelo et al., 2011). In that study, LR were isolated from frontal cortex of early motor stages of PD (PD), incidental PD (iPD) and healthy subjects with non-significant lesions (NSL). iPD subjects are those in which post-mortem study revealed Lewy body pathology in the brain stem but did not exhibited any motor symptoms, although some controversies remain around these cases, they could be considered as a previous stage of PD. The results showed important changes in the fatty acids composition of LR, with an increase of saturates and diminished levels of unsaturated fatty acids both in PD and iPD compared to controls. Therefore the unsaturation index was significantly decreased in the pathologic groups. More specifically, a great reduction was observed in docosahexaenoic acid (DHA), arachidonic acid (AA), docosapentaenoic acid (DPA) and linolenic acid in PD and iPD groups. Also the lipid classes in the PD group but especially in iPD group exhibited alterations compared to controls. In this regard, the ratio phospholipids to cholesterol was significantly increased. Remarkably, the authors performed a discriminant analysis on lipid raft composition in which the combination of the first and second canonical functions allowed a clear separation between the study groups (Figure 4). As it can be seen in the figure, fatty acid composition of LR, among other lipids, is key to discriminate between healthy and pathological cases. These results highlight the importance of LR alterations since early stages of development in PD and their potential involvement in the cognitive decline observed in PD patients.

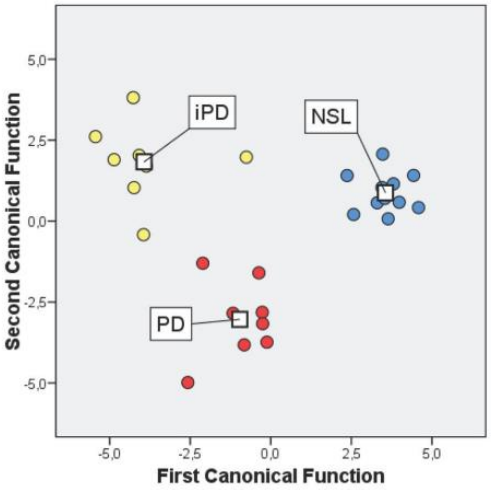

Structure matrix

Lipid species	Canonical Function	
	1	2
DHA	0.708*	0.316
AA	0.535*	0.209
22:5n-6	0.353*	0.168
18:1n-9	0.318*	-0.145
Sulfatides	0.155*	-0.154
18:0 DMA	0.055	0.810*
Cerebrosides	0.140	-0.264*

Figure 4. Discriminant function analyses of groups NSL, PD and iPD showing a clear separation between NSL, PD and iPD groups. Reproduced from (Fabelo et al., 2011).

The MPTP mouse model of Parkinson disease

In 1982 a number of patients with ages ranging from 26 to 42 years old started to exhibit a marked pattern of parkinsonism, which matched most of the motor and some of the non-motor features of PD and that responded to L-dopa. The age of the affected patients together with the suddenly initiation of the symptoms made unfeasible the diagnosis of PD. In all the cases identified only one factor was common: the symptoms had appeared shortly after they have self-administered intravenously with an abuse drug. The analysis of the substances injected revealed the presence of 1-methyl-4-phenyl-1,2,3,6-tetrahydropyridine (MPTP) which ends up being a by-product of the synthesis of MPPP, a meperidine analogue used as a drug of abuse. These findings were published a year after and although further confirmation was still necessary, the authors accurately identified

the MPTP as the causative agent. (J. Langston et al., 1983). The idea was supported by a previous case reported 3 years earlier in which a graduate student who was synthetizing his own drugs exhibited similar symptoms. The post-mortem analysis of this patient showed a profound degeneration in the dopaminergic neurons of the *substantia nigra* (Davis et al., 1979).

MPTP is a lipophilic molecule that can cross easily the blood-brain barrier when administered systemically. Once in the brain, it is transformed in the neurotoxic metabolite 1-methyl-4-phenylpyridinium (MPP^+), which in contrary is not permeable to this barrier (J.W. Langston et al., 1984; Markey et al., 1984). The transformation of MPTP into MPP^+ is mediated by astrocytes, more precisely the monoamine oxidase B (MAO B) (Heikkila et al., 1984). Astrocytes do not concentrate MPP^+, instead, it is released and specifically incorporated by dopaminergic neurons in the *substantia nigra* mediated by the dopamine transporter (DAT) (Shen et al., 1985). MPP^+ is then concentrated into the mitochondrial matrix by the electrochemical gradient of the inner membrane where it is able to inhibit the Complex I of the mitochondrial respiratory chain (Ramsay et al., 1986; Richardson et al., 2007). This inhibition leads to ATP depletion and finally neuronal death.

The discovery of MPTP ability to reproduce PD features in humans and its specific action over the dopaminergic neurons opened a completely new line of study in PD, making possible the creation of new animal models. The first animal models of PD using MPTP were produced in monkeys, which have been extensively used for study treatments against PD symptoms. However, the advantages of using mice as animal models have led to the majoritarian use of these rodents as PD model. The extraordinary impact of the MPTP animal models resides in the fact that prior to the development of the animal model there was a precise knowledge of the MPTP-induced parkinsonism in humans, therefore rendering a powerful model (J.W. Langston, 2017). Moreover, concepts such as the environmental factors as causative agent of PD and the involvement of mitochondrial dysfunction in its pathogenesis have emerged from studies using MPTP animal models.

Introduction

In order to produce a valid MPTP mouse model there are certain factors that must be taken into account. In the first instance, the mouse strain is of remarkable importance since there are great differences in the susceptibility to MPTP between different ones. The origin of these differences is yet not completely clear. One of the factors that play a role in MPTP susceptibility is the MAO B expression, but others such as tolerance to oxidative stress have also been considered (Meredith & Rademacher, 2011). The C5BL/6 is the mouse strain that exhibits the highest sensitivity to this neurotoxic showing a marked loss in nigrostriatal neurons and therefore is the one that has been extensively used. The second parameter that must be considered is the regimen of administration of MPTP. Different approaches have been used in this respect ranging from the acute regimens to the chronic ones. Initially, models employed repeated injections (1 or 2 hours intervals) over a short period of time (1-2 days) accumulating a total amount of 80 mg/kg. This acute regimen produced a severe loss of dopaminergic neurons in a short period of time, but was accompanied by high mortality rates (Sonsalla & Heikkila, 1986). Subchronic administration regimen use lower doses that are injected daily over a period of 5 to 10 days depending on the precise model. This schedule of administrations produces a progressive but less severe loss of dopaminergic neurons that can better resemble the progression of PD (Bezard et al., 1997). It has been reported that in this model the cell loss is produced by apoptosis while in the acute regimen the death mechanisms are different (Tatton & Kish, 1997). Furthermore, chronic intoxication models require longer treatment periods (4 to 5 weeks) in which the dosage may vary as well as the frequency of injection. This models exhibit a higher cell loss that remain long periods after the treatments. In some cases, chronically intoxicated mice exhibit α-synuclein inclusions in the remaining dopaminergic neurons, while this feature is absent in acute or subacute regimens (Meredith & Rademacher, 2011).

Lipid alterations in MPTP mouse model

A recent study from our group has analysed the alterations in the lipid composition of LR and NR membrane fractions from the same MPTP mouse model that will be further analysed in the present work (Canerina-Amaro et al., 2019). The study analysed cerebellum, midbrain and cortex from mice aged until 6 or 14 months and treated with MPTP following a subchronic administration regimen aimed to evoke the progressive development of PD. Age-matched controls were included in the analysis constituting two additional experimental groups. The results indicated several variations in the aged or MPTP-treated groups in the lipid composition of both LR and NR fractions that remarkably differed between the analysed areas. In midbrain, but not in cortex or cerebellum, cholesterol in LR fractions increased upon aging and exposure to MPTP. In all the areas analysed LR from the pathological-like groups exhibited a significant decrease in PUFA, DHA and AA that overall contributed to a decrease in the unsaturation index. These data, were in concordance with previous findings in human cortical LR from PD and dementia with Lewy body cases (Fabelo et al., 2011; Marín et al., 2017). When analysing the NR lipid profiles, it was noticeable that the variations observed opposed those in LR. This is, there were a decrease in cholesterol and an increase in PUFA in the aged or treated animals. Moreover, total phospholipids content was increased in aged treated mice. With these changes certain ratios of interest were subsequently altered. For all the analysed areas, the NR fractions from the aged mice exhibited increased ratios of PUFA/cholesterol, total phospholipids/PUFA and total phospholipids/cholesterol.

Altogether, the alterations observed in LR and NR fractions from the MPTP mouse model indicate that aging and the neurotoxic treatment, but especially the combination of both factors has an effect on the LR integrity in important brain areas related to PD (midbrain) and the cognitive decline (cortex) observed in late course of the pathology. Moreover, the altered lipid composition of LR structures may have an effect on their physicochemical properties.

Hypothesis and objectives

Hypothesis

Lipid rafts from neuronal membrane are particularly interesting structures since they constitute the gathering site for many membrane proteins and receptors. These platforms trigger signalling pathways related to neuronal preservation and brain functioning. A number of previous studies have shown altered lipid raft-mediated signalling pathways related to Parkinson disease. These alterations may be explained by modifications in the physicochemical properties of lipid rafts due to previously observed changes in their lipid composition, particularly in polyunsaturated fatty acid (PUFA), associated with the neuropathology.

Alterations in lipid composition from LR importantly affect the structure, interactions and role of resident proteins. These macromolecular complexes are mainly constituted by proteins that initiate intracellular signalling pathways crucial for neurogenesis, neuroprotection and neuronal functionality. Therefore, the analysis of these signalling platforms including both lipids and proteins may help to elucidate circuits of metabolic damage in early stages of Parkinson disease and eventually to allow therapeutic approaches to reduce the progression of this neurodegenerative disease.

This study may contribute to the development of new early diagnostic strategies and also the formulation of new therapeutic approaches. Consequently, the present research project focuses in the following objectives.

Objectives

1. Characterization of molecular alterations in lipid rafts from a toxicological murine model of Parkinson disease induced by MPTP. Brain regions involved in cognitive processes and motor control will be

analysed. This general objective comprises the following specific objectives:

a. Study of protein composition of lipid raft microdomains in the murine model and the possible modifications after MPTP treatment.
b. Study of possible interactions between α-synuclein and other proteins related to neurodegenerative processes in LR microdomains.
c. Analysis of post-translational modifications in α-synuclein.
d. Determination of ganglioside profile in lipid raft microdomains from the murine model.

2. Study of energy metabolism in a cellular model of Parkinson disease:
   a. In resting conditions.
   b. In response to an excitatory event.
3. Validation in LR samples from Parkinson disease patients of results obtained from the murine model of Parkinson disease (objective 1). This objective will focus mainly in distribution of proteins of interest.

Altogether, the development of these objectives aims to progress in the understanding of early pathological events initiated in neuronal membrane microdomains which might act as a trigger for the development of Parkinson disease. Particularly, they will contribute to improving the knowledge about potential alterations both in the activity and interaction between lipid raft resident proteins that take part in several responses related to neuronal survival and brain function preservation. Additionally, the study of metabolic flux in cortical neurons will bring light to the effect of the neurotoxin MPTP, mediated by its metabolite MPP^+. Therefore, the research here proposed would allow progressing in the understanding of neuroprotection mechanisms and neurotoxicity related to Parkinson disease and would provide new tools in the therapeutic approaches, both preventive and palliative ones.

Materials and Methods

1. Materials

1-Methyl-4-phenyl-1,2,3,6-tetrahydropyridine hydrochloride (MPTP-HCl), 1-Methyl-4-phenylpyridinium iodide (MPP^+ iodide), Cholera toxin B subunit-horseradish peroxidase (CTB-HRP), SIGMAFAST DAB with Metal Enhancer, trypsin, penicillin/streptomycin, poly-l-lysine, propidium iodide, 2-Deoxy-D-glucose (2DG) and sodium-L-lactate were purchased from Sigma. 4-15% Mini-PROTEAN TGX Precast Protein Gels, Precision Plus Protein Dual Color Standards, Trans-Blot Turbo Mini PVDF transfer packs, Blotting Grade Blocker, ReadyPrep 2-D Cleanup Kit, immobilized pH 3-10 gradient strips for two-dimensional gel electrophoresis and Clarity Wester ECL Substrate were from Bio-Rad. DeStreak rehydration solution was from GE Healthcare. Complete protease inhibitor cocktail and DNAseI were purchased from Roche Diagnostics. Hank's balanced salt solution (HBSS), Neurobasal medium, horse serum, B-27 Supplement and GlutaMAX Supplement were from Gibco. Calcein AM was from Molecular Probes. The Dynabeads Antibody Coupling Kit was from Invitrogen. CellTiter 96 AQueous One Solution Cell Proliferation Assay kit was from Promega and the Lactate Reagent from Beckman Coulter. Anti-tyrosine hydroxylase antibody (AB152) was from Millipore, antibodies used for immuno-detection or immuno-precipitation are listed in Table 3.

2. Animal handling and treatment

The PD animal model used for this study intends to resemble the slow progression of Parkinson disease. Administration of the neurotoxic MPTP in mouse has been extensively used as a well-accepted PD model. However the administration's schedule has been pointed out as an important factor in the extent of *nigral* degeneration. For this reason a subacute regimen of administration was performed (Bezard et al., 1997).

Materials and Methods

C57BL/6J mice were chosen since this strain is the most appropriate one for the establishment of the MPTP mouse model. Mice were housed in enriched cages with food and water ad libitum under a 12-h light/dark cycle in the Animal Facilities at La Laguna University. All procedures were performed in accordance with the European Community Directive (86/609/UE) and Universidad de La Laguna Ethics Committee guidelines for the care of laboratory animals.

Mice were aged until six or fourteen months and then treatments were performed. MPTP was dissolved in saline solution. Treated animals received daily injections of 4 mg MPTP/kg/day for 20 days. Littermates of these two groups were treated with saline following the same regimen. 43 days after finishing the treatments, mice were deeply anesthetized and sacrificed. Therefore, four experimental groups were established: W6 (control 6 month-old), M6 (MPTP treated 6 month-old), W14 (control 14 month-old), M14 (MPTP treated 14 month-old). Two different sets of samples were acquired; one set comprised of 3 animals per experimental group was processed for IHC. Another set with 4 animals per group was used for lipid raft isolation.

3. Human Brain Samples

Human brain tissue was obtained from the Institute of Neuropathology HUB-ICO-IDIBELL Biobank and the Hospital Clinic-IDIBAPS Biobank. All legal and ethical guidelines for Biomedical Research involving human subjects (Declaration of Helsinki) were followed and procedures counted with the approval of the local Ethics Committee. In a frame of 3-12 hours post-mortem autopsies were conducted and immediately brains were collected and bisected into hemispheres. The hemisphere intended for molecular studies was stored at -80ºC until used. LR isolation was processed in the Institute of Neuropathology, by Dr. I. Ferrer's group following the same protocol described in methods section 5. Fractions obtained were then delivered in dry-ice to our laboratory where they were further analysed.

LR isolation was preformed from frontal cortex tissue from clinically diagnosed and neuropathologically verified PD patients and the respective age-matched controls. The post-mortem delay was between 2 hours 15 minutes and 11 hours 45 minutes. Samples processed were from four cases of early PD stages (PD3-4; 3 male and 1 female, average age 70.1 ± 15.7 years), four cases of late stage (PD5-6; 3 male and 1 female, average age 78 ± 6.5 years) and another four cases of age-matched controls with no neurological symptoms and signs in which the neuropathological examination did not show abnormalities (2 male and 2 female, average age 70.5 ± 8.2 years).

4. Immunohistochemistry

In order to validate the effectiveness of MPTP treatments IHC stains to detect tyrosine hydroxylase (TH) were performed on brain slides containing the *substantia nigra*. Three individuals per animal group were analysed. For this analysis mice were anesthetized and perfused with 4% paraformaldehyde. Brains were extracted and post-fixed in 4% paraformaldehyde for 12 hours at room temperature followed by dehydration by immersion in graded ethanol:

- ethanol 70% (10-15')
- ethanol 80% (10-15')
- ethanol 90% (10-15')
- ethanol 96% (10-15')
- ethanol 100% (10-15') × 2

Brains were then incubated in methyl benzoate until they sank and then incubated for 1 hour in benzol. Prior to paraffin inclusion, samples were washed twice in liquid paraffin at 65ºC for 1 hour followed by one overnight wash. Finally brains were embedded in in paraffin blocs. Coronal 10 µm sections were obtained with a paraffin microtome and mounted on glass slides pre-treated with APS (3-Aminopropyl)-triethoxysilane.

Materials and Methods

Slides containing the *substantia nigra* were selected for TH IHC with help of a mouse brain atlas. Selected slides were deparaffinised by immersion in xylene and rehydrated using graded ethanol dilutions followed by washes with distilled water and phosphate-buffered saline (PBS):

- xylene (15 minutes) × 2
- ethanol 100% (10 minutes) × 2
- ethanol 96% (10 minutes)
- ethanol 90% (10 minutes)
- ethanol 80% (10 minutes)
- ethanol 70% (10 minutes)
- water (10 minutes) × 2
- TBS (10 minutes) × 2

For antigen retrieval slides were boiled for 15 minutes in 20 mM citrate buffer (pH 6) followed by 3 washes in tris-buffered-saline (TBS). Anti-tyrosine hydroxylase antibody was diluted 1:500 in TBS and slides were incubated overnight at room temperature. After 3 washes in TBS, slides were incubated 2 hours at RT with anti-rabbit-HRP antibody diluted 1:200 in TBS. Slides were washed 3 times with TBS and signal was developed using SIGMAFAST DAB (3,3'-Diaminobenzidine tetrahydrochloride) with metal enhancer. Before permanently mounting the slides with Eukitt, washing in distilled water and dehydration was performed:

- TBS (10 minutes) × 2
- water (10 minutes) × 2
- ethanol 70% (10 minutes)
- ethanol 80% (10 minutes)
- ethanol 90% (10 minutes)
- ethanol 96% (10 minutes)
- ethanol 100% (10 minutes) × 2
- xylene (15 minutes) × 2

Stained slides were photographed and TH-positive neurons were counted using ImageJ software. Total number of TH-positive neurons per animal was calculated as the sum of all TH-positive neurons in the sections analysed. To ensure no slides containing dopaminergic neurons from s*ubstantia nigra* were omitted from analysis, slides surrounding this area were processed for IHC until no TH signal appeared.

5. Lipid raft isolation

Brain samples intended for lipid raft isolation were dissected, immediately frozen and stored at -80ºC until processed. Lipid rafts were obtained from Cortex (Co), midbrain (Md) and cerebellum (Cb) samples following a previously described method (Mukherjee et al., 2003). Basically, this protocol makes use of the physical properties of lipid raft microdomains. These structures are detergent resistant and exhibit a low density compared to the rest of the membrane. This allows its purification using a detergent-containing buffer and a sucrose gradient. All the procedure must be performed in cold to ensure that low temperature prevents from protein and lipid degradation. Samples were homogenized in 1 ml of homogenization buffer (Table 1).

Homogenates were centrifuged at 500 *g* for 5 minutes at 4ºC. Supernatants were collected, transferred to clean 1.5 ml tubes and incubated at 4ºC for 1 hour using an orbital rotor. Buffer A described in Table 1 was used for dissolving sucrose at three different concentrations: 80%, 36% and 15%. 800 µL of homogenate were thoroughly mixed with an equal volume of 80% sucrose thus rendering a 40% of sucrose solution containing the sample. This sample was placed at the bottom of an ultracentrifuge tube and carefully overlaid with 8 mL of 36% sucrose solution followed with a third layer of 15% sucrose solution until the tube was completely filled (around 3.5 ml) (Figure 5A). Sucrose gradients were centrifuged at 150,000 *g* for 18 hours at 4ºC in a Beckman SW41Ti rotor. After centrifugation a cloudy layer is visible in the interphase between 15% and 36% sucrose solutions (Figure 5B). Six

fractions of 2 ml were carefully collected from the top to the bottom and the pellet was thoroughly mixed with the last 500 µL of the gradient and kept as a separate fraction for further analysis. Therefore from each sample 7 fraction were collected: F1-F6 and pellet (Figure 5C).

Reagent		Concentration
Buffer A	Tris-HCl, pH 8.0	50 mM
	$MgCl_2$	10 mM
	NaCl	150 mM
Triton X-100		1%
Glycerol		5%
NaF		20 mM
Na_3VO_4		1 mM
β-mercaptoethanol		5 mM
PMSF		1 mM
Complete protease inhibitor		1X

Table 1. Composition of the homogenization buffer.

Fractions F1 and F2 corresponded to lipid raft microdomains, whilst pellet comprised the non-raft fraction. Protein contents in each fraction were determined by the bicinchoninic acid (BCA) method and western blot assays were conducted in order to characterize the different fractions.

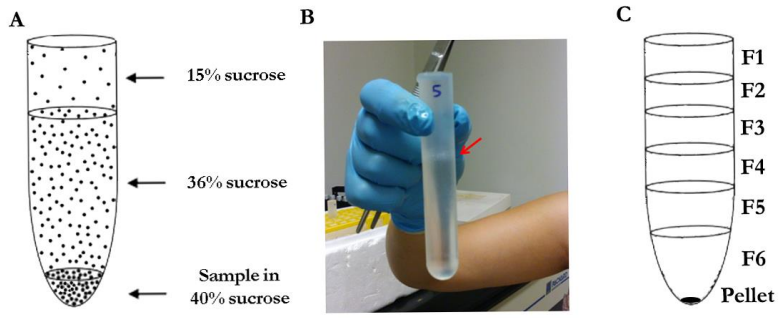

Figure 5. Representation of the sucrose gradient for lipid raft isolation. A) Scheme of the set up with sample and the discontinuous sucrose gradient before ultracentrifugation. B) Picture of the gradient after the ultracentrifugation. Notice the cloudy area (red arrow) that contains de lipid raft fraction. C) Scheme representing the fractions collected after ultracentrifugation separation.

6. Slot Blot analysis

Lipid rafts are characterized by a low content in proteins. This fact implies higher difficulties when trying to analyse the protein content in a detectable threshold by western blotting. For this reason we decided to analyse glutamate receptors by slot blot, which simplifies the procedure and improves the immuno-detection, rendering a better signal compared to western blot. Moreover, the availability of specific primary antibodies against the main brain gangliosides provides a simple way to determine the profile of gangliosides in LR samples using the slot blot set-up.

LR and NR samples were diluted in transference buffer (Table 2) using corresponding volumes for 2 µg of total protein in a final volume of 1 ml and 100 µl of diluted samples were spotted onto a nitrocellulose membrane sealed on a Slot-blot set-up (Bio-Rad) using a vacuum pump. After the transference membranes were blocked in detergent free-TBS containing 3.5% (w/v) of bovine serum albumin (BSA) for 1 hour at room temperature. Due to the characteristics of the

procedure, it is not possible to perform re-blot to detect different gangliosides or proteins in the same membrane. Therefore, replicates of each membrane were prepared using equal amounts of the same sample dilution. Membranes were incubated overnight at 4ºC with the specific primary antibodies: mouse monoclonal antibodies against GD1a, GD1b and GT1b gangliosides, rabbit monoclonal anti-mGluR5 and rabbit polyclonal anti-NMDAR2B. After 3 washes with TBS membranes were incubated with the corresponding secondary-HRP antibody. An additional membrane was incubated with cholera toxin B subunit-HRP diluted 1/20,000 in blocking solution for 45 min at room temperature. In all cases, signal was developed with Clarity Western ECL Substrate. Detection was performed with Chemie-Doc MP Imaging System (Bio-Rad) and its optical density analysed using Image Lab software.

Reagent	Concentration
Glycine	75 mM
Tris	25 mM
Methanol	20%

Table 2. Composition of the transfer buffer.

7. SDS-Page and Immunoblotting (Western Blot)

For protein analysis samples were resuspended in 4X loading buffer (Table 4) and heated at 95ºC for 5 minutes to linearize the proteins. Samples were then loaded in 15 or 10-well, 4-15% polyacrylamide precast gels (Mini-Protean-TGX gels, Bio-Rad) resolved by SDS-PAGE at 200 mV for approximately 30-35 minutes (Laemmli, 1970). Molecular weight marker ranging from 10 to 250 kDa was included in each gel for reference (Precision Plus Protein Dual Color Standards, Bio-Rad). Proteins were transferred to PVDF membranes using the Trans-Blot Turbo Transfer System and Mini PVDF Transfer Packs. Membranes were blocked

with BLOTTO (Bovine Lacto Transfer Technique Optimizer solution), which consisted of 5% non-fat milk in TBST, for 60 minutes and incubated with primary antibodies overnight at 4ºC with gentle agitation. Membranes were then washed 3 times for 10 minutes with TBST and incubated 1 hour at RT with the corresponding secondary antibody. After 3 washes in TBST signal was developed with Clarity Western ECL Substrate. Detection and quantification was performed with Chemie-Doc MP Imaging System and Image Lab software both from Bio-Rad. Table 3 shows the list of primary antibodies used.

Blots in which α-synuclein was analysed were subjected to mild fixation immediately before the blocking step. This fixation was intended to prevent α-synuclein detachment from blotted membranes (Lee & Kamitani, 2011). Immediately after transfer step membranes were incubated with TBS + 0.4% para formaldehyde (PFA) for 30 minutes at room temperature.

Antibody	**Type**	**Dilution**	**Supplier**
Anti-Alpha-synuclein [MJFR1] (ab138501)	Rabbit monoclonal	1:1,000	Abcam
Anti-Alpha-synuclein [4D6] (ab1903)	Mouse monoclonal	1:1,000	Abcam
Anti-Alpha-synuclein [EPR20535] (ab212184)	Rabbit monoclonal	1:5,000	Abcam
Anti-Alpha-synuclein (phospho S129) (ab59264)	Rabbit polyclonal	1:1,000	Abcam
Anti-Aggregated Alpha-Synuclein, clone 5G4 (MABN389)	Mouse monoclonal	1:1,000	Millipore
Anti-Alpha-Synuclein filament [MJFR-14-6-4-2] (ab209538)	Rabbit monoclonal	1:1,000	Abcam
Anti-Flotillin 1 (ab41927)	Rabbit polyclonal	1:1,000	Abcam

Anti-Na+/K+ ATPase α-1 (05-369)	Mouse monoclonal	1:1,000	Millipore
Anti-VDAC1 (ab14734)	Mouse monoclonal	1:1,000	Abcam
Anti-PrP (5B2) (sc-47730)	Mouse monoclonal	1:500	Santa Cruz Biotechnology
Anti-Amyloid Precursor Protein [Y188] (ab32136)	Rabbit monoclonal	1:1,000	Abcam
Anti-beta Amyloid (ab2539)	Rabbit polyclonal	1:1,000	Abcam
Anti-β-Actin (a5441)	Mouse monoclonal	1:5,000	Sigma
Anti-mGluR1a (ab183712)	Rabbit monoclonal	1:2,000	Abcam
Anti-Metabotropic Glutamate Receptor 5 [EPR2425Y] (ab76316)	Rabbit monoclonal	1:5,000	Abcam
Anti-Glutamate Receptor 1 (AMPA subtype) [EPR5479] (ab109450)	Rabbit monoclonal	1:2,000	Abcam
Anti-NMDAR2B (ab65783)	Rabbit polyclonal	1:1,000	Abcam
Anti-GD1a-1	Mouse	1:1,000	From Ronald L. Schnaar laboratory (Schnaar et al., 2002)
Anti-GD1b-1	Mouse	1:1,000	
Anti-GT1b-2b	Mouse	1:2,000	

Table 3. Antibodies used for western blot, slot blot and 2-D electrophoresis.

Reagent	Concentration
Tris-HCl	125 mM
SDS	4.6%
Glycerol	20%
ß-mercaptoethanol	10%
Bromophenol blue	4×10^4 %

Table 4. Loading buffer composition.

8. Two-dimensional gel electrophoresis

LR and NR samples were prepared for two-dimensional gel electrophoresis using the ReadyPrep 2-D cleanup Kit from Bio-Rad. Corresponding volumes for approximately 15 μg of total protein from each sample were submitted to the protocol described by the manufacturer and resuspended in 125 μL of DeStreak rehydration solution (GE Healthcare). At this point, samples were applied to immobilized pH gradient 7 cm-length strips pH 3-10 and processed for isoelectrofocusing (IEF) using a PROTEAN IEF cell from BioRad in a 2 steps programme. First step consisted in active rehydration performed at 5,000 V in a rapid slope for 14 hours. In a second step isoelectrofocusing was conducted up to 20,000 V/h. The IEF was performed overnight at RT. IEF strips were then reduced in equilibration buffer containing 2% (w/v) dithiothreitol (DTT), followed by alkylation in the same buffer but containing 2.5% (w/v) iodoacetamide (IAA). Both reduction and alkylation were performed for 15 min at room temperature. After this procedure, strips were loaded on 12.5% homemade SDS-polyacrylamide gels for second dimension resolution. After loading the strips, the set up was covered with 1% low-melting agarose solution and subjected to electrophoresis at a constant voltage of 100 mV for approximately 90 minutes. Resolved proteins were transferred to PVDF membranes. Fixation with PFA was performed as explained

previously. To detect phosphorylated proteins/epitopes, we blocked in TBST + 5% BSA instead of BLOTTO.

9. Primary cultures

Primary cultures were obtained from C57BL/6J mice E17 embryo brains (purchased from Janvier Laboratory) (Ref#: 31676432) (Bartlett & Banker, 1984). Pregnant mice were sacrificed in a CO_2 chamber followed by cervical dislocation and embryos were collected by C-section. Cortices were dissected on Hanks' Balanced Salt Solution (HBSS,) supplemented with Ca^{2+} and Mg^{2+} (1.26 mM $CaCl_2$, 0.49 mM $MgCl_2$ and 0.4 mM $MgSO_4$). Tissue was minced with scalpel and washed 3 times with HBSS without Ca^{2+}/Mg^{2+} followed by digestion with trypsin/DNAse I solution (0.25% trypsin and 1 mg/ml DNAseI, in HBSS) for 15 minutes with agitation every 5 minutes. After digestion, 3 washes with HBSS without Ca^{2+}/Mg^{2+} were performed to completely remove any Trypsin. Tissue was then dissociated by pipetting through horse serum pre-coated Pasteur pipette. Homogenate was transferred to a 15 ml tube on top of 8 ml of 1:1 mix of culture medium and horse serum and centrifuged for 5 minutes at 900 rpm. The pellet was resuspended in 5 ml of culture medium and thoroughly dissociated by pipetting. Cells were seeded on Poly-L-Lysine-coated culture vessels at a density of 1,500,000 cells/ml for "Seahorse" assays or 500,000 cells/ml for other assays. The culture medium was Neurobasal (Gibco) supplemented with B27 (Lifetech), 2 mM GlutaMax (Life Technologies) and 1% Penicillin/Streptomycin (Sigma).

10. Viability assays

Viability assays were performed using the calcein/propidium iodide uptake assay (Mattson et al., 1995). In live cells calcein AM is transformed into green fluorescent calcein dye by intracellular esterase activity and that is retained in the cytoplasm due to its ionic charge. Meanwhile, live cells are impermeable to propidium iodide (PI). Conversely, in dying cells, the compound can enter into the nucleus, as the integrity of the plasma membrane is compromised and it intercalates in nucleic acid, increasing its red fluorescence. Therefore, when added in combination calcein (Invitrogen) and PI to cell cultures it yields green fluorescent live cells and red fluorescent dead cells. Neurons were plated on a M24 well plate at a density of 250,000 cells/well in a volume of 500 µl. To assess the viability, calcein and PI were added to a final concentration of 1 µM and 2 µM respectively. Cells were then incubated for 20-30 min at 37ºC. Three random fields were chosen for each well and live and dead cells were counted manually using Zeiss Axiovert 40 CFL fluorescence microscope (Zeiss, Overkochen, Germany). Viability was estimated as percentage (%) of alive cells/total cells.

11. Treatments

11.1. MPP^+ in primary cultures of cortical neurons

In primary cultures of cortical neurons MPP^+ (Sigma) was used instead of MPTP to assure its uptake and metabolic processing by the neurons in culture. To determine the optimal dose of MPP^+, we conducted viability assays after 24 hour treatment with different concentrations of MPP^+, with the aim of finding the higher concentration of the neurotoxic that produced a moderate reduction on viability. 100 mM to 1 mM stock solutions of MPP^+ in PBS were prepared fresh for every experiment. After testing a range of concentrations, we selected 50 µM MPP^+ to treat neurons for either 24 hours or 4 hours followed by 20 hours of recovery with

the appropriated medium without MPP^+. Control groups were treated with the same volume of PBS in each case.

11.2. Glutamate in primary cultures of cortical neurons

Treatments with glutamate (Sigma) were used to simulate the physiological challenges to what neurons are usually exposed. Viability assays where conducted to determine a dose that alone, would represent a non-toxic stimulus, but that in combination with MPP^+ could increase the mortality. 1 M stock solution of glutamate was prepared in PBS and frozen at -20ºC. For the different assays neurons were exposed to different doses of glutamate ranging from 2 µM to 100 µM for a 20 minute period. For viability and lactate determination assays medium was replaced after exposure to eliminate the glutamate. Control neurons were treated with PBS and medium replacement at the same times that in treated neurons.

12. Mitochondrial respiration assays

Measurements of oxygen consumption rate (OCR) constitute a good approach to mitochondrial functionality assessment. The Extracellular Flux Analyzer Instrument (XF24, Agilent/Seahorse Biosciences) allows the sequential injection of up to 4 compounds in between OCR measurements thus allowing estimations of bioenergetics parameters such as basal respiration, maximal respiratory capacity or increase in respiratory rate in response to certain compounds that, altogether, can give important information about mitochondrial fitness (Ribeiro et al., 2015; M. Wu et al., 2007). For each use one XF24 cell culture plate, one XF24 sensor cartridge and a utility plate are required. Neurons were plated into the XF24 cell culture microplate at a density of 150,000 cells/well in 100 µl of culture medium. Cells were allowed to differentiate for 4-5 days before the measurements. Wells A1 and D6 were left empty for background correction. The

day before the experiment the cartridge has to be hydrated with XF24 calibration solution and incubated at 37ºC overnight in a CO_2-free incubator. On the day of the experiment the cartridge is loaded with appropriate concentration of the required drugs. Immediately before starting the experiment, culture medium was replaced with assay medium (DMEM without bicarbonate, supplemented with 10 mM glucose and 1 mM pyruvate). Cells were washed once with 300 µl of assay medium and finally brought to 600 µl of assay medium. After medium replacement cells were kept at 37ºC in a CO_2-free incubator while establishing instrument settings and cartridge calibration.

The basic assay involves OCR measurement followed by progressive injection of the ATP synthase inhibitor oligomycin, the uncoupling agent carbonyl cyanide 4-(trifluoromethoxy) phenylhydrazone (FCCP) and the mitochondrial complex III inhibitor antimycin, with OCR measurements in between and at the end of the injections. This basic protocol would consist of the following steps:

a) Calibrate probes
b) Equilibrate
c) Mix—2 min
d) Wait—2 min
e) Measure—3 min
f) Repeat steps c–e , three times
g) Inject oligomycin (Final concentration of 0.5 µM)
h) Repeat steps c–e , three times
i) Inject FCCP (Final concentration of 0.25 µM)
j) Repeat steps c–e , three times
k) Inject antimycin (Final concentration of 4 µM)
l) Repeat steps c–e , three times
m) End protocol.

Using this protocol a series of parameters represented in Figure 6 can be estimated:

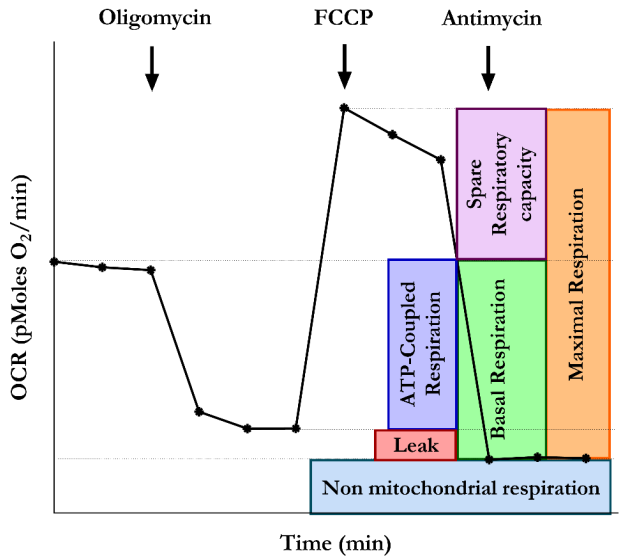

Figure 6. Schematic representation of a typical experiment for determination of the oxygen consumption rate (OCR) by extracellular flux analysis (Seahorse) and the derivation of different metabolic parameters. The sequential injection of oligomycin, FCCP and antimycin induces changes in the OCR that allow to determine key parameters in the characterization of mitochondrial fitness (Adapted from Simarro et al., 2010).

- Basal respiration (BR): Total mitochondrial respiration in normal conditions.

- ATP-Coupled Respiration (ATP-CR): Fraction of the respiration that is linked to ATP production.

- Maximal respiration (MR): Maximal respiration that the mitochondria could achieve in case of increased metabolic demand.

- Spare respiratory capacity (SRC): reserve in mitochondrial respiratory capacity to respond to a raise in energy demand.

- Proton Leak (PL): fraction of the respiration that is not transformed into ATP, due to loss of protons.

- Non mitochondrial respiration: Oxygen consumed by other or oxygen-consuming cellular systems, excluding the mitochondria.

The compounds injected during the assay were modified to study the effect of glutamate. Two different assays were performed:

- An injection of 10 μM glutamate followed by the previously described injections of oligomycin, FCCP and antimycin.
- Progressive injections of glutamate for a final concentration of 10, 50 and 100 μM, respectively and an injection of oligomycin for a final concentration of 0.5 μM. Therefore only parameters that were possible to estimate following this experimental design were basal respiration and ATP-Coupled respiration at the different concentrations of glutamate.

13. Lactate determination

Quantification of lactate production was performed as an indicator of the glycolytic pathway diverted away from oxidative phosphorylation. Quantification was performed with the Lactate Reagent kit (Beckman Coulter). This system is based on the development of two coupled reactions catalysed by Lactate oxidase (1) and Peroxidase (2) that finally renders a chromogen that can be quantified by its absorbance at 520 nm. The reactions are the following:

1. Lactate + O_2 → Pyruvate + H_2O_2

2. H_2O_2 + 4-Aminoantipyrine + H^+ donor (TOOS) → Chromogen

Primary cortical neurons were grown in M6 well plate at a density of 1,000,000 cells/well in a volume of 2 ml. At the beginning of the experiment the culture medium was replaced for 1 ml of fresh Neurobasal supplemented with N2. Two type of controls were used; 2-Deoxy-D-glucose (2DG) 30 mM to inhibit glycolysis and assess lactate production by non-glycolytic processes and oligomycin 1 μM as positive control that forces the maximal production of lactate by preventing

mitochondrial ATP production. 30 µl aliquots of medium were taken at 2, 4 and 6 hours after medium replacement (Katsu-Jiménez et al., 2019). Immediately after the last aliquot was taken, the plates were washed with PBS and immediately frozen at -80ºC for subsequent extraction of total proteins and normalization. To quantify lactate content in medium aliquots colorimetric assay using the Lactate Reagent (Beckman Coulter) was performed. Standard curve of lactate (Sodium-L-Lactate, Sigma) ranging from 0-5 mM was prepared and 5 µl of each value were transferred into a M96 well plate. 5 µl of each medium aliquot previously collected were also transferred to the plate. Components B and C of the Beckman Coulter Lactate Reagent were mixed in a ratio of 5:1 and 95 µl of the mixture were added to each sample or standard curve value. After 20-25 minutes of incubation at RT in the dark, absorbance at 520 nm was measured using the Infinite 200Pro plate reader. The values of lactate were normalized against total protein contain for each sample.

14. ATP assay

For ATP quantification the CellTiter-Glo® Luminescent Cell Viability Assay (Promega) was used. This kit is based on the luciferin/luciferase pair. Luciferase has the ability to oxidise luciferin in the presence of ATP emitting light in the process. The limiting reagent in this reaction is ATP since both luciferin and luciferase are present in high abundance, therefore the amount of light emitted will be dependent on and proportional to the amount of ATP.

Neurons were plated on M96 well plate, with transparent bottom and black walls, at a density of 50,000 cells/well in 100 µl. To quantify the ATP production over a period of time, the medium was replaced for fresh one and time was counted from that point. In each experiment 4 to 8 wells were left without cells but containing medium for background correction. At the moment of the assay the CellTiter-Glo Buffer was poured into the vial containing the lyophilized CellTiter-Glo Substrate and mixed by gently inverting the vial. Using a multichannel pipette 100 µl of the reagent were added into each well and plate was gently mixed for 2

minutes and let sit for 10 more minutes. Luminescence was measured with the Infinite 200Pro plate reader.

15. Total protein extracts

Total protein extracts from primary cultures of cortical neurons were performed to normalize lactate production against total protein content. Neurons plated on M6 well plates were washed with PBS, after thoroughly aspirating PBS the plates were frozen at -80ºC. For the extraction, plates were brought to RT and 50 µl of lysis buffer (20 mM HEPES pH 7.4, 100 mM NaCl, 100 mM NaF, 5 mM EDTA, 1% Triton X-100, Complete proteinase inhibitor and phosphatase inhibitor) were added into each well. Cells were harvested with a cell scraper and cell suspension was transferred to pre-cooled 1.5 ml centrifuge tubes and kept on ice for 15 minutes. After 10 minutes centrifugation at 4ºC, 13.000 g, supernatant was collected and kept at -20ºC. Protein quantification was done by bicinchoninic acid assay in M96 (Pierce) plate format.

16. Statistical analysis

Quantitative data were represented as mean ± statistical error (SEM). In some cases data were previously normalized to control group and expressed as percentage, assuming control (W6) as 100%. Statistical analysis has been carried out using GraphPad Prism 7.00 software. Kruskal-Wallis test with Dunn's corrections for multiple comparisons was performed when comparing experimental groups. Two-way ANOVA with Sidak's multiple comparisons test was performed when analysing differences between experimental groups at different periods of time. Two-way ANOVA with Tukey's multiple comparisons test was performed when analysing differences between experimental groups in the different brain areas. Sample size is detailed for each experiment in the results section but can be

summarized as follows. IHC experiments were conducted with 3 animals per group. LR isolation and the corresponding analysis were conducted with 4 animals per group. Experiments for the metabolic characterization of MPP^+ exposure in primary cultures of cortical neurons were repeated 3 times from primary cultures obtained in independent culture sessions and from independent mice. Each experiment itself included repetitions up to 8 depending on the setup possibilities.

Results

1. Characterization of lipid rafts from the MPTP Parkinson Disease murine model.

1.1. Validation of the PD-like neurotoxic model

The aim of this study is evaluating both the effect of aging and neurotoxicity caused by MPTP, thus establishing a PD-like mouse model. For this reason, we used six and fourteen month-old animals that were either treated with MPTP or saline and established four experimental mice groups. Treated mice (M6 and M14) received daily dose of 4 mg MPTP/kg/day for 20 days. Littermates (W6 and W14) received saline following the same regimen. W6 was considered the control group for comparisons.

In the first instance, we wanted to verify the effectivity of the MPTP treatments conducted generating a valid Parkinson disease model. Therefore, immunohistochemistry assays against tyrosine hydroxylase (TH) were performed in mice brain sections comprising the *substantia nigra*. TH is a key enzyme in the synthesis of dopamine, so TH immunohistochemistry is extensively used as a marker for dopaminergic neurons. For each experimental group 3 animals were used.

The total number of TH-positive neurons in the *substantia nigra* showed a significant decrease in those mice treated with MPTP, both at 6 and 14 month-old animals in comparison with W6 (p W6 *vs* M6: 0.0132; W6 *vs* M14: 0.0194, Dunnett's multiple comparisons test) (Figure 7). This result indicates that treatments with MPTP reduced the number of dopaminergic neurons in this brain area, generating a lesion comparable to the one found in brains from PD patients and successfully producing a valid mouse model for studying PD.

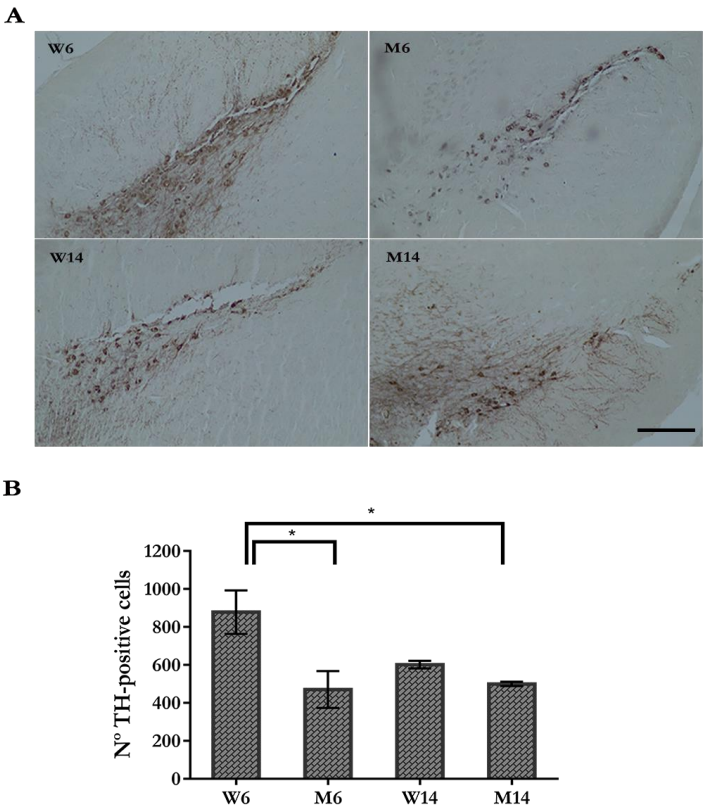

Figure 7. Tyrosine hydroxylase (TH) immunoreactivity in the *substantia nigra*. A) TH immunohistochemistry on brain slides from *substantia nigra* of the four experimental groups (W6: control 6 months, M6: MPTP treated 6 months; W14: control 14 months; M14: MPTP treated 14 months). Black bar = 100 µm. B) Quantification of TH-positive neurons in this area (* $p<0.05$, One-way ANOVA with Dunnett's multiple comparisons test. N= 3) Error bars represent SEM .Adapted from (Canerina-Amaro et al., 2019).

1.2. Lipid raft isolation and characterization

For lipid raft isolation mice brains of the different experimental groups were dissected and immediately frozen at -80ºC. The dissected structures that has been analysed in this study are three: cortex, midbrain and cerebellum. Cortex was selected based on previous studies that showed alteration in lipid rafts from this

brain area. Midbrain was selected for its implication in Parkinson disease since key areas in the development of the disease, such as *substantia nigra* and basal ganglia, are included in this region. Even when the isolation and lipid raft analysis of these areas would have been much more informative, it is not methodologically possible to perform the lipid raft isolation and analysis from such small structures. Therefore we opted for analysing midbrain. Cerebellum was used as control since no changes were expected. To the best of our knowledge, there are no reports showing cerebellar alterations in the mouse MPTP model of PD. Moreover, recent work from our group has found that lipid rafts in cerebellum are highly preserved in MPTP- treated mice (Díaz et al., 2019).

After lipid raft isolation we obtained 6 different fractions (F1 to F6) and a pellet (Figure 5). Theoretically, lipid rafts fractions should be contained in the interphase between the 15% and the 35% sucrose solutions. Remarkably, in this interphase a cloudy layer comprising the lipid rafts is visible after the ultracentrifugation step (Figure 5B). This fact constitutes an easy way to confirm that the isolation protocol has worked correctly. This layer is completely recovered in fractions F1 and F2. These two fractions were collected, mixed and analysed together. Pellet and fractions close to it would contain all the non-raft membranes and cytoplasmic content.

We quantified protein content of the fractions obtained by BCA. Results showed a remarkably low protein content in LR fractions, as expected, and higher content in the corresponding NR fractions. Then, we performed western blot analysis to evaluate the presence in the different fractions of proteins characteristic of both lipid raft and non-raft microdomains. Flotillin-1 is considered a scaffolding protein of lipid rafts and also PrPc has been shown to localize exclusively in lipid raft fractions. On the other hand, glyceraldehyde 3-phosphate dehydrogenase (GAPDH) and NeuN are characteristic proteins of non-raft fractions. The distribution of these proteins observed among the different fractions of our samples support the correct isolation of the lipid raft microdomains (Figure 8).

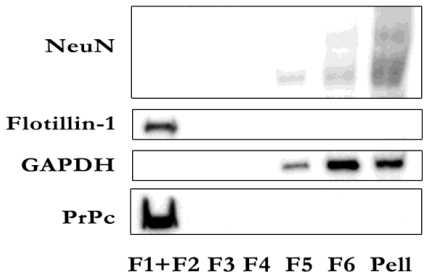

Figure 8. Immunoblotting of lipid raft fractions. Fractions 1 to 6 and pellet were separated by SDS-PAGE, transferred to PVDF membranes and incubated with the specific primary antibodies. Signal was developed by chemiluminescence. The localization of lipid raft resident proteins such as Flotillin-1 and Prion protein (PrPc) in fraction F1+F2 confirms the correct isolation of these microdomains. Glyceraldehyde 3-phosphate dehydrogenase (GAPDH) and NeuN are characteristic proteins of non-raft fractions. Illustration corresponds to fractions obtained from cortex of a W14 animal.

1.3. Gangliosides modifications of lipid raft fractions in response to MPTP treatment

Gangliosides are important part of the glycocalyx in nerve cells that preferentially reside in lipid rafts. There are just four types that comprise for the vast majority of gangliosides in mammal brains: GM1, GD1a, GD1b and GT1b. In general, gangliosides have self-aggregating properties and also tend to aggregate with other lipids and proteins. Particularly, some studies have reported association between GM1 and α-synuclein pointing to an inhibitory role in fibril formation (Martínez et al., 2007). Therefore, we have analysed the distribution of these glycolipids in lipid raft fractions previously isolated from cortex, midbrain and cerebellum in the four study cohorts: W6, M6, W14 and M14, four animals per group were used. Samples were analysed by slot-blot using cholera toxin subunit B to detect GM1 and specific antibodies directed against GD1a, GD1b and GT1b. Flotillin-1 was used as loading control for normalization. Normalized values were further referred as percentage of the control group (W6) for clarity.

Results

In general, the content of the gangliosides in lipid raft fractions isolated from cerebellum and midbrain did not show any significant difference between the experimental cohorts. However, the in the cortical area some differences were detected in GT1b and also a certain tendency can be noticed in GM1.

Content of GT1b ganglioside in cortical rafts exhibited variations between the experimental groups (p 0.0426, Kruskal-Wallis test). Comparisons between groups performed by Dunn's multiple comparisons test revealed that the cohort with a higher difference compared to the control group (W6) was the one comprised by old MPTP-treated animals (M14) (p= 0.1064) (Figure 9).

No significant differences were observed in the relative amount of GM1 between the study groups in any of the analysed areas, although a slight tendency to reduction after treatment was observed in cortex (p 0.0786, Kruskal-Wallis test) (Figure 9). The Dunn's multiple comparisons test pointed to the experimental group constituted by old MPTP-treated mice (M14) as the one with higher difference respect the control group (W6) (p= 0.1876), followed by young MPTP-treated animals (M6) (p= 0.2255 W6 *vs* M6).

In order to have an approximate idea of total gangliosides and taking into account that the four gangliosides analysed constitute the vast majority of total gangliosides in brain, we added together the densitometric values of all of them and performed the same normalization previously done (Figure 10). Results showed a significant difference in total gangliosides in raft fractions from cortex between experimental groups (p= 0.0199, Kruskal-Wallis test). Further comparison between groups revealed a strong tendency to reduction in total gangliosides after treatment, especially in aged animals (Dunn's multiple comparisons test: W6 *vs* M14 p= 0.0856; W6 *vs* M6 p= 0.1554). Therefore, the main alterations in ganglioside composition of LR fractions were found in the cortical area of the old and MPTP-treated mice (M14).

Results

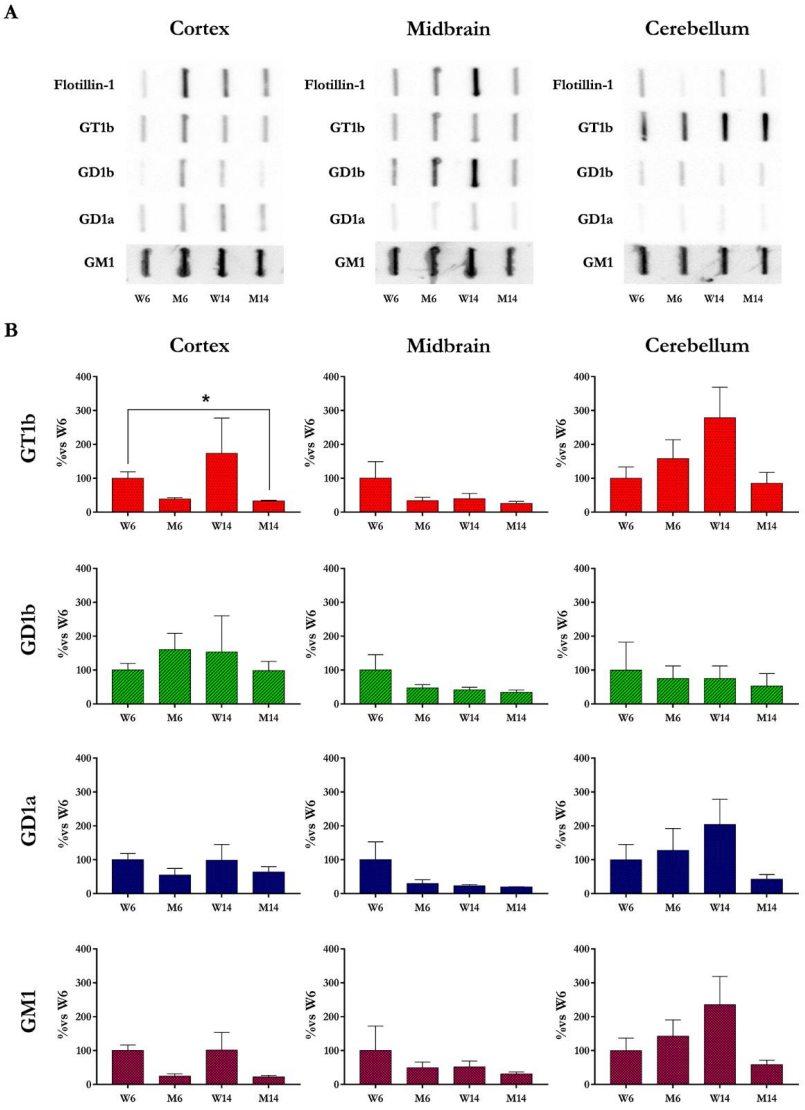

Figure 9. Distribution of main brain gangliosides in brain areas from the mouse cohorts. Lipid raft samples were transferred to PVDF membranes by slot blot and incubated with specific primary antibodies to detect gangliosides. A) Chemiluminescent detection of GM1, GD1a, GD1b and GT1b and the scaffolding protein Flotillin-1 from LR fractions from cortex, midbrain and cerebellum. B) Quantification of the gangliosides analysed was normalized using Flotillin-1 and then referred as percentage of the control group (W6) and compared to that control (W6: control 6 months, M6: MPTP treated 6 months; W14: control 14 months; M14: MPTP treated 14 months) (* $p<0.05$; Kruskal-Wallis test with Dunn's multiple comparison correction. N=4) Error bars represent SEM.

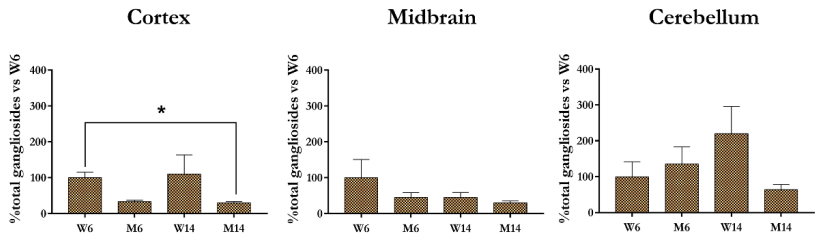

Figure 10. Total gangliosides from lipid raft fractions in cortex, midbrain and cerebellum. Densitometric values of the four gangliosides (GM1, GD1a, GD1b and GT1b) were added up and normalized against flotillin-1 and then referred as percentage of the control group (W6). Total gangliosides in lipid rafts from cortical area showed significant differences between the cohorts (W6: control 6 months, M6: MPTP treated 6 months; W14: control 14 months; M14: MPTP treated 14 months) (*p <0.05, Kruskal-Wallis test with Dunn's multiple comparison correction. N=4). Error bars represent SEM.

1.4. Protein alterations observed in lipid raft in response to MPTP treatment

One of the main goals of this work was analysing the possible alterations in lipid raft protein composition in response to MPTP treatment and aging. Therefore, we performed western blot analysis of both lipid raft and non-raft fractions obtained from cortex, midbrain and cerebellum of the experimental groups (W6, M6, W14 and M14). Blotted membranes were fixed in PFA immediately before blocking to avoid α-synuclein detachment from membrane and improve its immunodetection. Proteins analysed were selected attending to their actual or potential implications in development of PD according to our hypothesis. Both aggregated and monomeric forms of α-synuclein were analysed since it constitutes a key protein in PD. We were especially interested in the possible rearrangements in its distribution between LR and NR fractions and changes in its aggregation, as a factor related to the degree of toxicity. Additionally, several studies have shown a complex interaction between glutamate receptors mGluR5 and NMDAR2B, prion protein (PrPc) and α-synuclein that appears to be involved in cognitive impairment associated to PD (Diógenes et al., 2012; Ferreira et al., 2017; Urrea et al., 2018). For

this reason, we wanted to analyse the distribution of PrPc and glutamate receptors mGluR5, NMDAR2B. The ionotropic glutamate receptor 1 AMPA subtype (AMPA) and the metabotropic glutamate receptor 1 (mGluR1) were included in the study for comparison. In other line, voltage dependent anion channel (VDAC) has been demonstrated to be involved in neurotoxicity by amyloid-β (Fernández-Echevarría et al., 2014). Therefore, VDAC and APP distribution was also analysed as a relevant pathological comparison with other neurodegenerative proteinopathies in which "lipid raft aging" has been previously described (Fabelo et al., 2012).

The described proteins of interest were analysed by western blot as described above. Due to difficulties in normalization of protein values in the LR and NR fractions observed during the current study we opted for a double normalization. Proteins detected in LR fractions were normalized by flotillin-1 while proteins from NR fractions were normalized either by actin or tubulin-β. We chose to assume the LR-scaffolding protein flotillin-1 as a housekeeper since actin or tubulin did not appear in most samples from LR where other proteins were indeed detected. After this normalization, protein values were referred as percentage of the control group (W6) for clarification.

α-Synuclein was analysed using two different primary antibodies. Anti-α-synuclein [4D6] antibody from Abcam predominantly detected monomeric forms of the protein, so we limited to analyse the 16 kDa band obtained with this antibody. Then, membranes were reblotted to detect aggregated forms of the protein by incubation with anti-aggregated α-synuclein clone 5G4 antibody from Millipore. This antibody detected several bands of high molecular weight. The most evident ones were between 100 and 150 kDa (Figure 11). Quantification of aggregated α-synuclein included all the high molecular weight bands (Figure 11).

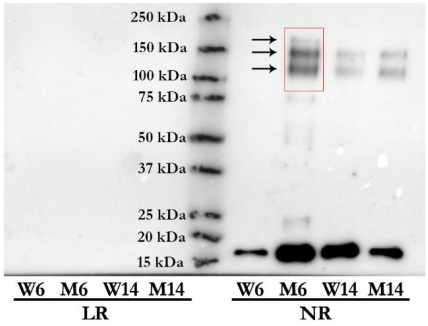

Figure 11. Representative image of α-synuclein detection by immunoblotting. Merged image between the colorimetric (visible) and chemiluminescent modes showing both the immunosignal and the molecular weight marker. Arrows indicate the most prominent high molecular weight bands and the red rectangle illustrates the quantified area. Notice that monomeric α-synuclein is saturated in this picture due to the effect of reblot to detect aggregated α-synuclein.

Due to previous works showing interaction between α-synuclein and GM1 ganglioside (Martínez et al., 2007), we expected to find this protein in LR fractions. However, our results showed a predominately distribution of α-synuclein in non-raft fractions across all areas and experimental groups in this study (Figure 12). A deeper analysis of this point will be cover in discussion section.

Densitometric values of α-synuclein, both monomeric and aggregated forms, were normalized using actin and then referred as percentage of the control group (W6). Percentage of aggregated α-synuclein versus total α-synuclein was also estimated using densitometric values of aggregated and monomeric forms (prior to their normalization against control) using the following formula:

$$\% = \frac{\text{aggregated}}{\text{aggregated} + \text{monomeric}} \times 100$$

Data were analysed by 2-way ANOVA establishing the area as one factor (cortex, midbrain and cerebellum) and the experimental groups (W6, M6, W14 and

M14) as the second factor. Results showed that, in general, there is an effect of the area in the content of α-synuclein. The multiple comparison test showed that for aggregated α-synuclein and the ratio of aggregated α-synuclein *vs* total α-synuclein, there was a significant higher content in cortex respect midbrain and cerebellum, while there were no differences between midbrain and cerebellum. Conversely, when analysing monomeric α-synuclein, there was no significant difference between cortex and the other areas investigated, although the midbrain was significantly higher than cerebellum. Table 5 summarises the *p*=s obtained after the Tukey's multiple comparison test between areas. Comparisons between areas were performed taking the mean values between the different experimental groups.

Tukey's multiple comparisons test results			
	Monomeric	Aggregated	Ratio aggregated *vs* total
Cortex *vs* Midbrain	ns	<0.0001	<0.0001
Cortex *vs* Cerebellum	ns	<0.0001	<0.0001
Midbrain *vs* Cerebellum	0.0112	0.0669	ns

Table 5. Summary of 2-way ANOVA *p*-values for multiple comparison test of α-synuclein content between different areas.

We did not find any statistical difference across the experimental groups in midbrain or cerebellum but cortical area exhibited a great increase in aggregated α-synuclein in response to both MPTP treatment and aging. In young treated animals (M6) mean value of aggregated α-synuclein shows an increase of 5 times respect the control (W6). In old animals, both treated or control that increment gets to 8-10 times higher (Figure 12B). In concordance with these data, estimation of the percentage of aggregated α-syn versus total α-syn shows similar increase after treatment and aging (Figure 12C). Content of the monomeric forms of α-synuclein were not significantly altered after treatment or aging.

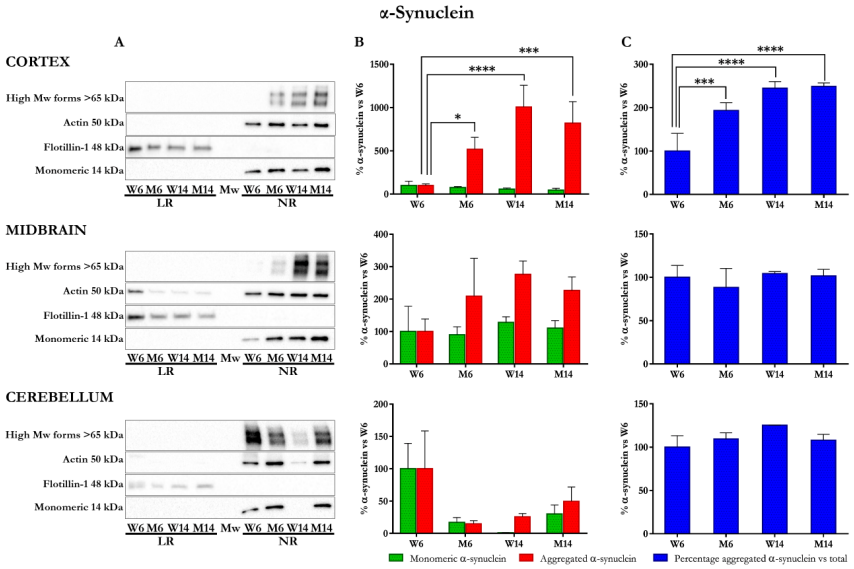

Figure 12. Analysis of α-synuclein distribution in LR and NR fractions. Lipid raft (LR) and non-raft (NR) samples were separated by SDS-PAGE, transferred to PVDF membranes and incubated with the specific primary antibodies. A) Chemiluminescent detection of α-synuclein, actin and flotillin-1 in LR and NR samples from the four experimental groups (W6: control 6 months, M6: MPTP treated 6 months; W14: control 14 months; M14: MPTP treated 14 months) in cortex, midbrain and cerebellum. Specific antibodies against both aggregated and monomeric α-synuclein were used to detect the different forms of this protein. NR fractions were normalised with actin and LR with flotillin-1. B) Quantification of monomeric (green) and aggregated (red) α-synuclein. C) Percentage of aggregated α-synuclein in comparison to total α-synuclein Data are referred to control group as 100% (*p <0.05, ***p<0.001, ****p <0.0001 Two-way ANOVA with Dunnett's multiple comparisons test. N=4). Error bars represent SEM.

PrPc distribution in LR and NR was also analysed. Results showed that PrPc is exclusively located in LR fractions in all areas studied. In cortical area ANOVA analysis showed a significant decrease in aged experimental group (W14) compared to the control (p= = 0.0033, Kruskal-Wallis with Dunn's multiple comparisons test). The observed decrease seams to affect also the MPTP treated groups, although it is not significant. No changes can be assessed in PrPc content in midbrain or cerebellum (Figure 13). For comparison of PrPc content between the different areas

of study two-way ANOVA was conducted. PrPc content in LR fractions from cortex was significantly lower than in midbrain or cerebellum, while there were no differences between these two areas (Table 6).

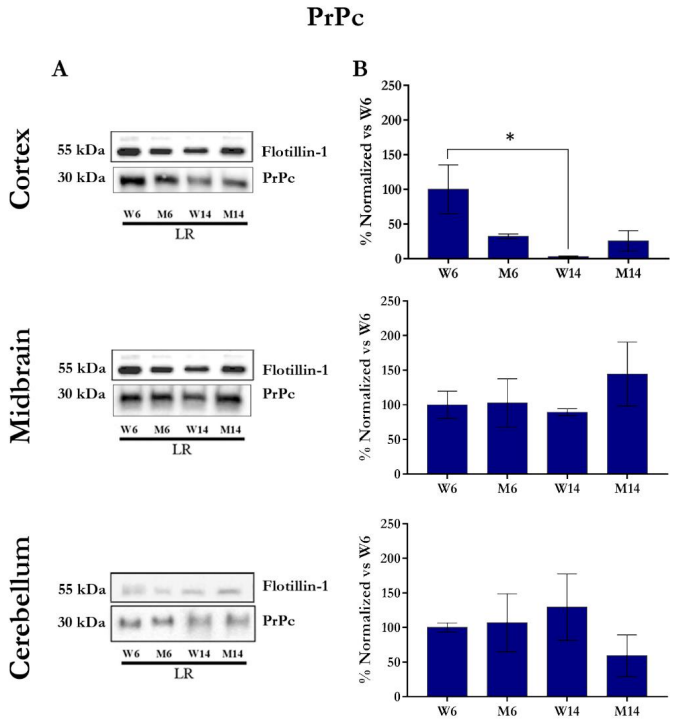

Figure 13. Analysis of prion protein (PrP) distribution in lipid raft (LR) fractions. Lipid raft samples were separated by SDS-PAGE, transferred to PVDF membranes and incubated with the specific primary antibodies. A) Chemiluminescent detection of PrPc and flotillin-1 from the mouse cohorts (W6: control 6 months, M6: MPTP treated 6 months; W14: control 14 months; M14: MPTP treated 14 months) in cortex, midbrain and cerebellum. B) Quantification of PrPc. Data are normalised by flotillin-1 and referred to control group (W6) as 100% Error bars show SEM. (*p <0.05, Kruskal-Wallis with Dunn's multiple comparisons test. N=4).

Analysis of VDAC showed the expected location exclusive to LR fractions. When analysing the effect of aging or MPTP treatment we found a significant decrease in cortical VDAC in young treated and old not treated animals, but not in

those with both factors (M14) (Figure 14). No changes were detected between the experimental groups either in midbrain or cerebellum. No alterations were found when comparing the different areas of study (Table 6).

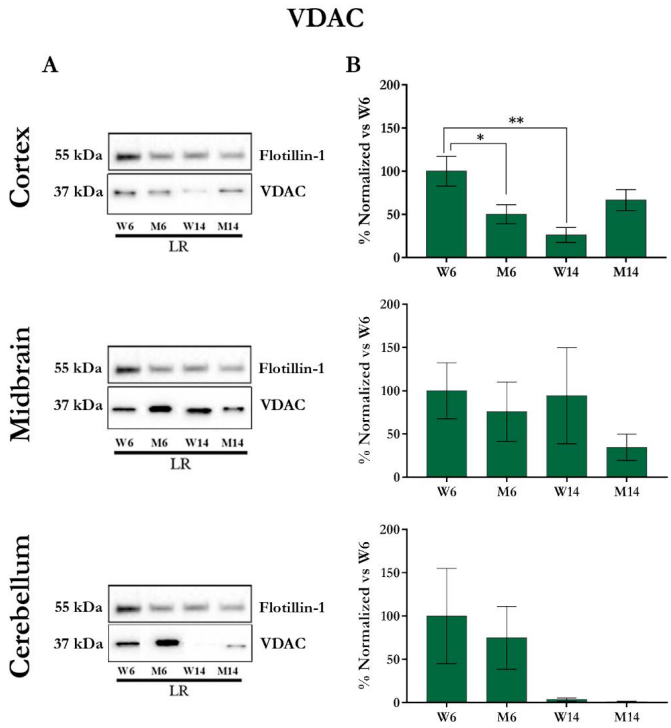

Figure 14. Analysis of voltage dependent anion channel (VDAC) distribution in lipid raft (LR) fractions. Lipid raft samples were separated by SDS-PAGE, transferred to PVDF membranes and incubated with the specific primary antibodies. A) Chemiluminescent detection of VDAC and flortillin-1 from the four experimental groups (W6: control 6 months, M6: MPTP treated 6 months; W14: control 14 months; M14: MPTP treated 14 months) in cortex, midbrain and cerebellum. B) Quantification of VDAC normalized by flotillin-1 and referred to control group as 100% (*p <0.05, **p<0.01. Kruskal-Wallis with Dunn's multiple comparisons test. N=4). Error bars represent SEM.

Amyloid precursor protein (APP) was predominately distributed in NR fractions. Even though some LR samples appeared to contain some APP, the content of this proteins was not significant enough for the analysis. Therefore, we

only quantified APP amount present in NR fractions for consistence. No changes were detected in APP values from NR samples between the experimental groups at any of the study areas (Figure 15). Comparison between areas showed a lower content of APP in cerebellum (Table 6).

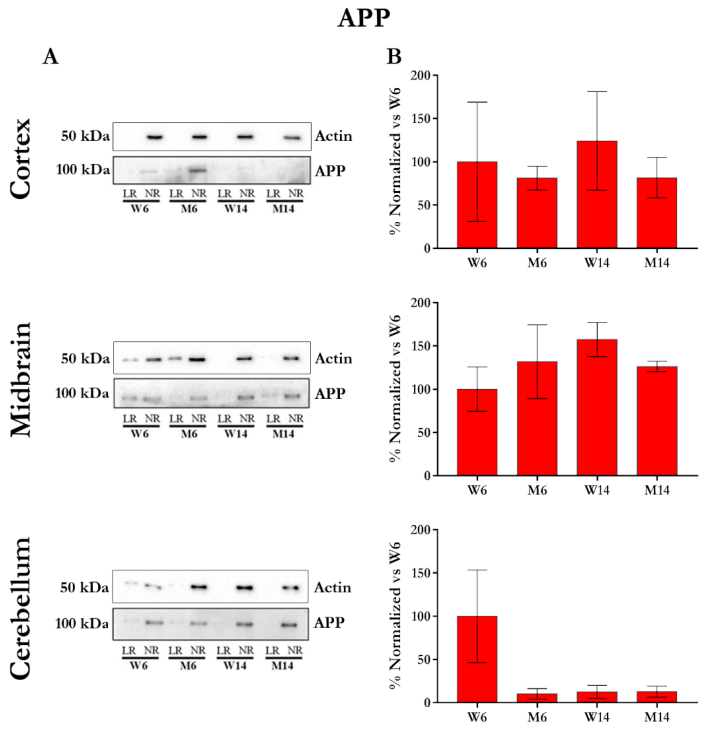

Figure 15. Analysis of amyloid precursor protein (APP) distribution in lipid raft (LR) and non-raft (NR) fractions. Samples were separated by SDS-PAGE, transferred to PVDF membranes and incubated with the specific primary antibodies. A) Chemiluminescent detection of APP in LR and NR fractions from the experimental groups (W6: control 6 months, M6: MPTP treated 6 months; W14: control 14 months; M14: MPTP treated 14 months) in cortex, midbrain and cerebellum. B) Quantification of APP in NR fractions. Data are normalised by actin and referred to control group as 100%. (Kruskal-Wallis with Dunn's multiple comparisons test. N=4). Error bars show SEM.

Tukey's multiple comparisons test results			
	PrPc	VDAC	APP
Cortex *vs* Midbrain	0.0054	ns	ns
Cortex *vs* Cerebellum	0.0195	ns	ns
Midbrain *vs* Cerebellum	ns	ns	0.0020

Table 6. Summary of 2-way ANOVA *p*-values for multiple comparison test of PrPc, VDAC and APP content between the different areas.

Analysis of glutamate receptors by western blot presented several difficulties, mainly due to their high molecular weight (over 250 kDa for mGluR5 dimer). Therefore we opted for analysing samples by slot blot. LR and NR samples were diluted in transfer buffer and transferred to PVDF membranes. Six replicate membranes with the same volume of sample were loaded to minimize variations.

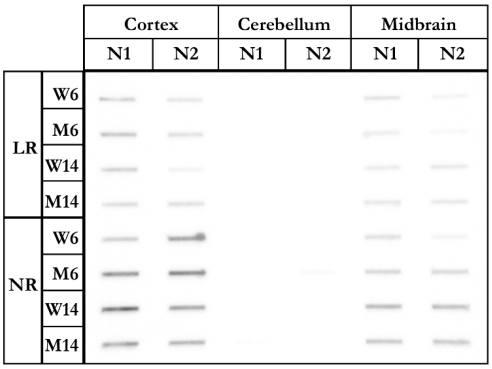

Figure 16. Representative scheme on the setup of slot blot assay performed. Lipid raft (LR) and non-raft (NR) fractions of all areas analysed by slot blot were loaded by duplicate (N1 and N2) in the same membrane. Image corresponds to mGluR5 chemiluminescent immunodetection.

Results

Each replicate was incubated with a different primary antibody: mGluR1, mGluR5, AMPA, NMDAR2B, flotillin-1 and tubulin-β. The setup allowed analysing in the same membrane two samples for LR and NR fractions from the four mouse cohorts and the three areas analysed in this study (Figure 16). LR samples were normalised against flotillin-1, while tubulin-β was used in NR samples for the same purpose. Values are expressed as optical density per square millimetre (OD/mm²).

In the first instance, we wanted to determine the distribution of the analysed receptors among the different areas of study. For this reason we made a simple estimation of total content for each glutamate receptor in each area by adding up the values obtained for LR and NR fractions in the control group (W6). This analysis indicated a different distribution of the receptors in the three brain regions. Noticeably, the receptors content in cerebellum changed widely in comparison to both cortex and midbrain. In contrast, no differences were found between cortex and midbrain for the different glutamate receptors. AMPA and mGluR1 presented a higher expression in cerebellum, while mGluR5 remained undetectable. For NMDAR2B no significant change was observed, but again, cerebellum presented a tendency to a lower content in comparison with other areas (Figure 17, Table 7).

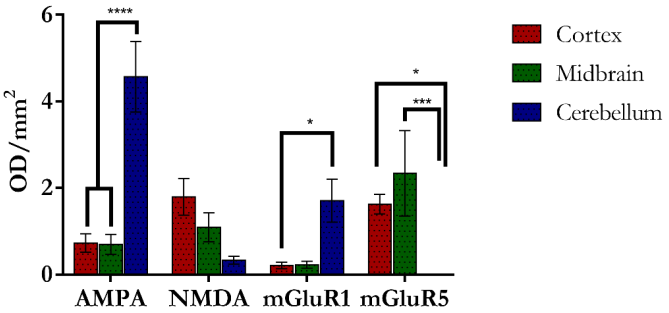

Figure 17. Comparison of total expression for glutamate receptors between cortex, midbrain and cerebellum analysed by slot blot. Graph was elaborated with the quantification from figures 18 to 21. Comparison was established using the control group (W6). Values were estimated as the sum of densitometric values of lipid raft and non-raft fractions and expressed as optical density per square millimetre (OD/mm²) (Two-way ANOVA with Tukey's multiple comparisons test. N=4). Error bars represent SEM.

Tukey's multiple comparisons test results				
	AMPA	NMDAR2B	mGluR1	mGluR5
Cortex *vs* Midbrain	0.9985	0.4971	0.9998	0.4946
Cortex *vs* Cerebellum	<0.0001	0.0556	0.0497	0.0293
Midbrain *vs* Cerebellum	<0.0001	0.4511	0.0520	0.0010

Table 7. Summary of 2-way ANOVA *p*-values for multiple comparison test of glutamate receptors distribution between areas in the control group.

Once we have assessed the differences in glutamate receptors expression between areas we wanted to analyse their distribution in LR and NR fractions and the possible effects of aging and MPTP treatment. Using the densitometric values for LR and NR fractions two new parameters were estimated and compared between experimental groups in the study areas. Firstly, the total amount of the glutamatergic receptor was estimated by simply adding up values from LR and NR (Panel C in Figure 18 to Figure 21). In order to have a clear view of the predominant distribution of the receptors among the LR and NR and to facilitate the analysis of the possible changes in this distribution, we estimated the ratio LR/total, using the densitometric values for LR and the previously estimated sum of LR and NR. In the graphical representation a dotted line was included at the value of 50%, indicating that in the cases were the value is lower than that, the distribution is predominant to the NR fractions and in those higher than the indicated dotted line the distribution is of the receptor is mainly to the LR fraction (Panel D Figure 18 to Figure 21).

In general, all the glutamate receptors analysed were mainly located at NR fractions. With little exceptions, LR content of glutamate receptors was significantly lower than NR content (p=<0.05, Mann Whitney test) and in many cases almost undetectable with the protocol performed. This lower distribution to LR fractions is clearly shown when the ratio of the corresponding receptor in LR versus the total content is estimated (Panel D, Figure 18 to Figure 21). In cerebellum, LR content of

Results

AMPA shows a tendency contrary to the previously described, where LR content appears to be higher than NR, however this result is not statistically significant (p= = 0.1143, Mann Whitney test) (Figure 18D). The amount of the metabotropic glutamate receptor 5 (mGluR5) in LR fractions is more evident. In cortex still presents a significantly lower content than in NR, but in midbrain the abundance in LR and NR is similar (p = 0.4857, Mann Whitney test) (Figure 21).

Analysis of the effect of aging or MPTP treatment over glutamate receptors revealed very little variations. NMDAR2B or mGluR1 did not exhibit any difference at all after aging or treatment (Figure 19, Figure 20). For AMPA, we found a severe diminution in cerebellar LR fractions in the old treated experimental group, M14 (Figure 18). Midbrain mGluR5 content in NR fractions shows a decrease in all treated or aged mice in comparison with the control group (Figure 21).

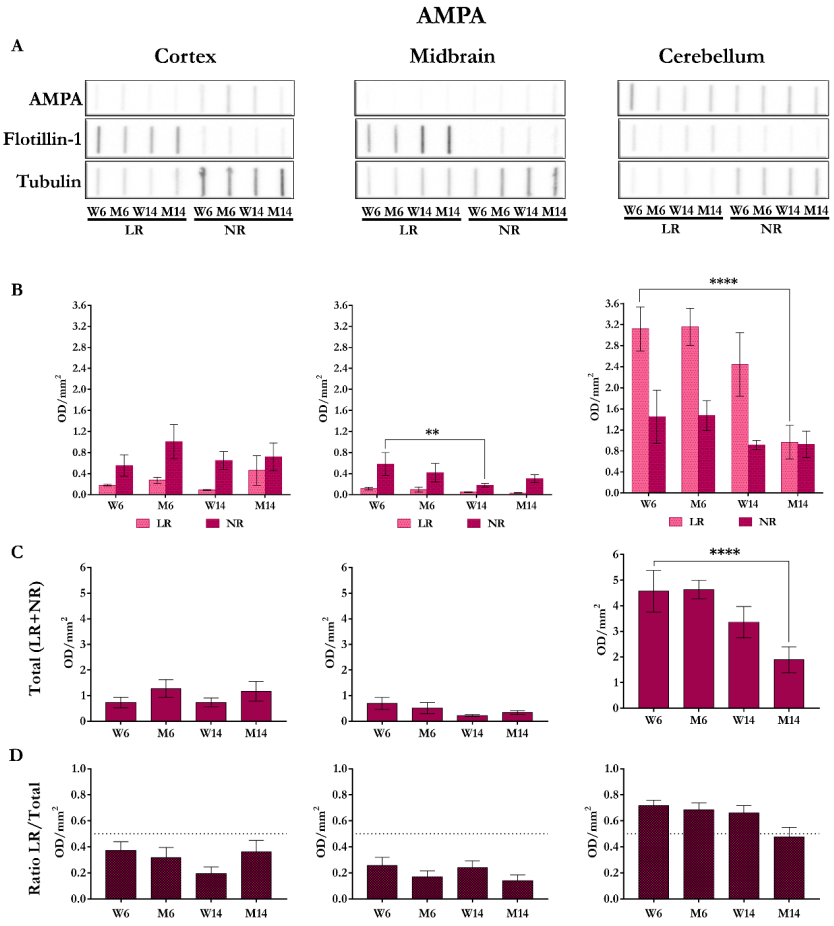

Figure 18. Analysis of ionotropic glutamate receptor AMPA subtype. Lipid raft (LR) and non-raft (NR) samples were transferred to PVDF membranes by slot blot and incubated with specific primary antibody. A) Chemiluminescent detection of AMPA, flotillin-1 and tubulin analysed in LR and NR fractions from cortex, midbrain and cerebellum of the four experimental groups (W6: control 6 months, M6: MPTP treated 6 months; W14: control 14 months; M14: MPTP treated 14 months). B) Quantification of AMPA normalised against flotillin-1 in LR samples and tubulin in NR samples. C) Estimations of total AMPA calculated as the addition of values from LR and NR. D) Ratio of AMPA found in LR fractions *vs* total AMPA (**p <0.01, ****p <0.0001 Two-way ANOVA with Dunnett's multiple comparisons test. N=4). Error bars represent SEM.

Results

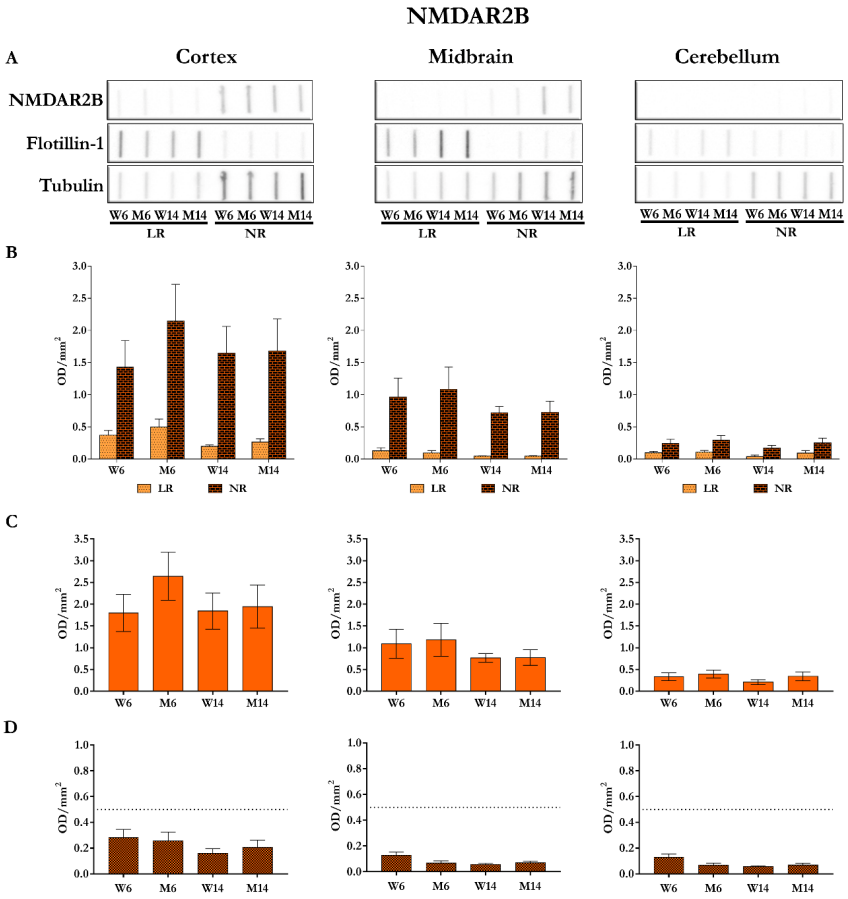

Figure 19. Analysis of ionotropic glutamate receptor NMDAR2B subtype. Lipid raft (LR) and non-raft (NR) samples were transferred to PVDF membranes by slot blot and incubated with specific primary antibody. A) Chemiluminescent detection of NMDAR2B, flotillin-1 and tubulin analysed in LR and NR fractions from cortex, midbrain and cerebellum of the mouse cohorts (W6: control 6 months, M6: MPTP treated 6 months; W14: control 14 months; M14: MPTP treated 14 months). B) Quantification of NMDAR2B normalised against flotillin-1 in LR samples and tubulin in NR samples. C) Estimations of total NMDAR2B calculated as the addition of values from LR and NR. D) Ratio of NMDAR2B found in LR fractions *vs* total NMDAR2B. (No statistical differences are found between experimental groups. Two-way ANOVA with Dunnett's multiple comparisons test. N=4). Error bars represent SEM.

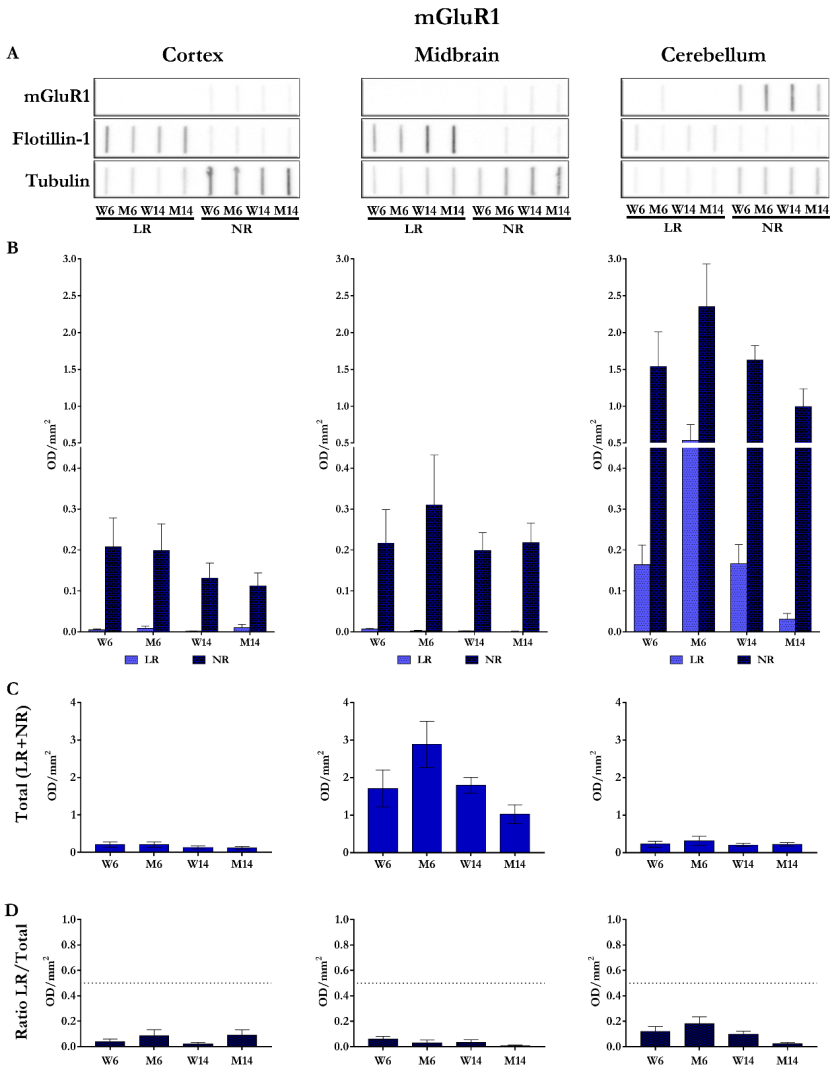

Figure 20. Analysis of metabotropic glutamate receptor 1. Lipid raft (LR) and non-raft (NR) samples were transferred to PVDF membranes by slot blot and incubated with specific primary antibody. A) Chemiluminescent detection of mGluR1, flotillin-1 and tubulin analysed in LR and NR fractions from cortex, midbrain and cerebellum of the experimental groups (W6: control 6 months, M6: MPTP treated 6 months; W14: control 14 months; M14: MPTP treated 14 months). B) Quantification of mGluR1 normalised against flotillin-1 in LR samples and against tubulin in NR samples. C) Estimations of total mGluR1 calculated as the addition of values from LR and NR. D) Ratio of mGluR1 found in LR fractions *vs* total mGluR1 (No statistical differences are found between experimental groups. Two-way ANOVA with Dunnett's multiple comparisons test. N=4). Error bars represent SEM.

Results

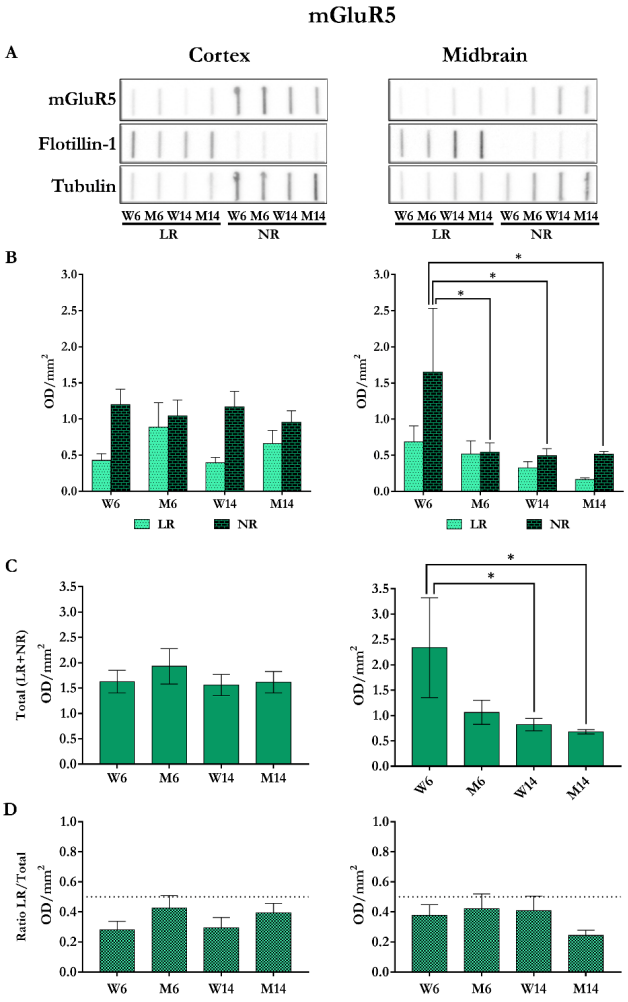

Figure 21. Analysis of metabotropic glutamate receptor 5. Lipid raft (LR) and non-raft (NR) samples were transferred to PVDF membranes by slot blot and incubated with specific primary antibody. A) Chemiluminescent detection of mGluR5, flotillin-1 and tubulin analysed in LR and NR fractions from cortex, midbrain and cerebellum of the four experimental groups (W6: control 6 months, M6: MPTP treated 6 months; W14: control 14 months; M14: MPTP treated 14 months). B) Quantification of mGluR5 normalised against flotillin-1 in LR samples and against tubulin in NR samples. C) Estimations of total mGluR5 calculated as the addition of values from LR and NR. D) Ratio of mGluR5 found in LR fractions *vs* total mGluR5 (*$p < 0.05$ Two-way ANOVA with Dunnett's multiple comparisons test. N=4). Error bars represent SEM.

Remarkably, no significant differences were found in the ratio LR *vs* Total for any of the receptors analysed in any area as a consequence of aging or treatment. This indicates that the experimental conditions did not induce a shift in the distribution among LR and NR fractions.

1.5. Post-translational modifications of α-synuclein

One of the most relevant post-translational modification observed in α-synuclein is the phosphorylation at Ser129 (Barrett & Greenamyre, 2015). This seems to be the most pathologically relevant form of α-synuclein since it has been highly associated with aggregation and Lewy body generation. Considering the abundance of aggregated forms of α-synuclein found, especially in cortical area, of aged and MPTP treated mice, we decided to analyse the phosphorylation of α-synuclein at Ser129. Non-raft fractions from cortex, midbrain and cerebellum of the mouse cohorts (W6, M6, W14 and M14) were analysed by two-dimensional electrophoresis using immobilized pH gradient strips pH 3-10 for the first dimension and 12.5% SDS-polyacrylamide gels for the second dimension resolution. Membranes were fixed in PFA and blocked with 5% BSA in TBST. Membranes were first incubated with anti-pSer129 α-synuclein antibody to detect only the phosphorylated α-synuclein at Ser129 and then reblotted with anti α-synuclein (4D6 clone) antibody to detect other forms of α-synuclein, including both monomeric and high molecular weight forms.

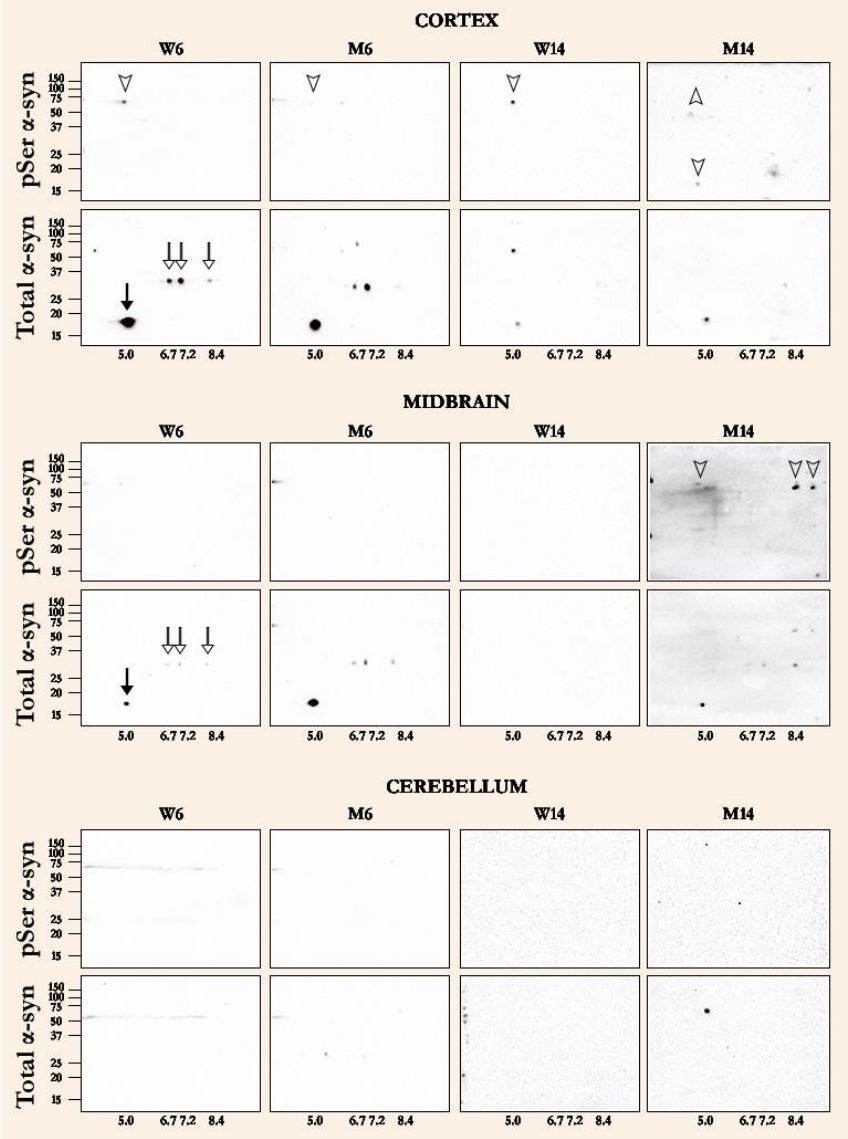

Figure 22. 2-D immunoblotting of non-raft (NR) fractions showing the pattern of isoforms of α-synuclein in cortex, midbrain and cerebellum. Samples were separated by isoelectrofucusing followed by SDS-PAGE. Proteins were transferred to PVDF membranes and incubated first with phosphorylated α-syn at Ser129 (pSer α-syn, upper panels) and then with anti α-syn 4D6 clone antibody (lower panels). Arrows indicate the predominant non-phosphorylated forms of α-syn, monomeric (solid arrow) or aggregated (hollow arrows). Arrowheads indicate phosphorylated high molecular weight forms. Values in abscissa indicates the estimated isoelectric point for the different isoforms of α-syn.

Results

Almost no signal was detected in NR fractions from cerebellum at any of the experimental groups (Figure 22, bottom). In the control group (W6) from cortex and midbrain, total α-synuclein was resolved in 4 predominant isoforms with estimated isoelectric points (p*I*) of 5.0, 6.7, 7.2 and 8.4 (Figure 22, left). The most abundant corresponds to the p*I* of 5.0 (solid arrow), which represents the native monomeric isoform. This isoform was attenuated in the aged and MPTP treated cohorts, in parallel with the increased accumulation of higher MW α-syn isoforms (arrowheads). Phosphorylated α-syn appears as high MW forms, especially in the midbrain of M14 cohort (Figure 22, middle right).

2. Study of energy metabolism in a cellular model of Parkinson disease

After analysing the effects of MPTP in a mouse model of PD, we wanted to get further understanding of the effect on the energy metabolism of this neurotoxic compound. With that aim and taking into account that the cortical area is key in this study, we produced primary cultures of cortical neurons which provide a feasible approach for the metabolic analysis using different experimental procedures. Although there is wide evidence that demonstrates that MPTP selectively blocks the complex I in the respiratory chain of the mitochondria, to the best of our knowledge, the characterization of MPTP effect on energy metabolism in cortical neurons have not been performed yet. Since primary cultures do not contain the glial cells that in primates and rodents transform MPTP into the toxic metabolite MPP^+, we opted for directly using the metabolite in the following assays instead of MPTP. We perform this metabolic characterization in two different conditions. First in resting conditions, in the absence of any stimulus and then simulating the physiological conditions developed by the excitatory neurotransmitter glutamate.

In both conditions, the metabolic characterization was focused on three main studies. First of all, the mitochondrial respiration and all the parameters derived from the oxygen consumption rate (OCR) that can be measured with the Extracellular Flux Analyzer Instrument (XF24, Agilent/Seahorse Biosciences). For simplicity, we will refer to this study as "Seahorse assay". The second study consisted on measurement of the lactate production as an indicator of glycolytic pathway diverted away from oxidative phosphorylation. Finally, the determination of total ATP production by CellTiter-Glo® Luminescent Cell Viability Assay (Promega). All these studies were conducted using three experimental groups of primary cortical neurons:

- Neurons treated with MPP^+ for 24 hours (MPP^+ 24h) to evaluate the effects on the long term.

- Neurons treated during 4 hours followed by 20 hours of recovery without the presence of the neurotoxic (MPP^+ 4h) to evaluate whether the neurons were able to recover of neurotoxicity.
- A control group treated with saline.

In order to characterize the effect of MPP^+ on energy metabolism, we first search for a non-lethal dose that allowed producing the effect while neurons stay alive. This determination is of great importance since the following assays require neurons to be alive in a high percentage for obtaining accurate results.

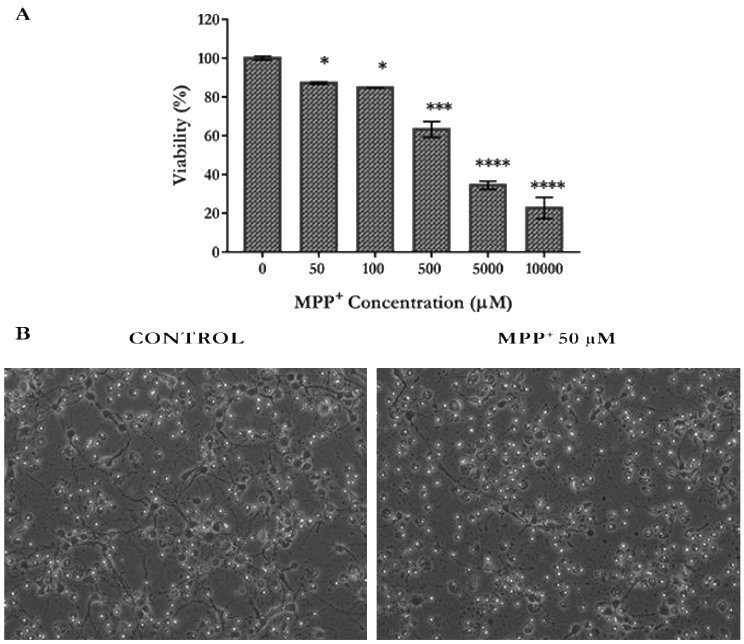

Figure 23. Effect of MPP^+ on neuronal viability. Cultured neurons were treated with different doses of MPP^+ and after 24 hours viability rate was estimated as percentage of alive neurons/total. A) Graph showing the reduction on viability rate as the concentration of MPP^+ increases. Error bars show SEM (* $p<0.05$, *** $p<0.001$, **** $p<0.0001$; Kruskal-Wallis test with Dunn's correction for multiple comparisons. N=3). B) Photomicrograph in light field of control and MPP^+ treated neurons. No major morphological differences are observed between control neurons and those treated with 50 µM MPP^+ for 24 hours.

Results

Viability assays were conducted after 24 hour treatment at different doses of MPP^+ ranging from 50 μM to 10 mM. For each MPP^+ dose 3 replicate wells were analysed and for each well at least 3 fields were counted. As expected, higher reduction on viability rate was observed at the higher concentrations, obtaining results consistent with a dose dependent mortality. At 50 μM MPP^+ the viability rate was 87% and neurons morphology remain not visibly altered (Figure 23). This significant but not severe decrease in viability provides an optimal dose to perform the following metabolic characterization. Thus, we selected that dose of 50 μM MPP^+ for the following experiments.

2.1. MPP^+ effect in resting/standard conditions

In the first instance, we performed the characterization of energy metabolism in the different experimental groups of primary neurons in the absence of any physiological perturbation. *Seahorse* assay to measure the mitochondrial respiration consisted on the basic assay in which OCR measurements alternated with progressive injections of oligomycin, FCCP and antimycin. Assays were repeated three times and each one included 7-8 wells for each experimental condition (control, MPP^+ 24h and MPP^+ 4h).

A severe impairment on mitochondrial respiration was found in neurons treated with MPP^+ for 24 hours, while those treated only for 4 hours appeared less severely affected (Figure 24). Basal respiration and ATP coupled respiration were dramatically reduced and almost completely blocked in response to long exposure to the neurotoxic. Also, the maximal respiration was greatly reduced in that group. For the neurons with the shorter exposure to MPP^+, reduction in these parameters, although significant, was less pronounced and showed intermediate values between neurons treated for 24 hours and controls. The spare respiratory capacity was also decreased in response to MPP^+ treatments. However, in contrast with the previously described parameters, the reduction was more marked in those treated for the shorter period.

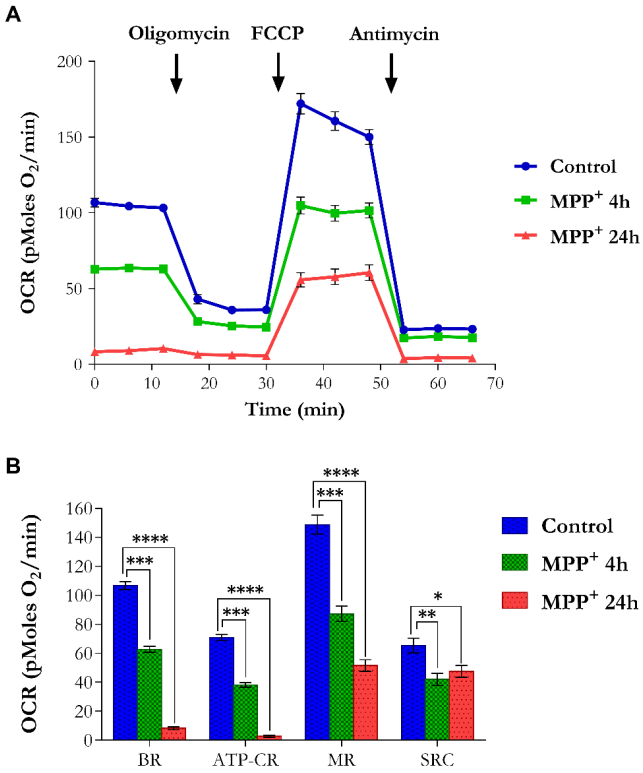

Figure 24. Effect on the mitochondrial respiration of MPP⁺ exposure. Neurons were seeded on XF24 cell culture microplates and MPP⁺ treatments performed. A) Oxygen consumption rate (OCR) measures in real time in response to sequential injections of oligomycin, FCCP and antimycin. B) Metabolic parameters derived from OCR measurements; basal respiration (BR), ATP- coupled respiration (ATP-CR), maximal respiration (MR) and spare respiratory capacity (SRC). Error bars show SEM (* p<0.05, *** p<0.001, **** p<0.0001; Kruskal-Wallis test with Dunn's correction for multiple comparisons N=3).

Since we found such severe impairment in the mitochondrial respiration of MPP⁺-treated neurons, we searched for alternative energy sources. The lactate production and release to the medium was assessed as an indicator of glycolytic flux. MPP⁺ treatments were performed for either 4 or 24 hours. Each experiment included two replicated wells for each experimental group. Immediately before

starting the lactate assay media was replaced and following that point, aliquots of media were recovered every two hours. As expected, the lactate concentration in the medium increased with time of exposure in all experimental groups. Neurons treated with MPP^+ for 24 hours showed a dramatic increase in lactate production compared to control neurons or those treated for shorter time (Figure 25). This result indicates a marked shift in to the glycolytic pathway in the neurons when the mitochondria are blocked.

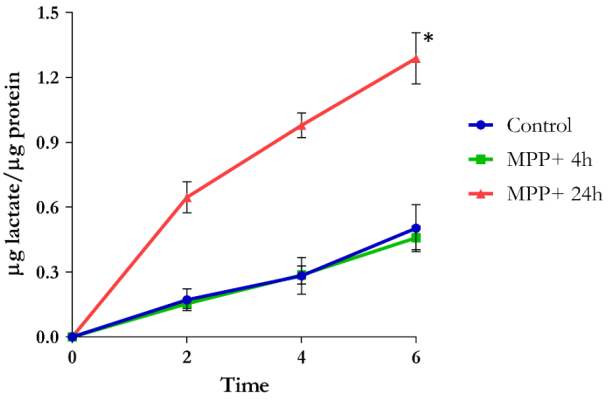

Figure 25. Lactate concentration in medium from neurons exposed to MPP^+. Neurons were seeded on M6 plates and treatments with MPP^+ performed. At the moment of the assay media was replaced with fresh one and aliquots were recovered after 2, 4 and 6 hours. A higher lactate production is observed in response to longer exposure to MPP^+. Error bars show SEM (* p<0.05; Kruskal-Wallis test with Dunn's correction for multiple comparisons. N=3).

Finally, in order to get a general view of the energetic status of the cultured neurons in response to MPP^+, quantification of total ATP production was performed. Each assay included 8 wells for each experimental group and the additional controls. Results showed a drastic reduction on ATP levels of neurons treated with MPP^+ as compared to controls, being more pronounced on those with the longer exposures (Figure 26).

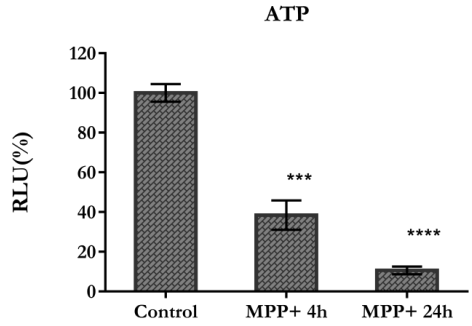

Figure 26. ATP levels on the different study groups. Cells were seeded on M96 plates and MPP^+ treatments were performed as corresponding. For ATP quantification media was replaced by the CellTiter-Glo® reagent and luminescence was measured. Values are expressed in relative luminescence units (RLU) and normalized against control. Error bars show SEM (*** $p<0.001$, **** $p<0.0001$; Kruskal-Wallis test with Dunn's correction for multiple comparisons N=3).

Overall, the characterization of energy metabolism in neurons treated with the neurotoxic metabolite MPP^+ indicates that the blockade of mitochondria is compensated with an increase in the glycolytic pathway, but this compensation is not enough to maintain the normal ATP levels.

2.2. MPP^+ effect under excitatory conditions

The severe impairment in mitochondrial respiration previously demonstrated in response to MPP^+ exposure contrasts with the low mortality observed in these neurons. However, *in vivo* MPP^+ is known to produce a very different result, with significant depletion of neurons affected. A possible explanation for this difference may reside in the physiological challenges that neurons experience *in vivo*. To evaluate this possibility we tried to reproduce such conditions. Glutamate constitutes the main excitatory neurotransmitter in brain (Zhou & Danbolt, 2014). Combined treatments of MPP^+ and glutamate were performed on primary cortical

neurons to determine whether a physiological challenge may exacerbate the neurotoxic effect of MPP^+ previously demonstrated.

First of all, viability assays to determine a suitable dose of glutamate were performed. We wanted to know the relative effect on viability at the different doses of glutamate for further comparison when combined treatments with MPP^+ would be performed. After 20 minute treatment with the different doses of glutamate, media was replaced to eliminate the neurotransmitter. Viability rates decreased rapidly at concentrations between 1 and 10 µM. Higher concentrations did not longer reduce viability (Figure 27).

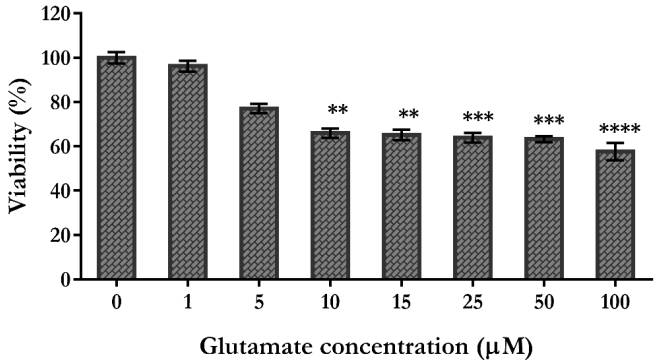

Figure 27. Viability rates in response to different doses of glutamate. Cells were seeded on M96 plates. After 24 hours glutamate treatments were performed for 20 minutes. Viability was determined by calcein/propidium iodide uptake assay and viability rates were normalized to control without glutamate. Error bars show SEM (** p<0.01, *** p<0.001, **** p<0.0001; Kruskal-Wallis test with Dunn's correction for multiple comparisons N=3).

Mitochondrial respiration in response to glutamate treatment was evaluated. The first series of experiments consisted on a single glutamate injection for a final concentration of 10 µM followed by injections of oligomycin, FCCP and antimycin. This experimental design allowed determining the main respiratory parameters in response to a moderate dose of glutamate and comparing those between the

different MPP^+ treatments. Control neurons showed a higher basal respiration. Therefore, cell respiration linked with ATP production was also higher compared to treated neurons. This difference was also higher in the neurons treated for the longer period. However, the increase in the respiration in response to glutamate injection was not different between the neurons treated with MPP^+ for 24 hours or controls (Figure 28).

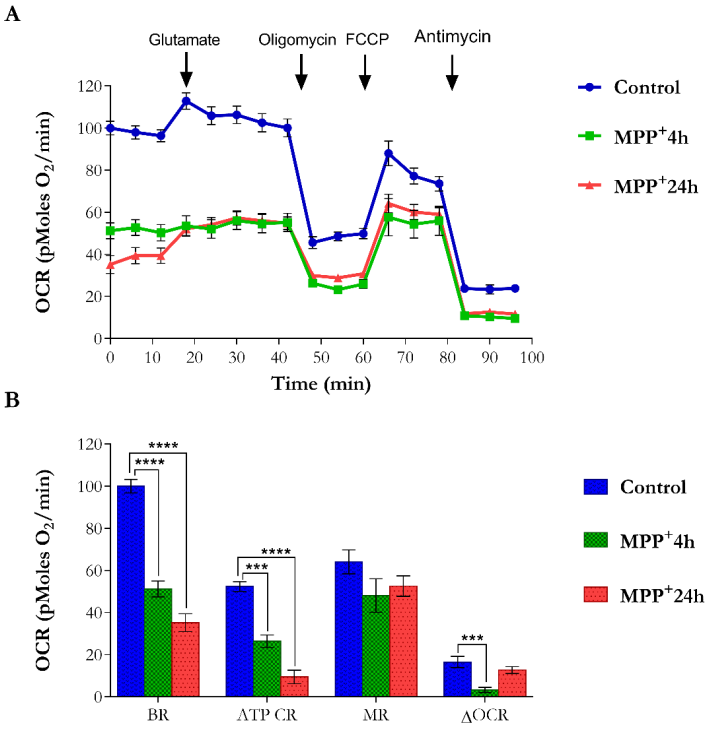

Figure 28. Mitochondrial respiration in response to glutamate and MPP^+. Arrows indicate glutamate injections. Oligomycin, FCCP and antimycin injections were performed as explained in Figure 24. A) Respiration in real time after 10 µM glutamate. Values are normalized to basal respiration of control. B) Metabolic parameters derived from oxygen consumption rate (OCR) quantification. Δ OCR represents OCR increase in response to glutamate. Error bars show SEM (***p<0.001, **** p<0.0001; Kruskal-Wallis test with Dunn's correction for multiple comparisons N=3).

Results

In a second series of experiments consecutive injections of glutamate accounting for 10, 50 and 100 μM were realized followed by oligomycin injection. With this design, we aimed to evaluate the ability to increase the respiration in response to an accumulated physiological challenge. Again, control neurons exhibited a higher basal respiration (Figure 29A) and the values of ATP coupled respiration were always higher in the control neurons, independently of the dose of glutamate. The MPP^+ treated neurons showed a reduction in the respiration linked to ATP production that was higher in those neurons treated for the longer period of time (Figure 29B). None of the experimental groups showed an increase in the respiratory rate after exposure to 100 μM glutamate. Interestingly, the ability to increase the oxygen consumption in response to the glutamate administration was lower in the neurons treated for 24 hours, which were able to increase their respiration only in response to the first glutamate injection at a concentration of 10 μM but not in the following ones. In contrast, control or 4 hours treated neurons were able to increase it also when the glutamate increased up to 50 μM (Figure 29C).

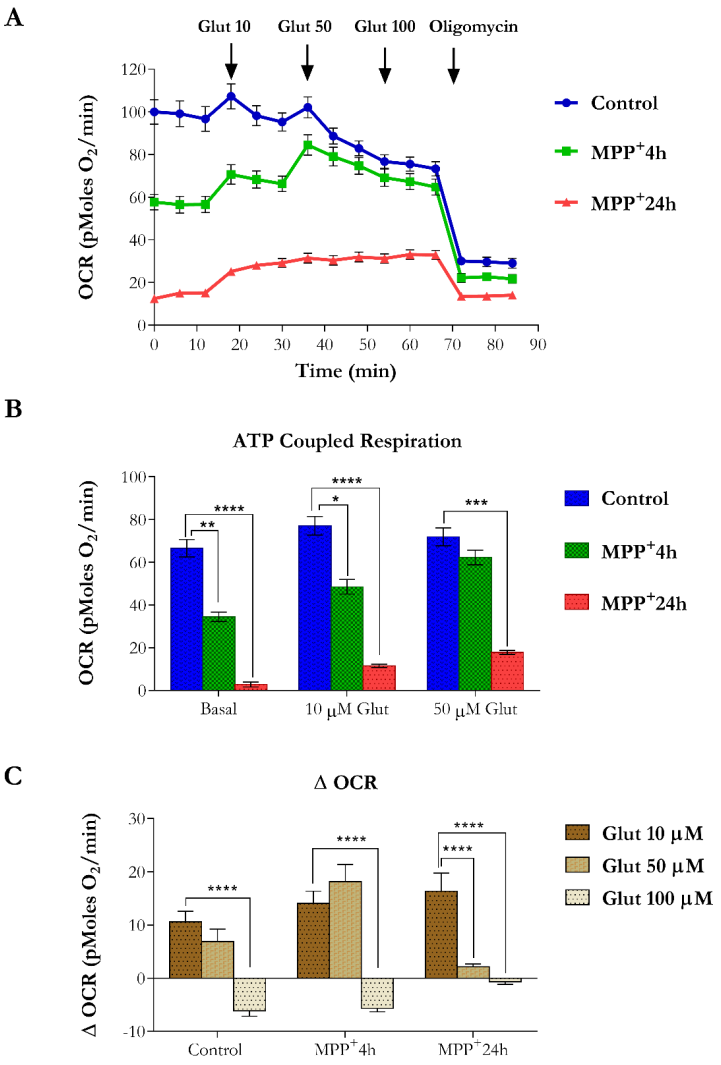

Figure 29. Mitochondrial respiration in response to glutamate injections of increasing concentration: 10, 50 and 100 µM in combination with MPP⁺. Oxygen consumption rate (OCR) of cultured neurons from the different experimental groups was measured after the sequential injection of growing glutamate concentrations. Arrows indicate glutamate injections. After glutamate injections only oligomycin was injected. A) Respiration in real time after successive glutamate injections. B) ATP coupled respiration at the different concentrations of glutamate, derived from the OCR quantification in A. C) OCR increment in response to each glutamate injection. Error bars show SEM (*p<0.05, ** p<0.01, ***p<0.001, **** p<0.0001; Kruskal-Wallis test with Dunn's correction for multiple comparisons N=3).

Results

Similarly to the characterization performed in resting conditions, lactate quantification was performed for the combined treatments of MPP^+ and glutamate to evaluate the role of the physiological challenge in the damaged neurons and their ability to shift for an alternative energy source. Treatments with MPP^+ were performed for the corresponding period right before the assay. At the beginning of the experiment the medium was replaced and the first set of aliquots was collected after 1 hour. Immediately after collecting this first aliquot, glutamate was added in a concentration of 50 μM and further aliquots were collected at 2, 4 and 6 hours. A higher lactate production was observed in neurons treated with MPP^+ for 24 hours compared the other experimental groups similarly to the results obtained in resting conditions. An interesting result is observed when analysing the effect of glutamate on lactate production in the different experimental groups. Neurons increase their lactate production in response to the physiological challenge exerted by glutamate and this capacity to respond decreases in response to the MPP^+ damage. This phenomenon can be observed as in intact control neurons lactate production was increased in response to glutamate. The mild damage produced by 4 hours MPP^+ treatment results in a non-statistically significant tendency to increase such production. Finally, the 24 hours treated group showed an opposite effect, presenting a decrease in lactate after the glutamate exposure (Figure 30).

Finally, determination of ATP levels was performed to obtain a general scenario of the energy state. Quantification was conducted immediately after 20 minute treatment with glutamate at the different concentrations previously used, this is, control without glutamate, 10 μM and 50 μM. A decrease in ATP levels was observed in response to both MPP^+ and glutamate (Figure 31). Some differences were detected at the two glutamate doses in the presence of the neurotoxic. However, the results are not fully conclusive taking into account the higher demand of ATP triggered by glutamate, thus partially masking the real ATP production. The methodology used reports the end-point ATP levels, not allowing to detect the real time changes in response to glutamate stimulation.

Overall, these results demonstrate that neurons are able to activate other metabolic pathways in response to the MPP^+ insult, thus ensuing cell survival. However, in conditions that require a higher activation of metabolism to produce an adequate response, like in glutamate stimulation, cortical neurons damaged by MPP^+ are not able to exhibit a response according to the requirements.

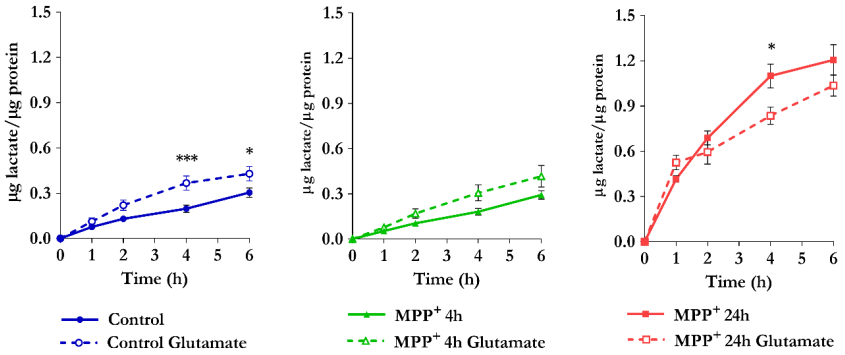

Figure 30. Lactate production in response to glutamate. Neurons were seeded on M6 plates and MPP^+ treatments were performed. Then, neurons were treated with glutamate or saline for 20 minutes and media was replaced with fresh one. Medium aliquots were recovered after 2, 4 and 6 hours for lactate concentration determination. Error bars show SEM (*p<0.05, ***p<0.001; Two-way ANOVA with Sidak's multiple comparisons test N=3).

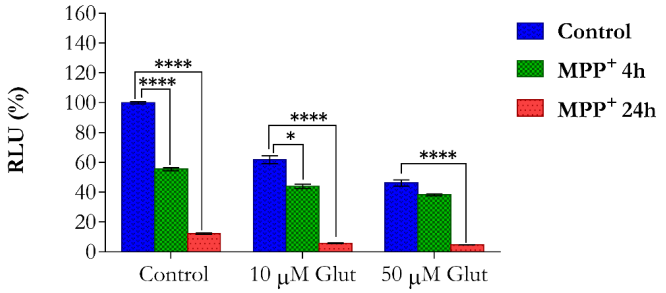

Figure 31. ATP quantification after treatment with MPP^+ and glutamate. Neurons treated with MPP^+ for 4 or 24 hours and controls were further treated with 10 or 50 µM of glutamate for 20 minutes and ATP was immediately quantified. Error bars show SEM (* p<0.05, ** p<0.01, ***p<0.001, **** p<0.0001; Kruskal-Wallis test with Dunn's correction for multiple comparisons N=3).

3. Analysis of lipid rafts from Parkinson disease patients

The previous study of lipid raft and non-raft microdomains conducted on the PD mouse model revealed that the cortical area was the one that exhibited the most relevant alterations after MPTP treatment or aging. These results match reports of altered lipid composition from PD and iPD brains specifically in lipid rafts from frontal cortex (Fabelo et al., 2011). Therefore, we focused on the analysis of LR protein alterations in frontal cortex from PD brains. Additionally, aggregation of α-synuclein in the aged MPTP treated mice was one of the most interesting alterations observed in cortical area. For this reason, we focused on the study of this protein, paying especial attention to its different aggregation stages.

Lipid rafts were isolated from human *post-mortem* brain tissue collected from clinically diagnosed and neuropathologically verified PD patients and the respective controls. Two pathological groups were establish attending to the development of the disease; a group of early development (PD 3-4, Braak classification) and a group of late development (PD 5-6). Control group was comprised by samples from age-matched individuals with no neurological symptoms. Four cases were included in each group.

Fractions obtained were processed by western blot in order to verify the distribution of LR microdomains among the fractions. Distribution of flotillin-1 was used as an indicator of the presence of lipid raft microdomains and APP and PrPc were included for comparison with other neurodegenerative diseases. For a deeper analysis of α-syn distribution, several primary antibodies directed against different aggregation and phosphorylation states of the protein were selected. The anti-α-syn [MJFR1] from Abcam was chosen since it mainly detects monomeric forms of the protein. The anti-aggregated α-syn (clone 5G4) from Millipore and the anti-α-syn (phospho-S129) were selected to detect the corresponding high molecular weight and phosphorylated forms of the protein respectively. Finally, the anti-α-syn filament [MJFR-14-6-4-2] - conformation-Specific antibody was especially intended to detect the fibrillary forms of the protein. Not all the antibodies were suitable for

western blot analysis due to the characteristics of the target. Therefore, we opted for performing the immunoblotting detection of α-synuclein by slot blot, a technique that allows the detection of protein in their native configuration. In this assay, we also included the analysis of GM1 ganglioside by incubation with cholera toxin B subunit. All forms of α-synuclein and GM1 were normalized using β-tubulin.

Western blot analysis was conducted in order to assess the distribution of certain proteins of interest among the LR and NR fractions. Fractions F1 to F6 from each sample were resolved by SDS-PAGE and transferred to PVDF membranes. Due to limited volume sample availability, analysis by western blot was performed with a reduced number of samples that did not allow quantification and adequate statistical comparisons between groups. However, this analysis allowed to verify that LR microdomains were located, as usual, at fractions 1 and 2 and that the non-raft membranes were located at fractions 5-6. Flotillin-1 was distributed exclusively in fractions 1 and 2 in all cases, confirming LR localization. Similarly, PrPc was found in those fractions corresponding to LR microdomains, reproducing the previous findings in the mouse model.

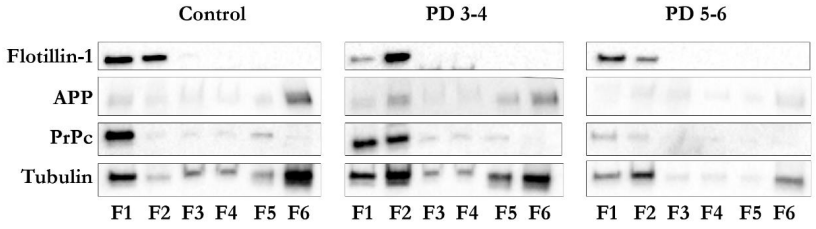

Figure 32. Immunoblot of fractions obtained from human brains. Fractions 1 to 6 obtained from the three experimental groups (control, PD stages 3-4 and PD stages 5-6) were separated by SDS-PAGE, transferred to PVDF membranes and incubated with the specific primary antibodies. Chemiluminescent detection is shown. Lipid raft resident proteins such as Flotillin-1 and PrPc appeared in fractions 1 or 2 thus confirming the correct isolation of fractions. Tubulin was present among all the collected fractions and therefore it serves as a housekeeper protein. No statistical analysis was performed due to restricted number of samples.

Results

In the case of APP, the distribution appears to be predominantly to the NR with only a very subtle distribution in LR fractions. Further assays may be required to establish the potential modifications in the amount of APP with the progress of the disease. Tubulin-β was located both in LR and NR fractions in all cases (Figure 32). Therefore tubulin-β was further used to normalise densitometric values in all fractions.

Analysis of GM1 revealed an increase of this glycolipid in LR from late stage of PD. Additionally, this ganglioside is even detectable in the NR fraction of this same group (Figure 33). Although it is not expected to find GM1 out of the LR fractions, this fact may be indicative of an increased synthesis in response to the pathologic disruption of LR microdomains.

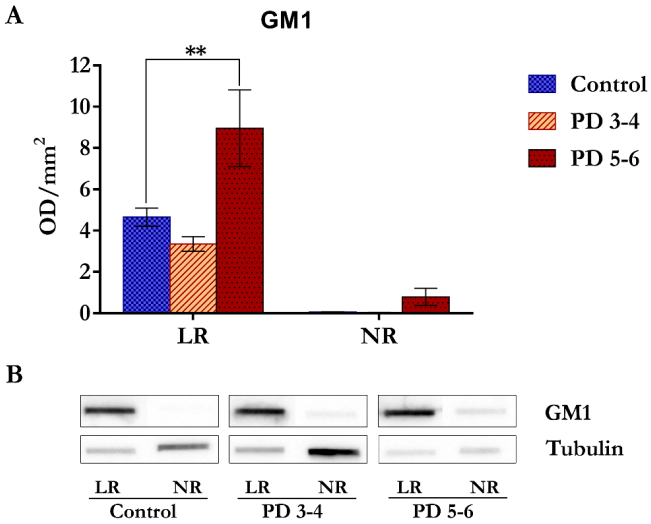

Figure 33. Analysis of GM1 ganglioside in lipid rafts from frontal cortex of PD patients. Lipid raft (LR) and non-raft (NR) samples from the three experimental groups (control, PD stages 3-4 and PD stages 5-6) were analysed by slot blot using cholera toxin to detect GM1. A) Quantification of slot blot immunodetection of GM1 normalised against β-tubulin. B) Image from slot blot showing GM1 and β-tubulin immunoblot. (** $p = < 0.01$ Two-way ANOVA with Dunnett's multiple comparisons test. N=4). Error bars represent SEM.

Contrary to the previously observed in the mouse PD model, α-synuclein appears both in LR and NR fractions from human frontal cortex samples. This distribution among the membrane microdomains varies for the different states of aggregation and phosphorylation of the protein. For an easier interpretation of the distribution of α-syn among the membrane microdomains, we estimated the ratio between α-syn detected in LR *vs* total α-syn, being the total α-syn the sum of densitometric values obtained from LR and NR. In this sense, a values lower than 50% indicates a predominantly NR distribution, while values over 50% indicate that α-syn mainly appears in LR membranes.

Monomeric α-syn locates predominantly at NR fractions (Table 8, Figure 34). Multiple t-test comparing LR *vs* NR content of monomeric α-syn shows that, except in the cases of advanced PD (stages 5-6), the NR content is significantly higher than the corresponding in LR fractions. In NR fractions, advanced PD cases present a significant increase in the monomeric forms of α-syn (Figure 34).

Aggregated α-synuclein appears in similar abundance both in LR and NR fractions for all the pathological and control cases. However, in the NR fractions the advanced PD cases shown a significant increase of this aggregated α-syn, similar to the observed for the monomeric form (Figure 34).

Comparison between LR and NR content for the different forms of α-synuclein				
	Monomeric	**Aggregated**	**Fibrillary**	**pSer129**
Control	0.0123	ns	0.04185	1.9×10^{4}
PD 3-4	2×10^{5}	ns	0.06658	0.00845
PD 5-6	ns	ns	0.04185	0.00227

Table 8. Summary of *p*-values obtained from the multiple t-tests with Holm-Sidak correction performed comparing LR and NR content for the different forms of α-synuclein.

Results

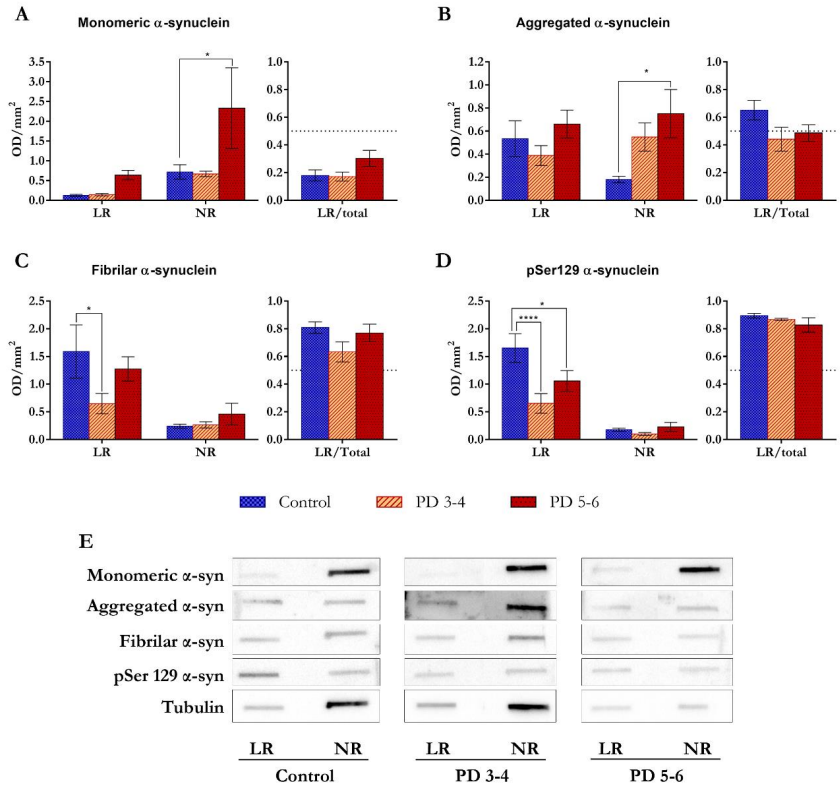

Figure 34. Analysis of α-synuclein in lipid raft and non-raft fractions from frontal cortex of PD brains. Lipid raft (LR) and non-raft (NR) samples from the three experimental groups (control, PD stages 3-4 and PD stages 5-6) were analysed by slot blot using different primary antibodies directed against α-synuclein. A-D) Quantification of different forms of α-synuclein detected in LR and NR fractions and the corresponding ratio LR *vs* NR; monomeric (A), aggregated (B), fibrillary (C) and phosphorylated at serine 129 (D). E) Immunoblot of the different forms of α-synuclein analysed. Statistical significance is shown for the comparison between pathological cases respect the control group in both LR and NR fractions (*p <0.05, **p<0.01, ****p <0.0001 Two-way ANOVA with Dunnett's multiple comparisons test. N=4). Error bars represent SEM.

Fibrillary and phosphorylated α-synuclein forms show a trend to distribute predominantly to LR fractions (Table 8, Figure 34). There is a decrease of both fibrillary and phosphorylated α-syn at early stages of the pathology (PD 3-4)

compared to the control cases. This reduction is less evident in advanced PD, suggesting that the main redistribution in the post-translational forms of α-syn take place mainly at the first stages of PD. This phenomenon may be related to the early changes in the lipid environment within membrane microstructures occurring during asymptomatic stages of the pathology that may affect the lipid interactions of α-syn within the lipid microenvironment (Fabelo et al., 2011).

Discussion

Parkinson disease represents a severe disabling pathology that affects millions of people worldwide. The impact of this disorder is only expected to grow even more in the near future due to the aging of population. Present therapies are still uncomplete, focused only on treating the symptoms but do not provide a cure. Moreover, diagnosis is frequently established in advanced stages of the disease further reducing treatment possibilities. Therefore, early detection is a key goal in the research of PD that would open the possibility for the development of more effective treatments. Lipid raft impairment has been found as an early condition in the development of PD and other neurodegenerative disorders. In this study, we have focused on LR anomalies occurring with the progression of the disease that may correlate with the acceleration of the pathological events.

MPTP mouse model characterization

The MPTP mouse model has been one of the most used in PD research since the discovery of the neurotoxic effects of this meperidine analogue reproducing a Parkinson-like phenotype. The different regimens of administration that have been performed conduce to different levels of affectation that may serve to reproduce different characteristics of the disorder (Bezard et al., 1997; Jackson-Lewis & Przedborski, 2007; Schlachetzki et al., 2016). In this study, we used low doses of MPTP sustained over a prolonged period of time which intended to resemble the slow progression of the disease better than other acute intoxication regimens. We further combined the MPTP intoxication with aging of mice in an attempt to reproduce a model that would also enable to study the lipid raft aging process (Díaz et al., 2018; Fabelo et al., 2012).

Diagnosis of PD is still mainly based on motor symptoms (Armstrong & Okun, 2020) although there is strong evidence that points to the development of non-motor symptoms prior to the motor ones. These motor symptoms of PD have been estimated to appear when at least 50-70% of dopaminergic neurons in the

substantia nigra are lost (Mahlknecht et al., 2015; Schapira et al., 2017). This fact has a clear implication in the irreversibility of the disease at the moment of diagnosis and emphasises the need for an earlier diagnosis and a better knowledge of the events that occur at the onset of PD (Noyce & Bandopadhyay, 2017). In this study, we wanted to focus on the early stages of development of the pathology. In our model, the dopaminergic loss observed represented less than the 50 % (Figure 7) in the aged and MPTP-treated mice (M14) compared to control mice. Indeed, the aged-untreated animals (W14) exhibited a subtle loss of dopaminergic neurons that was not significantly different from controls (W6) or the aged-treated (M14) mice, in line with previous observations (Credle et al., 2015; Gao et al., 2013). This fact highlights the mild effect of the intoxication and the importance of aging in the proposed model. Therefore, these animals would represent an early stage of the PD phenotype. Since the implications of lipid raft alterations occurs in these early stages (Marín et al., 2013), this model would be appropriate for the desired analysis.

Since the main interest of this study is analysing the changes in cortical LR related to the Parkinson-like phenotype in the mouse model, we wanted to better characterise the effects of MPTP on cortical neurons. It is widely accepted that MPTP administration selectively affects dopaminergic neurons from the *substantia nigra* due to the high affinity of MPP^+ (the actual toxic metabolite of MPTP) for the dopamine transporter (DAT), which is highly expressed on those neurons (J. W. Langston, 2017; Shen et al., 1985).

Previous work from our group found the alteration of cortical LR at stages previous to severe nigrostriatal depletion (Fabelo et al., 2011). Hence, the effects found cannot be a consequence of such depletion but may represent an independent phenomenon. Following this rationale, the changes found in cortical LR from the mouse model may not represent a consequence of the depletion of dopaminergic neurons, but on the contrary, serve as an early indicator of the future dopaminergic degeneration (Marín et al., 2013; Marín, 2011). This would necessary require a direct effect of MPTP (or MPP^+) in the cortical area of mice. Therefore we wanted to assess whether MPTP would have an effect or not on this brain area.

Discussion

The available assays to determine energy metabolism fitness based on cell cultures provide a powerful tool (Ferrick et al., 2008). Therefore, we used primary cultures obtained from mouse cortex since this model facilitates the execution of the required assays to characterise energy metabolism (Katsu-Jiménez & Giménez-Cassina, 2019). This model also represents the closest approach to our study system. *In vivo*, the MPTP action mechanism comprises its conversion into MPP^+ mediated by monoamine oxidase B (MAO B) from astrocytes (Heikkila et al., 1984).

We performed a series of experiments to better characterise the effects of MPP^+ on energy metabolism of mouse cortical neurons. The results obtained demonstrated that at relatively low doses of MPP^+, cortical neurons remain alive (Figure 23), even when they present a severe impairment of mitochondrial respiration (Figure 24). This is possible due to the switch to an alternative source of energy provided by the anaerobic glycolytic pathway (Figure 25)(Hui et al., 2008; Katsu-Jiménez et al., 2019). However, it was also observed that the ability to respond to physiological challenges that require a higher energy production would be severely affected after MPP^+ exposure (Figure 26).

The metabolic parameters obtained from the analysis of oxygen consumption rate (OCR) reveals the severe impairment of mitochondria in response to MPP^+. Firstly, the drastic reduction in the basal respiration (BR) and the ATP coupled respiration (ATP-CR) indicates an important blockade of the electron transport chain and an almost null production of ATP by this pathway (Smolina et al., 2017). Secondly, the maximal respiration (MR) and the spare respiratory capacity (SRC) are also significantly reduced in comparison with controls. This indicates that, in the case that an extra energy supply is required, neurons would not have the possibility to comply with it (Figure 24). This idea is supported by results obtained in experiments that included the administration of a low dose of glutamate, which acting as an excitatory neurotransmitter will demand an increase in the ATP production by mitochondria (Jekabsons & Nicholls, 2004; Yadava & Nicholls, 2007; Zhou & Danbolt, 2014). Indeed control neurons responded to glutamate increasing

their OCR, with the corresponding increase in the ATP production while MPP^+-treated neurons were not able to exhibit such increase (Figure 28 and Figure 29).

In general, the reduction of all these parameters was less pronounced in the neurons that were treated with MPP^+ for only four hours and then were allowed to recovery in the absence of MPP^+. However, in all the cases the reduction in comparison with control neurons was statistically significant. This may indicate that a shorter period of exposure produces a less severe affectation but the effects produced are permanent.

As previously mentioned, the impairment in mitochondrial respiration is somehow compensated by an increase in the ATP production by anaerobic pathways. This can be noticed as an increment in the lactate production by those neurons exposed to MPP^+ (Figure 25) (Rosa et al., 2005). However combined treatments of MPP^+ and glutamate, demonstrate that the neurotoxic effect leads the neurons to an exhausted state in which the additional requirement of energy caused by glutamate stimulation cannot be accomplished (Figure 30) (Jekabsons & Nicholls, 2004). Nonetheless, this switch to the anaerobic pathway does not allow in any circumstance to maintain the normal neuronal activity regarding to energy production (Figure 26 and Figure 31).

Therefore, low doses of MPTP produce a severe impair in the energetic metabolism but do not directly lead to neuronal death in the cortical neurons. This impairment may traduce in further cellular alterations like those observed in the cortical area of the MPTP-treated mice.

These results demonstrate that, in mice, cortical neurons may be affected by MPTP administration, even when those effects are not translated into a clear neuronal death, comparable to that seen in the dopaminergic neurons from the *substantia nigra*. Therefore, they support the suitability of the MPTP mouse model to analyse the early events occurring during the development of the PD phenotype in cortical brain areas.

Lipid alterations in LR from the murine model

After ensuring the suitability of our murine model, we firstly focused on a deep lipidomic analysis of both LR and NR fractions obtained from different brain regions. Analysis of ganglioside composition of lipid raft fractions from the different brain regions analysed showed changes in the cortical area. Gangliosides have been reported as regulators in neurodegeneration associated to α-syn pathology (Ariga, 2014; Schnaar, 2016). Particularly, *in vitro* studies have demonstrated the binding of GM1 ganglioside to α-syn and reported this binding to promote the α-helical structure of the protein and inhibit the fibril formation (Martínez et al., 2007). Here, we did not observe differences in LR GM1 content related to the pathological conditions at any of the brain areas analysed. However, GT1b exhibited a significant decrease in the cortical LR of aged animals exposed to MPTP. A similar result was observed when analysing the total ganglioside content in these microdomains. The total ganglioside content was estimated as the addition of the different ganglioside analysed (GM1, GD1a, GD1b and GT1b). Therefore, the observed differences may be explained mainly by the marked decrease of GT1b. Indeed, the descendant trend observed in the other gangliosides also contributed to this observation (Figure 9 and Figure 10). The effects of alterations in other ganglioside apart from GM1 on α-syn membrane regulation and neurodegeneration have been little explored (Badawy et al., 2018). However, our results may indicate that any of the main brain ganglioside species may play a role in the lipid raft modifications related to neuropathological events. For instance, misfolding and aggregation of α-syn is enhanced by distinct gangliosides in a specific manner (Gaspar et al., 2018). It is also important to note that, according to the biosynthetic pathway (Figure 3), GT1b ganglioside is the most complex one among those four that are present in the mouse brain (Schnaar, 2016). Therefore the reduction in this ganglioside species together with the similar tendency observed in the rest of gangliosides may indicate a general propensity to ganglioside decline in response to the pathological conditions recreated in this model (Huebecker et al., 2019).

Discussion

Although not directly analysed in this study, it is important to mention the previously observed differences of other lipid classes in this PD model since they constitute the vast majority of lipid alterations that could potentially lead to the signalling unbalances in which this work focuses. The most significant variations observed in the murine model membrane microdomains analysed affected PUFA, cholesterol (Cho), saturated fatty acids (SFAs) and phospholipids. Those changes were more evident when analysing different ratios of interest like Cho/PUFA, PL/PUFA, SFA/PUFA and unsaturation index (UI). Both LR and NR fractions were evaluated and the effects of aging and MPTP treatment detected at them were in many cases opposite indicating a sort of shift of certain lipids from LR to NR microdomains or vice versa (Canerina-Amaro et al., 2019).

One of the most remarkable variations observed in response to aging and MPTP exposure occurred in the cortical and midbrain raft fractions and included PUFA such as DHA and AA. This result correlates with those observed in previous works from our group performed in human LR from PD patients (Fabelo et al., 2011). These two fatty acids have been demonstrated to be involved in α-synuclein binding to membrane and aggregation. More specifically, the binding of α-syn to lipid microdomains requires the combination of PUFA (AA or DHA), oleic acid and phosphatidylserine (PS) (Kubo et al., 2005). AA and DHA in phospholipid vesicles can induce aggregation of α -syn (Perrin et al., 2001). In this sense, it is important to note that PS has also been found altered in the LR fractions from our murine model. In relation to PUFA variations, the UI in LR showed a diminution in response to both age and treatment. This indicator is related to the ability of membrane to deal with oxidative stress and the physicochemical properties of the membrane, regarding their flexibility (Krishna & Periasamy, 1999). With the decrease in UI membranes present more viscous and liquid-ordered lipid rafts in comparison with controls. Overall, the observed modifications in lipid composition may affect the interactions with LR resident proteins and dynamics of α-synuclein may be profoundly affected by the changes observed in lipid content of LR in cortex and midbrain.

Discussion

Cholesterol represents a key molecule in lipid rafts structures and plays an important role in the stability of these microdomains. Alterations of Cho were observed both in LR (only in midbrain) and in NR, exhibiting converse tendencies in each membrane microdomain. Despite this fact, alterations in this component do not appear to be a crucial factor in α-syn dynamics in relation to membrane LR (Kubo et al., 2005). Although we have focused on lipid alterations that lead to changes in protein signalling, the reverse interactions have also been proposed, with α-syn enhancing altered lipid conformations that exerts a neurotoxic effect (Hellstrand et al., 2013; Zhu & Fink, 2003). Supporting this idea, the α-syn genetically depleted mouse model shows increased content of PUFA (Sharon et al., 2003).

It is especially remarkable that the described lipid modifications in response to MPTP exposure are similar to those previously reported by our group in other neurodegenerative scenarios that include both mouse models and human brain samples from AD and PD patients. The Cho and PUFA imbalances together with the lower unsaturation index are a common characteristic observed in the cortex of the APP/PS1 mouse model (Fabelo et al., 2012), in frontal cortex of human PD brains (Fabelo et al., 2011), in frontal cortex of DLB patients (Marín et al., 2017) and in early stages of AD in human frontal cortex (Díaz et al., 2018). Therefore, the PD-like lesion exerted by MPTP accelerates the normal aging process of LR microdomains in cognitive and motor mice brain areas, producing an earlier development of neuropathological features.

All the above mentioned LR alterations are in agreement with the hypothesis of "lipid raft aging", according to which the LR microdomains undergo a normal process of aging characterized by modifications in lipid classes' distribution and proportions. These normal lipid raft aging is exacerbated during the progression of pathological neurodegenerative processes. Importantly, cortical alterations of LR appear at very early developmental stages both in PD and AD, when the neuropathology still remains mainly asymptomatic. In this sense, such LR

aberrations may act as a predictor of risk for further development of neuropathologies (Marín et al., 2016).

Protein alterations in LR from the murine model

The lipid analysis of lipid raft fractions performed revealed severe alterations in the PD-like model obtained by combination of aging and MPTP intoxication. Therefore, we further wanted to determine whether these alterations in the lipid matrix of LR microstructures conditioned the distribution and interactions of the proteins embedded in this signalling platforms, as well as others that have been shown relevant for the development of PD phenotype. Since α-syn is a key protein in the pathogenesis of PD our analysis has focused on its distribution among the membrane domains, its aggregation state and the posttranslational modifications that may be associated to the course of the PD phenotype (Mehra et al., 2019; Oueslati, 2016; Villar-Piqué et al., 2016).

α-Syn was vastly found in NR fractions across all the brain regions analysed in the different mouse cohorts studied. In general, an important accumulation of high molecular weight (Mw) forms was observed but specifically the cortical area showed a significant increase in those aggregated α-syn species in response to both aging and neurotoxic insult by MPTP. A similar accumulation of high Mw α-syn forms has been reported in the transgenic mice producing an altered mutant form of α-syn, E57K (Rockenstein et al., 2014). Despite the fact that the precise identity and pathological character of this aggregates is difficult to stablish due to the exceedingly complex and not well-known nature of α-syn biochemistry (Benskey et al., 2016; Mor et al., 2016), there is a certain concern about the association between this kind of high Mw α-syn species with neuropathological states. Additionally, monomeric (14kDa) forms of the protein were found in NR fractions. These monomeric forms have been widely reported in different cell types, including nerve cells and represent α-syn native, physiological forms (Bartels et al., 2011; Dettmer et al., 2016).

Remarkably, in raft fractions α-syn was negligible with only a faint and inconsistent amount of the monomeric forms in some young healthy controls. This finding does not fit with previous works showing interaction between this protein and GM1 which is located exclusively in LR (Martínez et al., 2007). Indeed, our slot blot analysis demonstrated that GM1 was exclusively distributed in LR. Therefore, in our samples, there is no interaction between α-synuclein and GM1. We mostly attribute this difference between our results and previous works to the different model in which the study was performed (tissue *vs in vitro*) and to the fact that gangliosides have self-aggregating properties that *in vitro* may lead to the artificial formation of aggregates with α-syn that is not found in our tissue samples. Alternatively, it might respond to a poor detection capability due to the low amount of protein present in this microdomains and the inherent difficult detection of α-syn (Lee & Kamitani, 2011).

Together with aggregation, phosphorylation of α-syn has been widely implicated in PD associated neurotoxicity. Particularly, phosphorylation at Serine 129 (pS129) has been reported to be an important component of Lewy bodies present in different synucleinopathies (Fujiwara et al., 2002). Analysis by 2-D immunoblotting in our mouse cohorts revealed that pS129 α-syn was mainly present in NR from midbrain of aged mice, where it appeared in the form of high Mw aggregates. The accumulation of high Mw phosphorylated α-syn in the PD-like cohort concurs with the reduction in the isoform corresponding to the unmodified α-syn monomer that was present in the control animals (Gould et al., 2014; Luth et al., 2015). Thus, a certain correlation between pS129 α-syn enhancement and aggregation could be established, reflecting that α-syn phosphorylation is age-dependent and relates to local micro-environmental changes. Also, pS129 α-syn appears to correlate with lipid modifications related to MPTP insult, further evidencing the relation of α-syn processing with neuronal membrane lipid homeostasis (Samuel et al., 2016).

The self-aggregation of certain proteins is a phenomenon shared by several neurodegenerative diseases commonly known as proteinopathies. It has been

proposed that amyloid-β (Aβ), prion protein (PrPc) and α-syn (the proteins that aggregate in such pathologies) may share similar biophysical and biochemical properties that affect the aggregation process and their interaction with membranes (Goedert, 2015; Goedert et al., 2017; Ugalde et al., 2016). In this sense, it has been also proposed that α-syn exhibits prion-like propagation that account for the progressive affectation within the nervous system (Angot et al., 2010). LR microdomains are considered key platforms for the regulation of prion-like seeding of several neurodegenerative diseases, including PD (Arbor et al., 2016; Kazlauskaite et al., 2003). Due to this common mechanism we further wanted to evaluate whether the lipid alterations previously described also influenced the behaviour of such related proteins including PrPc and APP.

Here, we have found a decrease of PrPc in the PD-like mice that was also affected by aging. This data correlates with previous reports of decreasing PrPc related to human aging and AD-related neurodegeneration (Whitehouse et al., 2010). Nonetheless, other studies have shown a different behaviour of PrPc in response to aging in mouse hippocampus, suggesting that PrPc trafficking may be region-dependent (Agostini et al., 2013). Moreover, the interaction between α-syn and PrPc in the membrane have been reported to be involved in cognitive decline (Ferreira et al., 2017). However, we did not find such interaction in our mouse cohorts and, indeed, both proteins were localized to different membrane fractions. This may be due to the small amount of protein content represented in the lipid raft fractions that did not allow to precisely detect possible low amounts of α-syn. Despite the fact that we could not find such interaction, we observed a correlation between the decrease of these two proteins in response to aging and MPTP neurotoxicity, suggesting that lipid unbalances may affect the interrelation of these markers. In this line, we suggest that GM1 might be a key lipid involved in the modulation of pathological behaviour and interaction of α-syn and PrPc. Supporting this idea, previous studies have set binding of PrPc to GM1 as a required condition for PrPc-related neurodegeneration (Botto et al., 2014). Moreover, clustering of amyloidogenic proteins in structures like LR may promote toxic cross-seeding. An

example of this is the finding that the formation of cytosolic aggregates of α-syn is promoted by scrapie PrP and Aβ (Morales et al., 2010; Mougenot et al., 2011). When analysing APP, we found a predominant distribution in NR fractions that did not appear to be affected by the PD-like phenotype.

Overall, our data indicate that alterations in the lipid matrix of membrane microdomains occurring during aging and PD-like toxicity may promote α-syn trafficking, enhancement of toxic conformational rearrangements and increased phosphorylation that lead to pathological aggregation. The abnormal lipid composition of rafts may promote the rearrangement of other pathologically relevant protein species, such as PrPc, that may contribute to neurodegeneration.

Alterations in LR from frontal cortex of PD brains

After analysing the lipid and protein modifications exhibited by lipid raft microdomains in our murine PD model, we further evaluated whether such aberrations, especially in α-syn distribution and aggregation pattern, were conserved in the frontal cortex of human brains affected by PD. Remarkably, the lipid matrix of raft membranes in the murine MPTP model showed similar changes to those previously observed in human brains since early stages of PD. As previously mentioned, those lipid modifications consisted on a great reduction in PUFA, especially DHA, AA, DPA and linolenic acid, with an increase in saturated fatty acids. Consequently, the unsaturation index was significantly decreased in the pathologic subjects. Also phospholipids were more abundant in LR fractions at early stages of PD compared to healthy controls (Fabelo et al., 2011).

We performed a ganglioside analysis in those LR and NR fractions obtained from frontal cortex of early stages of PD (PD 3-4) and PD at stages 5-6. This analysis was limited to GM1 and determined that, as expected, GM1 localises to LR fractions. A significant increase in this lipid species was observed in the samples from late stages of PD. In this case the LR from early stages of PD did not appear

to be affected contrary to the previous observations in which the early stages showed the most important alterations in the lipid matrix of LR. Indeed, in mice, GM1 was not affected and only GT1b, a more complex ganglioside, exhibited a decrease in response to PD-like conditions. In this sense, the increase in GM1 observed here might be a sort of late compensation to other ganglioside alterations (Schnaar et al., 2014).

Regarding α-syn distribution and aggregation pattern we found a main difference when comparing to results obtained in mice. In this case, samples from human frontal cortex exhibited a generalised presence of α-syn in LR membrane fractions and even some forms of this protein were more abundant in those microdomains than in NR fractions. This finding reinforces the idea that, in mice, the absence of α-syn in LR shown in this work might be due to a deficiency in detection associated to the lower amount of the protein and the inherent difficulties for detecting this protein (Newman et al., 2013). In order to get a more precise picture of α-syn behaviour in PD brains we analysed different forms of the protein by using specific primary antibodies directed against monomeric, aggregated, fibrillary and phosphorylated (S129) α-syn. We found that the distribution among the LR and NR fractions for each form as well as their changes in the pathological cases were different. Here, it is important to note that while LR fractions represent specific membrane microdomains, the NR includes both the non-raft membranes as well as cytosolic components (Fabelo et al., 2012). In this sense, the methodological approach used here does not allow to completely distinguish whether the α-syn species detected in the NR fractions are attached to other non-raft membranes or belong to possible intracytoplasmic aggregates, for instance. Related to this, several reports have suggested that binding of α-syn to membranes prevents cytotoxicity (Davidson et al., 1998; Martínez et al., 2007). The precise pathological character of the different α-syn forms analysed remains controversial (Alam et al., 2019). In this sense, it is widely accepted that the monomeric forms represent the native non-pathological forms of the protein. However, other studies have pointed to those forms as potentially cytotoxic since they are prone to pathological aggregation while

only the α-syn tetramer represents the physiological form of the protein (Bartels et al., 2011). According to this idea, the increase in monomeric α-syn observed in the NR fraction of late stage PD brains compared to healthy controls would be representative of the pathological character of those forms. Indeed, a similar increment of aggregated α-syn is observed in those same fractions. Together, this would indicate that cortical NR fractions of PD brains in late stages would accumulate not only toxic high Mw aggregates of α-syn but also the monomeric forms that would promote further aggregation. However, the results obtained from the analysis of fibrillary and phosphorylated α-syn forms are difficult to interpret. Although both forms are generally considered as pathological ones (Alam et al., 2019), they are more abundant in the LR fractions of the healthy controls compared both to the early and late stage of PD. Remarkably in all cases, these α-syn forms are more abundant in LR fractions than in NR. A possible explanation for this observation may be related to a lower detection in NR fractions that might accumulate higher amounts of this species in insoluble intracytoplasmic inclusions characteristics of the PD pathology (Newman et al., 2013). Considering this option and the inherent difficulty for α-syn detection, an infra-estimation of such pathological α-synuclein forms appears reasonable.

Interestingly, α-syn aggregation is a common event in different synucleopathies. For example, in the frontal cortex of cases with DLB α-syn aggregates were also detected (Marín et al., 2017). DLB is a synucleinopathy characterized by widespread α-syn accumulation in different brain areas, including cortex (Jellinger, 2018; Jellinger & Korczyn, 2018; McKeith et al., 2004). Although stronger evidence is still required, α-syn aggregation in DLB may follow a similar mechanism to the one proposed here, being a consequence of the detachment form LR caused by lipid aberrations in such structures (Marín et al., 2017). Overall, these data indicate that rearrangements of α-syn leading to its NR location are closely related to synucleinopathies, most probably due to the lipid impairment proved in membrane microdomains (Fabelo et al., 2011; Marín et al., 2017). To support this idea, previous studies have shown that specific lipid association is relevant in the

initiation of α-syn aggregation, enabling the core seed for further aggregation (Cole et al., 2002).

In order to summarise the molecular modifications of lipid raft microdomains observed in this work, we have depicted a schematic representation of the most relevant alterations occurring during the neurodegenerative process related to PD pathology (Figure 35).

Overall, the molecular aberrations here presented in lipid rafts microdomains represent an early event in the neuropathological development of PD. The proteins analysed have been selected on the basis of previous knowledge about the course of the pathology. This work would benefit from a systematic proteomic analysis that allowed the determination of other alterations in proteins. This possibility has not been explored here due to the limitations of the methodological approach available for threshold detection of protein amounts.

In the course of PD, the cardinal symptoms that allow accurate diagnosis appear very late, when the neurodegeneration has already achieved an irreversible condition (Noyce & Bandopadhyay, 2017). Thus, the development of early diagnosis biomarkers is key to open the possibility of treatments that effectively restrain the progression of the pathology. Currently, there are not accurate well-established early diagnosis biomarkers available (Lotankar et al., 2017; Parnetti et al., 2019). Over the last years, intensive research has been performed with the aim of finding accurate cerebrospinal fluid (CSF) or blood biomarkers. In these sense, CFS may provide a good pathway for exploring central nervous system events and it might reflect the aggregation of α-syn observed during the development of PD (Sierks et al., 2011). An analogue strategy might be used to explore the possible CSF or blood representation of the early molecular aberrations described in this work.

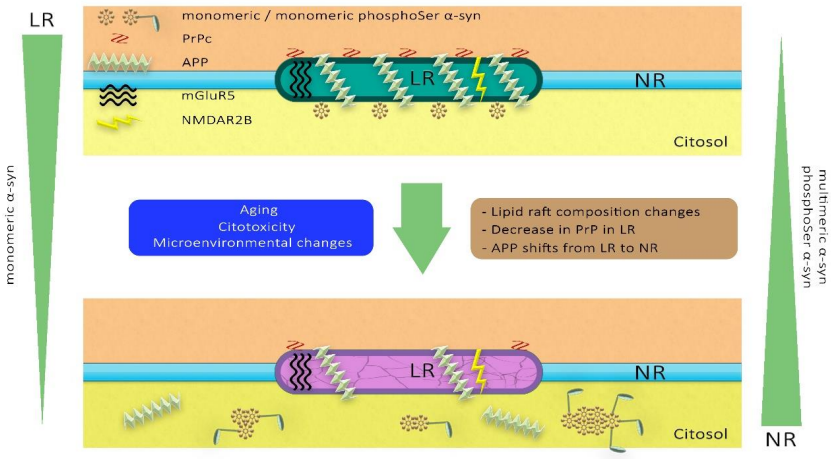

Figure 35. Schematic representation of hypothetical model of lipid raft alterations and their functional and structural consequences. Healthy lipid raft microdomains (up) may be affected by several stimuli that would alter their strictly regulated chemical composition and therefore their physicochemical properties. Such alterations would facilitate pathological changes in proteins including glutamate receptors, PrPc and APP and induce aberrations in the aggregation and phosphorylation of α-synuclein associated with PD pathology (down). Reproduced from (Canerina-Amaro et al., 2019).

Conclusions

Conclusions

1. Lipid rafts from the MPTP mouse model exhibited important alterations that affected both the lipid matrix and the proteins related to those microdomains. Among the different brain areas analysed, the cortex was the one that showed a more prominent affectation regarding the protein modifications.

2. Pathological aging in the mouse model is associated with ganglioside alterations in cortex, being the more complex gangliosides those that exhibit a higher alteration.

3. In the Parkinson disease mouse model, α-synuclein localises exclusively to non-raft fractions. This protein accumulation is increased during brain aging and enhanced in correlation with the pathological progression.

4. The α-synuclein forms that have been associated with higher toxicity, this is the high molecular weight aggregates and those phosphorylated at the serine 129, are especially increased in aged pathological mice.

5. The glutamatergic receptors analysed in this study did not show any remarkable variation in their distribution among the membrane microdomains or their expression.

6. MPP^+ at the dose of 50 μM for 24 hours impairs energy metabolism in primary cortical neurons leading to reduced levels of ATP, even though the cells are still viable.

7. Impairment in energy metabolism induced by MPP^+ reduces the capacity of cortical neurons to respond to a physiological challenge.

8. In cortical human brain samples from advanced stages of Parkinson disease GM1 profile is altered.

9. Contrary to observed in the mice model, in human samples α-synuclein appears both in lipid raft and non-raft fractions, but its relative

abundance in both compartments depends on the aggregation and phosphorylation state.

10. The cortical area of human brains affected by Parkinson disease shows variations in the different forms of α-synuclein. These changes depend on the form and the membrane microdomain analysed. In general, those forms associated with a higher toxicity were increased in the non-raft fractions of samples at late stages of Parkinson disease.

Bibliography

Bibliography

Abeliovich, A., Schmitz, Y., Fariñas, I., Choi-Lundberg, D., Ho, W. H., Castillo, P. E., … Rosenthal, A. (2000). Mice lacking α-synuclein display functional deficits in the nigrostriatal dopamine system. *Neuron*, *25*(1), 239-252. https://doi.org/10.1016/S0896-6273(00)80886-7

Agostini, F., Dotti, C. G., Pérez-Cañamás, A., Ledesma, M. D., Benetti, F., & Legname, G. (2013). Prion Protein Accumulation in Lipid Rafts of Mouse Aging Brain. *PLoS ONE*, *8*(9), e74244. https://doi.org/10.1371/journal.pone.0074244

Alam, P., Bousset, L., Melki, R., & Otzen, D. E. (2019). α-Synuclein Oligomers and Fibrils: a Spectrum of Species, a Spectrum of Toxicities. *Journal of Neurochemistry*, *150*(5), 522-534. https://doi.org/10.1111/jnc.14808

Angot, E., Steiner, J. A., Hansen, C., Li, J. Y., & Brundin, P. (2010). Are synucleinopathies prion-like disorders? *The Lancet Neurology*, *9*(11), 1128-1138. https://doi.org/10.1016/S1474-4422(10)70213-1

Arbor, S. C., LaFontaine, M., & Cumbay, M. (2016). Amyloid-beta Alzheimer targets - protein processing, lipid rafts and amyloid-beta pores. *The Yale journal of biology and medicine*, *89*(1), 5-21.

Ariga, T. (2014). Pathogenic role of ganglioside metabolism in neurodegenerative diseases. *Journal of Neuroscience Research*, *92*(10), 1227-1242. https://doi.org/10.1002/jnr.23411

Armstrong, M. J., & Okun, M. S. (2020). Diagnosis and Treatment of Parkinson Disease: A Review. *JAMA - Journal of the American Medical Association, 323*(6), 548-560. https://doi.org/10.1001/jama.2019.22360

Aureli, M., Grassi, S., Prioni, S., Sonnino, S., & Prinetti, A. (2015). Lipid membrane domains in the brain. *Biochimica et Biophysica Acta - Molecular and Cell Biology of Lipids*, *1851*(8), 1006-1016. https://doi.org/10.1016/j.bbalip.2015.02.001

Badawy, S. M., Okada, T., Kajimoto, T., Hirase, M., Matovelo, S. A., Nakamura, S., … Nakamura, S.I. (2018). Extracellular α-synuclein drives sphingosine 1-phosphate receptor subtype 1 out of lipid rafts, leading to impaired inhibitory G-protein signaling. *Journal of Biological Chemistry*, *293*(21), 8208-8216. https://doi.org/10.1074/jbc.RA118.001986

Bibliography

Bandres-Ciga, S., Diez-Fairen, M., Kim, J. J., & Singleton, A. B. (2020). Genetics of Parkinson's disease: An introspection of its journey towards precision medicine. *Neurobiology of Disease*, *137*(104782) 1-9. https://doi.org/10.1016/j.nbd.2020.104782

Barrett, P. J., & Greenamyre, J. T. (2015). Post-translational modification of α-synuclein in Parkinson's disease. *Brain Research*, *1628*, 247-253. https://doi.org/10.1016/j.brainres.2015.06.002

Bartels, T., Choi, J. G., & Selkoe, D. J. (2011). α-Synuclein occurs physiologically as a helically folded tetramer that resists aggregation. *Nature*, *477*(7362), 107-111. https://doi.org/10.1038/nature10324

Bartlett, W. P., & Banker, G. A. (1984). An electron microscopic study of the development of axons and dendrites by hippocampal neurons in culture. I. Cells which develop without intercellular contacts. *Journal of Neuroscience*, *4*(8), 1944-1953. https://doi.org/10.1523/jneurosci.04-08-01944.1984

Beitz, J. M. (2014). Parkinson's disease: a review. *Frontiers in Bioscience*, *6*(3), 65-74. https://doi.org/10.2741/s415

Benskey, M. J., Perez, R. G., & Manfredsson, F. P. (2016). The contribution of alpha synuclein to neuronal survival and function - Implications for Parkinson's disease. *Journal of Neurochemistry*, *137*(3), 331-359. https://doi.org/10.1111/jnc.13570

Betarbet, R., Sherer, T. B., MacKenzie, G., García-Osuna, M., Panov, A. V., & Greenamyre, J. T. (2000). Chronic systemic pesticide exposure reproduces features of Parkinson's disease. *Nature Neuroscience*, *3*(12), 1301-1306. https://doi.org/10.1038/81834

Bezard, E., Dovero, S., Bioulac, B., & Gross, C. (1997). Effects of Different Schedules of MPTP Administration on Dopaminergic Neurodegeneration in Mice. *Experimental Neurology*, *148*(1), 288-292. https://doi.org/10.1006/exnr.1997.6648

Bido, S., Soria, F. N., Fan, R. Z., Bezard, E., & Tieu, K. (2017). Mitochondrial division inhibitor-1 is neuroprotective in the A53T-α-synuclein rat model of Parkinson's disease. *Scientific Reports*, *7*(1), 1-13.

https://doi.org/10.1038/s41598-017-07181-0

Bieberich, E. (2018). Sphingolipids and lipid rafts: Novel concepts and methods of analysis. *Chemistry and Physics of Lipids*, *216*, 114-131. https://doi.org/10.1016/j.chemphyslip.2018.08.003

Biosa, A., Sandrelli, F., Beltramini, M., Greggio, E., Bubacco, L., & Bisaglia, M. (2017). Recent findings on the physiological function of DJ-1: Beyond Parkinson's disease. *Neurobiology of Disease*, *108*, 65-72. https://doi.org/10.1016/j.nbd.2017.08.005

Bosco, D. A., Fowler, D. M., Zhang, Q., Nieva, J., Powers, E. T., Wentworth, P., … Kelly, J. W. (2006). Elevated levels of oxidized cholesterol metabolites in Lewy body disease brains accelerate α-synuclein fibrilization. *Nature Chemical Biology*, *2*(5), 249-253. https://doi.org/10.1038/nchembio782

Bose, A., & Beal, M. F. (2016). Mitochondrial dysfunction in Parkinson's disease. *Journal of Neurochemistry*, *139*(S1), 216-231. https://doi.org/10.1111/jnc.13731

Botto, L., Cunati, D., Coco, S., Sesana, S., Bulbarelli, A., Biasini, E., … Palestini, P. (2014). Role of lipid rafts and GM1 in the segregation and processing of prion protein. *PLoSONE*, *9*(5) e98344. https://doi.org/10.1371/journal.pone.0098344

Boussicault, L., Kacher, R., Lamazière, A., Vanhoutte, P., Caboche, J., Betuing, S., & Potier, M. C. (2018). CYP46A1 protects against NMDA-mediated excitotoxicity in Huntington's disease: Analysis of lipid raft content. *Biochimie*, *153*, 70-79. https://doi.org/10.1016/j.biochi.2018.07.019

Braak, H., Del Tredici, K., Rüb, U., De Vos, R. A. I., Jansen Steur, E. N. H., & Braak, E. (2003). Staging of brain pathology related to sporadic Parkinson's disease. *Neurobiology of Aging*, *24*(2), 197-211. https://doi.org/10.1016/S0197-4580(02)00065-9

Brás, I. C., Domínguez-Meijide, A., Gerhardt, E., Koss, D., Lázaro, D. F., Santos, P. I., … Outeiro, T. F. (2020). Synucleinopathies: Where we are and where we need to go. *Journal of Neurochemistry*, *153*(4), 433-454. https://doi.org/10.1111/jnc.14965

Canerina-Amaro, A., Pereda, D., Díaz, M., Rodríguez-Barreto, D., Casañas-Sánchez,

Bibliography

V., Heffer, M., … Marín, R. (2019). Differential Aggregation and Phosphorylation of Alpha Synuclein in Membrane Compartments Associated With Parkinson Disease. *Frontiers in Neuroscience*, *13*(382), https://doi.org/10.3389/fnins.2019.00382

Cardellach, F., Martí, M. J., Fernández-Solá, J., Marín, C., Hoek, J. B., Tolosa, E., & Urbano-Márquez, A. (1993). Mitochondria1 respiratory chain activity in skeletal muscle from patients with parkinson's disease. *Neurology*, *43*(11), 2258-2262. https://doi.org/10.1212/wnl.43.11.2258

Chaturvedi, R. K., & Beal, M. F. (2008). Mitochondrial approaches for neuroprotection. *Annals of the New York Academy of Sciences*, *1147*, 395-412. https://doi.org/10.1196/annals.1427.027

Chen, X., de Silva, H. A. R., Pettenati, M. J., Rao, P. N., George-Hyslop, P. S., Roses, A. D., … Saitoh, T. (1995). The human NACP/α-synuclein gene: Chromosome assignment to 4q21.3-q22 and TaqI RFLP analysis. *Genomics*, *26*(2), 425-427. https://doi.org/10.1016/0888-7543(95)80237-G

Cole, N. B., Murphy, D. D., Grider, T., Rueter, S., Brasaemle, D., & Nussbaum, R. L. (2002). Lipid droplet binding and oligomerization properties of the Parkinson's disease protein α-synuclein. *Journal of Biological Chemistry*, *277*(8), 6344-6352. https://doi.org/10.1074/jbc.M108414200

Credle, J. J., George, J. L., Wills, J., Duka, V., Shah, K., Lee, Y. C., … Sidhu, A. (2015). GSK-3β dysregulation contributes to parkinson's-like pathophysiology with associated region-specific phosphorylation and accumulation of tau and α-synuclein. *Cell Death and Differentiation*, *22*(5), 838-851. https://doi.org/10.1038/cdd.2014.179

D. van Rooijen, B., M.A.E. Claessens, M., & Subramaniam, V. (2010). Membrane Interactions of Oligomeric Alpha-Synuclein: Potential Role in Parkinsons Disease. *Current Protein & Peptide Science*, *11*(5), 334-342. https://doi.org/10.2174/138920310791330659

Dauer, W., Kholodilov, N., Vila, M., Trillat, A. C., Goodchild, R., Larsen, K. E., … Hen, R. (2002). Resistance of α-synuclein null mice to the parkinsonian neurotoxin MPTP. *Proceedings of the National Academy of Sciences of the United States*

of America, *99*(22), 14524-14529. https://doi.org/10.1073/pnas.172514599

Davidson, W. S., Jonas, A., Clayton, D. F., & George, J. M. (1998). Stabilization of α-Synuclein secondary structure upon binding to synthetic membranes. *Journal of Biological Chemistry*, *273*(16), 9443-9449. https://doi.org/10.1074/jbc.273.16.9443

Davis, G. C., Williams, A. C., Markey, S. P., Ebert, M. H., Caine, E. D., Reichert, C. M., & Kopin, I. J. (1979). Chronic parkinsonism secondary to intravenous injection of meperidine analogues. *Psychiatry Research*, *1*(3), 249-254. https://doi.org/10.1016/0165-1781(79)90006-4

Del Tredici, K., & Braak, H. (2016). Sporadic Parkinson's disease: Development and distribution of α-synuclein pathology. *Neuropathology and Applied Neurobiology*, *42*(1), 33-50. https://doi.org/10.1111/nan.12298

Dettmer, U., Selkoe, D., & Bartels, T. (2016). New insights into cellular α-synuclein homeostasis in health and disease. *Current Opinion in Neurobiology*, *36*, 15-22. https://doi.org/10.1016/j.conb.2015.07.007

Díaz, M., Fabelo, N., Ferrer, I., & Marín, R. (2018). "Lipid raft aging" in the human frontal cortex during nonpathological aging: gender influences and potential implications in Alzheimer's disease. *Neurobiology of Aging*, *67*, 42-52. https://doi.org/10.1016/j.neurobiolaging.2018.02.022

Díaz, M., Fabelo, N., Martín, V., Ferrer, I., Gómez, T., & Marín, R. (2014). Biophysical alterations in lipid rafts from human cerebral cortex associate with increased BACE1/AβPP interaction in early stages of Alzheimer's disease. *Journal of Alzheimer's Disease*, *43*(4), 1185-1198. https://doi.org/10.3233/JAD-141146

Díaz, M. L., Fabelo, N., & Marín, R. (2012). Genotype-induced changes in biophysical properties of frontal cortex lipid raft from APP/PS1 transgenic mice. *Frontiers in Physiology*, *3*, 1-10. https://doi.org/10.3389/fphys.2012.00454

Díaz, M., Luis-Amaro, A. C., Rodríguez-Barreto, D., Casañas-Sánchez, V., Pérez, J.-A., & Marín, R. (2019). Lipostatic Mechanisms Preserving Cerebellar Lipids in MPTP-Treated Mice: Focus on Membrane Microdomains and Lipid-Related Gene Expression. *Frontiers in Molecular Neuroscience*, *12*(93), 1-20.

https://doi.org/10.3389/fnmol.2019.00093

Diógenes, M. J., Dias, R. B., Rombo, D. M., Vicente Miranda, H., Maiolino, F., Guerreiro, P., … Outeiro, T. F. (2012). Extracellular Alpha-Synuclein Oligomers Modulate Synaptic Transmission and Impair LTP Via NMDA-Receptor Activation. *The Journal of Neuroscience*, *32*(34), 11750-11762. https://doi.org/10.1523/JNEUROSCI.0234-12.2012

Elbaz, A., Carcaillon, L., Kab, S. & Moisan, F. (2016). Epidemiology of Parkinson's disease. *Revue Neurologique*, *172*(1), 14-26. https://doi.org/10.1016/j.neurol.2015.09.012

Emmanouilidou, E., Melachroinou, K., Roumeliotis, T., Garbis, S. D., Ntzouni, M., Margaritis, L. H., … Vekrellis, K. (2010). Cell-produced α-synuclein is secreted in a calcium-dependent manner by exosomes and impacts neuronal survival. *Journal of Neuroscience*, *30*(20), 6838-6851. https://doi.org/10.1523/JNEUROSCI.5699-09.2010

Fabelo, N., Martín, V., Marín, R., Moreno, D., Ferrer, I., & Díaz, M. (2014). Altered lipid composition in cortical lipid rafts occurs at early stages of sporadic Alzheimer's disease and facilitates APP/BACE1 interactions. *Neurobiology of Aging*, *35*(8), 1801-1812. https://doi.org/10.1016/j.neurobiolaging.2014.02.005

Fabelo, N., Martín, V., Marín, R., Santpere, G., Aso, E., Ferrer, I., & Díaz, M. (2012). Evidence for Premature Lipid Raft Aging in APP/PS1 Double-Transgenic Mice, a Model of Familial Alzheimer Disease. *Journal of Neuropathology & Experimental Neurology*, *71*(10), 868-881. https://doi.org/10.1097/NEN.0b013e31826be03c

Fabelo, N., Martín, V., Santpere, G., Marín, R., Torrent, L., Ferrer, I., & Díaz, M. (2011). Severe alterations in lipid composition of frontal cortex lipid rafts from Parkinson's disease and incidental Parkinson's disease. *Molecular Medicine*, *17*, 1107-1118. https://doi.org/10.2119/molmed.2011.00119

Fernández-Echevarría, C., Díaz, M., Ferrer, I., Canerina-Amaro, A., & Marín, R. (2014). Aβ promotes VDAC1 channel dephosphorylation in neuronal lipid rafts. Relevance to the mechanisms of neurotoxicity in Alzheimer's disease. *Neuroscience*, *278*, 354-366. https://doi.org/10.1016/j.neuroscience.2014.07.079

Ferreira, D. G., Temido-Ferreira, M., Vicente-Miranda, H., Batalha, V. L., Coelho, J. E., Szegö, É. M., … Outeiro, T. F. (2017). α-synuclein interacts with PrPC to induce cognitive impairment through mGluR5 and NMDAR2B. *Nature Neuroscience*, *20*(11), 1569-1579. https://doi.org/10.1038/nn.4648

Ferrick, D. A., Neilson, A., & Beeson, C. (2008). Advances in measuring cellular bioenergetics using extracellular flux. *Drug Discovery Today*, *13*(5-6), 268-274. https://doi.org/10.1016/j.drudis.2007.12.008

Fortin, D. L., Nemani, V. M., Voglmaier, S. M., Anthony, M. D., Ryan, T. A., & Edwards, R. H. (2005). Neural activity controls the synaptic accumulation of α-synuclein. *Journal of Neuroscience*, *25*(47), 10913-10921. https://doi.org/10.1523/JNEUROSCI.2922-05.2005

Fujiwara, H., Hasegawa, M., Dohmae, N., Kawashima, A., Masliah, E., Goldberg, M. S., … Iwatsubo, T. (2002). α-synuclein is phosphorylated in synucleinopathy lesions. *Nature Cell Biology*, *4*(2), 160-164. https://doi.org/10.1038/ncb748

Gao, L., Hidalgo-Figueroa, M., Escudero, L. M., Díaz-Martín, J., López-Barneo, J., & Pascual, A. (2013). Age-Mediated Transcriptomic Changes in Adult Mouse Substantia Nigra. *PLoS ONE*, *8*(4), e62456. https://doi.org/10.1371/journal.pone.0062456

Gaspar, R., Pallbo, J., Weininger, U., Linse, S., & Sparr, E. (2018). Ganglioside lipids accelerate α-synuclein amyloid formation. *Biochimica et Biophysica Acta - Proteins and Proteomics*, *1866*(10), 1062-1072. https://doi.org/10.1016/j.bbapap.2018.07.004

GBD 2016 Neurology Collaborators. (2019). Global, regional and national burden of neurological disorders, 1990-2016: a systematic analysis for the Global Burden of Disease Study 2016. *The Lancet Neurology*, *18*(5), 459-480. https://doi.org/10.1016/S1474-4422(18)30499-X

Goedert, M. (2015). Alzheimer's and Parkinson's diseases: The prion concept in relation to assembled Aβ, tau and α-synuclein. *Science*, *349*(6248), 1255555-1255555. https://doi.org/10.1126/science.1255555

Goedert, M., Masuda-Suzukake, M., & Falcon, B. (2017). Like prions: The propagation of aggregated tau and α-synuclein in neurodegeneration. *Brain*,

Bibliography

140(2), 266-278. https://doi.org/10.1093/brain/aww230

Gould, N., Mor, D. E., Lightfoot, R., Malkus, K., Giasson, B., & Ischiropoulos, H. (2014). Evidence of native α-synuclein conformers in the human brain. *Journal of Biological Chemistry*, *289*(11), 7929-7934. https://doi.org/10.1074/jbc.C113.538249

Grassi, S., Giussani, P., Mauri, L., Prioni, S., Sonnino, S., & Prinetti, A. (2020). Lipid rafts and neurodegeneration: Structural and functional roles in physiologic aging and neurodegenerative diseases. *Journal of Lipid Research*, *61*, 636-654. https://doi.org/10.1194/jlr.TR119000427

Grünewald, A., Kumar, K. R., & Sue, C. M. (2019). New insights into the complex role of mitochondria in Parkinson's disease. *Progress in Neurobiology*, *177*, 73-93. https://doi.org/10.1016/j.pneurobio.2018.09.003

Guardia-Laguarta, C., Area-Gómez, E., Rüb, C., Liu, Y., Magrané, J., Becker, D., … Przedborski, S. (2014). α-synuclein is localized to mitochondria-associated ER membranes. *Journal of Neuroscience*, *34*(1), 249-259. https://doi.org/10.1523/JNEUROSCI.2507-13.2014

Hansen, C., Angot, E., Bergström, A. L., Steiner, J. A., Pieri, L., Paul, G., … Brundin, P. (2011). α-Synuclein propagates from mouse brain to grafted dopaminergic neurons and seeds aggregation in cultured human cells. *Journal of Clinical Investigation*, *121*(2), 715-725. https://doi.org/10.1172/JCI43366

Heikkila, R. E., Manzino, L., Cabbat, F. S., & Duvoisin, R. C. (1984). Protection against the dopaminergic neurotoxicity of 1-methyl-4-phenyl-1,2,5,6-tetrahydropyridine by monoamine oxidase inhibitors. *Nature*, *311*(5985), 467-469. https://doi.org/10.1038/311467a0

Hellstrand, E., Nowacka, A., Topgaard, D., Linse, S., & Sparr, E. (2013). Membrane Lipid Co-Aggregation with α-Synuclein Fibrils. *PLoS ONE*, *8*(10), e77235. https://doi.org/10.1371/journal.pone.0077235

Huebecker, M., Moloney, E. B., Van Der Spoel, A. C., Priestman, D. A., Isacson, O., Hallett, P. J., & Platt, F. M. (2019). Reduced sphingolipid hydrolase activities, substrate accumulation and ganglioside decline in Parkinson's disease. *Molecular Neurodegeneration*, *14*(40), 1-21. https://doi.org/10.1186/s13024-019-

0339-z

Hui, S. T. Y., Andres, A. M., Miller, A. K., Spann, N. J., Potter, D. W., Post, N. M., … Davis, R. A. (2008). Txnip balances metabolic and growth signaling via PTEN disulfide reduction. *Proceedings of the National Academy of Sciences of the United States of America*, *105*(10), 3921-3926. https://doi.org/10.1073/pnas.0800293105

Ingelsson, M. (2016). Alpha-synuclein oligomers-neurotoxic molecules in Parkinson's disease and other lewy body disorders. *Frontiers in Neuroscience*, *10*(408), 1-10. https://doi.org/10.3389/fnins.2016.00408

Jackson-Lewis, V., Blesa, J., & Przedborski, S. (2012). Animal models of Parkinson's disease. *Parkinsonism and Related Disorders*, *18*(S1) S183-S185. https://doi.org/10.1016/s1353-8020(11)70057-8

Jackson-Lewis, V., & Przedborski, S. (2007). Protocol for the MPTP mouse model of Parkinson's disease. *Nature Protocols*, *2*(1), 141-151. https://doi.org/10.1038/nprot.2006.342

Jakes, R., Spillantini, M. G., & Goedert, M. (1994). Identification of two distinct synucleins from human brain. *FEBS Letters*, *345*(1), 27-32. https://doi.org/10.1016/0014-5793(94)00395-5

Jankovic, J. (2008). Parkinson's disease: Clinical features and diagnosis. *Journal of Neurology, Neurosurgery and Psychiatry*, *79*(4), 368-376. https://doi.org/10.1136/jnnp.2007.131045

Jekabsons, M. B., & Nicholls, D. G. (2004). *In situ* respiration and bioenergetic status of mitochondria in primary cerebellar granule neuronal cultures exposed continuously to glutamate. *Journal of Biological Chemistry*, *279*(31), 32989-33000. https://doi.org/10.1074/jbc.M401540200

Jellinger, K. A. (2018). Dementia with Lewy bodies and Parkinson's disease-dementia: current concepts and controversies. *Journal of Neural Transmission*, *125*, 615-650. https://doi.org/10.1007/s00702-017-1821-9

Jellinger, K. A., & Korczyn, A. D. (2018). Are dementia with Lewy bodies and Parkinson's disease dementia the same disease? *BMC Medicine*, *16*(1), 1-16. https://doi.org/10.1186/s12916-018-1016-8

Bibliography

Katsu-Jiménez, Y., & Giménez-Cassina, A. (2019). Fibroblast growth Factor-21 promotes ketone body utilization in neurons through activation of AMP-dependent kinase. *Molecular and Cellular Neuroscience*, *101*(103415), 1-12 https://doi.org/10.1016/j.mcn.2019.103415

Katsu-Jiménez, Y., Vázquez-Calvo, C., Maffezzini, C., Halldin, M., Peng, X., Freyer, C., … Arnér, E. S. J. (2019). Absence of TXNIP in Humans Leads to Lactic Acidosis and Low Serum Methionine Linked to Deficient Respiration on Pyruvate. *Diabetes*, *68*(4), 709-723. https://doi.org/10.2337/db18-0557

Kazlauskaite, J., Sanghera, N., Sylvester, I., Vénien-Bryan, C., & Pinheiro, T. J. T. (2003). Structural changes of the prion protein in lipid membranes leading to aggregation and fibrillization. *Biochemistry*, *42*(11), 3295-3304. https://doi.org/10.1021/bi026872q

Krishna, M. M. G., & Periasamy, N. (1999). Location and orientation of DODCI in lipid bilayer membranes: Effects of lipid chain length and unsaturation. *Biochimica et Biophysica Acta - Biomembranes*, *1461*(1), 58-68. https://doi.org/10.1016/S0005-2736(99)00149-2

Kubo, S. I., Nemani, V. M., Chalkley, R. J., Anthony, M. D., Hattori, N., Mizuno, Y., … Fortin, D. L. (2005). A combinatorial code for the interaction of α-synuclein with membranes. *Journal of Biological Chemistry*, *280*(36), 31664-31672. https://doi.org/10.1074/jbc.M504894200

Laemmli, U. K. (1970). Cleavage of structural proteins during the assembly of the head of bacteriophage T4. *Nature*, *227*, 680-685.

Langston, J., Ballard, P., Tetrud, J., & Irwin, I. (1983). Chronic Parkinsonism in Humans due to a Product of Meperidine-Analog Synthesis. *Science*, *219*(4587), 979-980.

Langston, J. W. (2017). The MPTP Story. *Journal of Parkinson's Disease*, *7*(s1), S11-S19. https://doi.org/10.3233/JPD-179006

Langston, J. W., Irwin, I., Langston, E. B., & Forno, L. S. (1984). 1-Methyl-4-phenylpyridinium ion (MPP^+): Identification of a metabolite of MPTP, a toxin selective to the substantia nigra. *Neuroscience Letters*, *48*(1), 87-92. https://doi.org/10.1016/0304-3940(84)90293-3

Bibliography

Larsen, K. E., Schmitz, Y., Troyer, M. D., Mosharov, E., Dietrich, P., Quazi, A. Z., … Sulzer, D. (2006). α-Synuclein overexpression in PC12 and chromaffin cells impairs catecholamine release by interfering with a late step in exocytosis. *Journal of Neuroscience*, *26*(46), 11915-11922. https://doi.org/10.1523/JNEUROSCI.3821-06.2006

Ledesma, M. D., Martín, M. G., & Dotti, C. G. (2012). Lipid changes in the aged brain: Effect on synaptic function and neuronal survival, *51*(1), 23-35 https://doi.org/10.1016/j.plipres.2011.11.004

Lee, B. R., & Kamitani, T. (2011). Improved Immunodetection of Endogenous α-Synuclein. *PLoS ONE*, *6*(8), e23939. https://doi.org/10.1371/journal.pone.0023939

Levental, I., Grzybek, M., & Simons, K. (2010). Greasing their way: Lipid modifications determine protein association with membrane rafts. *Biochemistry*, *49*(30), 6305-6316. https://doi.org/10.1021/bi100882y

Lotankar, S., Prabhavalkar, S. K. & Bhatt, L. K. (2017). Biomarkers for Parkinson's Disease: Recent Advancement. *Neuroscience Bulletin*, *33*, 585-597. https://doi.org/10.1007/s12264-017-0183-5

Luk, K. C., Kehm, V., Carroll, J., Zhang, B., O'Brien, P., Trojanowski, J. Q., & Lee, V. M. Y. (2012). Pathological α-synuclein transmission initiates Parkinson-like neurodegeneration in nontransgenic mice. *Science*, *338*(6109), 949-953. https://doi.org/10.1126/science.1227157

Luth, E. S., Bartels, T., Dettmer, U., Kim, N. C., & Selkoe, D. J. (2015). Purification of α-synuclein from human brain reveals an instability of endogenous multimers as the protein approaches purity. *Biochemistry*, *54*(2), 279-292. https://doi.org/10.1021/bi501188a

Mahlknecht, P., Seppi, K., & Poewe, W. (2015). The concept of prodromal Parkinson's disease. *Journal of Parkinson's Disease*, *5*(4), 681-697. https://doi.org/10.3233/JPD-150685

Marín, Fabelo, N., Fernández-Echevarría, C., Canerina-Amaro, A., Rodríguez-Barreto, D., Quinto-Alemany, D., … Díaz, M. (2016). Lipid Raft Alterations in Aged-Associated Neuropathologies. *Current Alzheimer Research*, *13*(9), 973-984.

https://doi.org/10.2174/1567205013666160314150017

Marín, R. (2011). Signalosomes in the brain: relevance in the development of certain neuropathologies such as Alzheimer's disease. *Frontiers in Physiology*, *2*(23), 1-4. https://doi.org/10.3389/fphys.2011.00023

Marín, R., Fabelo, N., Martín, V., García-Esparcia, P., Ferrer, I., Quinto-Alemany, D., & Díaz, M. (2017). Anomalies occurring in lipid profiles and protein distribution in frontal cortex lipid rafts in dementia with Lewy bodies disclose neurochemical traits partially shared by Alzheimer's and Parkinson's diseases. *Neurobiology of Aging*, *49*, 52-59. https://doi.org/10.1016/j.neurobiolaging.2016.08.027

Marín, R., Rojo, J. A., Fabelo, N., Fernández, C. E., & Díaz, M. (2013). Lipid raft disarrangement as a result of neuropathological progresses: A novel strategy for early diagnosis? *Neuroscience*, *245*, 26-39. https://doi.org/10.1016/j.neuroscience.2013.04.025

Markey, S. P., Johannessen, J. N., Chiueh, C. C., Burns, R. S., & Herkenham, M. A. (1984). Intraneuronal generation of a pyridinium metabolite may cause drug-induced parkinsonism. *Nature*, *311*(5985), 464-467. https://doi.org/10.1038/311464a0

Maroteaux, L., Campanelli, J. T., & Scheller, R. H. (1988). Synuclein: A neuron-specific protein localized to the nucleus and presynaptic nerve terminal. *Journal of Neuroscience*, *8*(8), 2804-2815. https://doi.org/10.1523/jneurosci.08-08-02804.1988

Martín, V., Fabelo, N., Santpere, G., Puig, B., Marín, R., Ferrer, I., & Díaz, M. (2010). Lipid alterations in lipid rafts from Alzheimer's disease human brain cortex. *Journal of Alzheimer's Disease*, *19*(2), 489-502. https://doi.org/10.3233/JAD-2010-1242

Martínez, Z., Zhu, M., Han, S., & Fink, A. L. (2007). GM1 specifically interacts with α-synuclein and inhibits fibrillation. *Biochemistry*, *46*(7), 1868-1877. https://doi.org/10.1021/bi061749a

Mattson, M. P., Barger, S. W., Begley, J. G., & Mark, R. J. (1995). Chapter 10 Calcium, Free Radicals and Excitotoxic Neuronal Death in Primary Cell

Culture. *Methods in Cell Biology*, *46*, 187-216. https://doi.org/10.1016/S0091-679X(08)61930-5

McKeith, I., Mintzer, J., Aarsland, D., Burn, D., Chiu, H., Cohen-Mansfield, J., … Reid, W. (2004). Dementia with Lewy bodies. *Lancet Neurology*, *3*(1), 19-28. https://doi.org/10.1016/S1474-4422(03)00619-7

Mehra, S., Sahay, S., & Maji, S. K. (2019). α-Synuclein misfolding and aggregation: Implications in Parkinson's disease pathogenesis. *Biochimica et Biophysica Acta - Proteins and Proteomics*, *1867*(10), 890-908. https://doi.org/10.1016/j.bbapap.2019.03.001

Meredith, G. E., & Rademacher, D. J. (2011). MPTP mouse models of Parkinson's disease: An update. *Journal of Parkinson's Disease*, *1*(1), 19-33. https://doi.org/10.3233/JPD-2011-11023

Mor, D. E., Ugras, S. E., Daniels, M. J., & Ischiropoulos, H. (2016). Dynamic structural flexibility of α-synuclein. *Neurobiology of Disease*, *88*, 66-74. https://doi.org/10.1016/j.nbd.2015.12.018

Morales, R., Estrada, L. D., Díaz-Espinoza, R., Morales-Scheihing, D., Jara, M. C., Castilla, J., & Soto, C. (2010). Molecular cross talk between misfolded proteins in animal models of alzheimer's and prion diseases. *Journal of Neuroscience*, *30*(13), 4528-4535. https://doi.org/10.1523/JNEUROSCI.5924-09.2010

Mougenot, A.-L. J., Bencsik, A., Nicot, S., Vulin, J., Morignat, E., Verchère, J., … Baron, T. G. (2011). Transmission of Prion Strains in a Transgenic Mouse Model Overexpressing Human A53T Mutated α-Synuclein. *Journal of Neuropathology & Experimental Neurology*, *70*(5), 377-385. https://doi.org/10.1097/NEN.0b013e318217d95f

Mukherjee, A., Biswas, A., & Das, S. K. (2016). Gut dysfunction in Parkinson's disease. *World Journal of Gastroenterology*, *22*(25), 5742-5752. https://doi.org/10.3748/wjg.v22.i25.5742

Mukherjee, A., Arnaud, L., & Cooper, J. A. (2003). Lipid-dependent Recruitment of Neuronal Src to Lipid Rafts in the Brain. *Journal of Biological Chemistry*, *278*(42), 40806-40814. https://doi.org/10.1074/jbc.M306440200

Newman, A. J., Selkoe, D., & Dettmer, U. (2013). A new method for quantitative

immunoblotting of endogenous α-synuclein. *PLoS ONE*, *8*(11), 81314. https://doi.org/10.1371/journal.pone.0081314

Noyce A., Bandopadhyay R. (2017). Parkinson's disease: Basic Pathomechanisms and a Clinical Overview. In: Beart P., Robinson M., Rattray M., Maragakis N. (Eds.) *Neurodegenerative Diseases. Advances in Neurobiology, 15*. 55-92 Springer, Cham. https://doi.org/10.1007/978-3-319-57193-5_3

Oueslati, A. (2016). Implication of Alpha-Synuclein Phosphorylation at S129 in Synucleinopathies: What Have We Learned in the Last Decade? *Journal of Parkinson's Disease*, *6*, 39-51. https://doi.org/10.3233/JPD-160779

Oueslati, A., Fournier, M., & Lashuel, H. A. (2010). Role of post-translational modifications in modulating the structure, function and toxicity of α-synuclein. Implications for Parkinson's disease pathogenesis and therapies. In *Progress in Brain Research 183*, 115-145. https://doi.org/10.1016/S0079-6123(10)83007-9

Pan, B., Fromholt, S. E., Hess, E. J., Crawford, T. O., Griffin, J. W., Sheikh, K. A., & Schnaar, R. L. (2005). Myelin-associated glycoprotein and complementary axonal ligands, gangliosides, mediate axon stability in the CNS and PNS: Neuropathology and behavioral deficits in single- and double-null mice. *Experimental Neurology*, *195*(1), 208-217. https://doi.org/10.1016/j.expneurol.2005.04.017

Parker, W. D., Boyson, S. J., & Parks, J. K. (1989). Abnormalities of the electron transport chain in idiopathic parkinson's disease. *Annals of Neurology*, *26*(6), 719-723. https://doi.org/10.1002/ana.410260606

Parkinson, J. (1817). *An essay on the Shaking Palsy*. London: Sherwood, Neely and Jones.

Parnetti, L., Gaetani, L., Eusebi, P., Paciotti, S., Hansson, O., El-Agnaf, O., … Calabresi, P. (2019). CSF and blood biomarkers for Parkinson's disease. *The Lancet Neurology*, *18*, 573-586. https://doi.org/10.1016/S1474-4422(19)30024-9

Perrin, R. J., Woods, W. S., Clayton, D. F., & George, J. M. (2001). Exposure to Long Chain Polyunsaturated Fatty Acids Triggers Rapid Multimerization of Synucleins. *Journal of Biological Chemistry*, *276*(45), 41958-41962. https://doi.org/10.1074/jbc.M105022200

Pike, L. J. (2003). Lipid rafts: Bringing order to chaos. *Journal of Lipid Research*, *44*(4), 655-667. https://doi.org/10.1194/jlr.R200021-JLR200

Pike, L. J. (2006). Rafts defined: A report on the Keystone symposium on lipid rafts and cell function. *Journal of Lipid Research*, *47*(7), 1597-1598. https://doi.org/10.1194/jlr.E600002-JLR200

Ramsay, R. R., Salach, J. I., & Singer, T. P. (1986). Uptake of the neurotoxin 1-methyl-4-phenylpyridine (MPP^+) by mitochondria and its relation to the inhibition of the mitochondrial oxidation of NAD^+-linked substrates by MPP^+. *Biochemical and Biophysical Research Communications*, *134*(2), 743-748. https://doi.org/10.1016/S0006-291X(86)80483-1

Recasens, A., & Dehay, B. (2014). Alpha-synuclein spreading in Parkinson's disease. *Frontiers in Neuroanatomy*, *8*, 1-9. https://doi.org/10.3389/fnana.2014.00159

Ribeiro, S. M., Giménez-Cassina, A., & Danial, N. N. (2015). Measurement of Mitochondrial Oxygen Consumption Rates in Mouse Primary Neurons and Astrocytes. In: C. M. Palmeira & A. P. Rolo (Eds.), *Mitochondrial Regulation: Methods and Protocols*. 59-69. https://doi.org/10.1007/978-1-4939-1875-1_6

Richardson, J. R., Caudle, W. M., Guillot, T. S., Watson, J. L., Nakamaru-Ogiso, E., Seo, B. B., … Miller, G. W. (2007). Obligatory role for complex I inhibition in the dopaminergic neurotoxicity of 1-methyl-4-phenyl-1,2,3,6-tetrahydropyridine (MPTP). *Toxicological Sciences*, *95*(1), 196-204. https://doi.org/10.1093/toxsci/kfl133

Rockenstein, E., Nuber, S., Overk, C. R., Ubhi, K., Mante, M., Patrick, C., … Masliah, E. (2014). Accumulation of oligomer-prone α-synuclein exacerbates synaptic and neuronal degeneration *in vivo*. *Brain*, *137*(5), 1496-1513. https://doi.org/10.1093/brain/awu057

Rosa, R. B., Schuck, P. F., de Assis, D. R., Latini, A., Dalcin, K. B., Ribeiro, C. A. J., … Wajner, M. (2005). Inhibition of energy metabolism by 2-methylacetoacetate and 2-methyl-3-hydroxybutyrate in cerebral cortex of developing rats. *Journal of Inherited Metabolic Disease*, *28*(4), 501-515. https://doi.org/10.1007/s10545-005-0501-3

Samuel, F., Flavin, W. P., Iqbal, S., Pacelli, C., Renganathan, S. D. S., Trudeau, L. E.,

… Tandon, A. (2016). Effects of serine 129 phosphorylation on α-synuclein aggregation, membrane association and internalization. *Journal of Biological Chemistry*, *291*(9), 4374-4385. https://doi.org/10.1074/jbc.M115.705095

Schapira, A., Chaudhuri, K. R., & Jenner, P. (2017). Non-motor features of Parkinson disease. *Nature Reviews Neuroscience*, *18*(7), 435-450. https://doi.org/10.1038/nrn.2017.62

Schapira, A. H. V., Cooper, J. M., Dexter, D., Clark, J. B., Jenner, P., & Marsden, C. D. (1990). Mitochondrial Complex I Deficiency in Parkinson's Disease. *Journal of Neurochemistry*, *54*(3), 823-827. https://doi.org/10.1111/j.1471-4159.1990.tb02325.x

Schengrund, C. L. (2010). Lipid rafts: Keys to neurodegeneration. *Brain Research Bulletin*, *82*(1-2), 7-17. https://doi.org/10.1016/j.brainresbull.2010.02.013

Schlachetzki, J. C. M., Grimm, T., Schlachetzki, Z., Ben Abdallah, N. M. B., Ettle, B., Vöhringer, P., … Winkler, J. (2016). Dopaminergic lesioning impairs adult hippocampal neurogenesis by distinct modification of α-synuclein. *Journal of Neuroscience Research*, *94*(1), 62-73. https://doi.org/10.1002/jnr.23677

Schnaar, R. L. (2016). Gangliosides of the Vertebrate Nervous System. *Journal of Molecular Biology*, *428*(16), 3325-3336. https://doi.org/10.1016/j.jmb.2016.05.020

Schnaar, R. L., Fromholt, S. E., Gong, Y., Vyas, A. A., Laroy, W., Wayman, D. M., … Shiekh, K. A. (2002). Immunoglobulin G-class mouse monoclonal antibodies to major brain gangliosides. *Analytical Biochemistry*, *302*(15), 276-284. https://doi.org/10.1006/abio.2001.5540

Schnaar, R. L., Gerardy-Schahn, R., & Hildebrandt, H. (2014). Sialic acids in the brain: Gangliosides and polysialic acid in nervous system development, stability, disease and regeneration. *Physiological Reviews*, *94*(2), 461-518. https://doi.org/10.1152/physrev.00033.2013

Sharon, R., Bar-Joseph, I., Mirick, G. E., Serhan, C. N., & Selkoe, D. J. (2003). Altered Fatty Acid Composition of Dopaminergic Neurons Expressing α-Synuclein and Human Brains with α-Synucleinopathies. *Journal of Biological Chemistry*, *278*(50), 49874-49881. https://doi.org/10.1074/jbc.M309127200

Shen, R.-S., Abell, C. W., Gessner, W., & Brossi, A. (1985). Serotonergic conversion of MPTP and dopaminergic accumulation of MPP^+. *FEBS Letters*, *189*(2), 225-230. https://doi.org/10.1016/0014-5793(85)81028-0

Shi, Z., Sachs, J. N., Rhoades, E., & Baumgart, T. (2015). Biophysics of α-synuclein induced membrane remodelling. *Physical Chemistry Chemical Physics*, *17*(24), 15561-15568. https://doi.org/10.1039/c4cp05883f

Sierks, M. R., Chatterjee, G., McGraw, C., Kasturirangan, S., Schulz, P., & Prasad, S. (2011). CSF levels of oligomeric alpha-synuclein and beta-amyloid as biomarkers for neurodegenerative disease. *Integrative Biology*, *3*(12), 1188-1196. https://doi.org/10.1039/c1ib00018g

Simarro, M., Gimenez-Cassina, A., Kedersha, N., Lazaro, J.-B., Adelmant, G. O., Marto, J. A., … Anderson, P. (2010). Fast kinase domain-containing protein 3 is a mitochondrial protein essential for cellular respiration. *Biochemical and Biophysical Research Communications*, *401*(3), 440-446. https://doi.org/10.1016/J.BBRC.2010.09.075

Simons, K., & Ikonen, E. (1997). Functional rafts in cell membranes. *Nature*, *387*(6633), 569-572. https://doi.org/10.1038/42408

Singh, A., Zhi, L., & Zhang, H. (2019). LRRK2 and mitochondria: Recent advances and current views. *Brain Research*, *1702*, 96-104. https://doi.org/10.1016/j.brainres.2018.06.010

Smolina N., Bruton J., Kostareva A., Sejersen T. (2017). Assaying Mitochondrial Respiration as an Indicator of Cellular Metabolism and Fitness. In: Gilbert D., Friedrich O. (Eds.) *Cell Viability Assays. Methods in Molecular Biology,* 79-87. Humana Press, New York, NY. https://doi.org/10.1007/978-1-4939-6960-9_7

Sonnino, S., Aureli, M., Mauri, L., Ciampa, M. G., & Prinetti, A. (2015). Membrane lipid domains in the nervous system. *Frontiers in Bioscience - Landmark*, *20*(2), 280-302. https://doi.org/10.2741/4309

Sonsalla, P. K., & Heikkila, R. E. (1986). The influence of dose and dosing interval on MPTP-induced dopaminergic neurotoxicity in mice. *European Journal of Pharmacology*, *129*(3), 339-345. https://doi.org/10.1016/0014-2999(86)90444-9

Spillantini, M. G., Schmidt, M. L., Lee, V. M. Y., Trojanowski, J. Q., Jakes, R., &

Bibliography

Goedert, M. (1997). α-synuclein in Lewy bodies. *Nature*, *388*, 839-840. https://doi.org/10.1038/42166

Sulzer, D., & Edwards, R. H. (2019). The physiological role of α-synuclein and its relationship to Parkinson's Disease. *Journal of Neurochemistry*, *150*(5), 475-486. https://doi.org/10.1111/jnc.14810

Surguchov, A. (2008). Molecular and Cellular Biology of Synucleins. In: *International Review of Cell and Molecular Biology 270*, 225-317. https://doi.org/10.1016/S1937-6448(08)01406-8

Svennerholm, L., Boström, K., Jungbjer, B., & Olsson, L. (1994). Membrane lipids of adult human brain: Lipid composition of frontal and temporal lobe in subjects of age 20 to 100 years. *Journal of Neurochemistry*, *63*(5), 1802-1811. https://doi.org/10.1046/j.1471-4159.1994.63051802.x

Tatton, N. A., & Kish, S. J. (1997). *In situ* detection of apoptotic nuclei in the substantia nigra compacta of 1-methyl-4-phenyl-1,2,3,6-tetrahydropyridine-treated mice using terminal deoxynucleotidyl transferase labelling and acridine orange staining. *Neuroscience*, *77*(4), 1037-1048. https://doi.org/10.1016/S0306-4522(96)00545-3

Tysnes, O. B., & Storstein, A. (2017). Epidemiology of Parkinson's disease. *Journal of Neural Transmission*, *124*(8), 901-905. https://doi.org/10.1007/s00702-017-1686-y

Ueda, K., Fukushima, H., Masliah, E., Xia, Y., Iwai, A., Yoshimoto, M., … Saitoh, T. (1993). Molecular cloning of cDNA encoding an unrecognized component of amyloid in Alzheimer disease. *Proceedings of the National Academy of Sciences of the United States of America*, *90*(23), 11282-11286. https://doi.org/10.1073/pnas.90.23.11282

Ugalde, C. L., Finkelstein, D. I., Lawson, V. A., & Hill, A. F. (2016). Pathogenic mechanisms of prion protein, amyloid-β and α-synuclein misfolding: the prion concept and neurotoxicity of protein oligomers. *Journal of Neurochemistry*, *139*(2), 162-180. https://doi.org/10.1111/jnc.13772

Urrea, L., Segura-Feliu, M., Masuda-Suzukake, M., Hervera, A., Pedraz, L., García Aznar, J. M., … del Río, J. A. (2018). Involvement of Cellular Prion Protein in

α-Synuclein Transport in Neurons. *Molecular Neurobiology*, *55*(3), 1847-1860. https://doi.org/10.1007/s12035-017-0451-4

Vargas, K. J., Makani, S., Davis, T., Westphal, C. H., Castillo, P. E., & Chandra, S. S. (2014). Synucleins regulate the kinetics of synaptic vesicle endocytosis. *Journal of Neuroscience*, *34*(28), 9364-9376. https://doi.org/10.1523/JNEUROSCI.4787-13.2014

Villar-Piqué, A., Lopes da Fonseca, T., & Outeiro, T. F. (2016). Structure, function and toxicity of alpha-synuclein: the Bermuda triangle in synucleinopathies. *Journal of Neurochemistry*, *139*(S1), 240-255. https://doi.org/10.1111/jnc.13249

Volpicelli-Daley, L. A., Luk, K. C., Patel, T. P., Tanik, S. A., Riddle, D. M., Stieber, A., … Lee, V. M. Y. (2011). Exogenous α-Synuclein Fibrils Induce Lewy Body Pathology Leading to Synaptic Dysfunction and Neuron Death. *Neuron*, *72*(1), 57-71. https://doi.org/10.1016/j.neuron.2011.08.033

Whitehouse, I. J., Jackson, C., Turner, A. J., & Hooper, N. M. (2010). Prion protein is reduced in aging and in sporadic but not in familial Alzheimer's disease. *Journal of Alzheimer's Disease*, *22*(3), 1023-1031. https://doi.org/10.3233/JAD-2010-101071

Wood, S. J., Wypych, J., Steavenson, S., Louis, J. C., Citron, M., & Biere, A. L. (1999). α-Synuclein fibrillogenesis is nucleation-dependent: Implications for the pathogenesis of Parkinson's disease. *Journal of Biological Chemistry*, *274*(28), 19509-19512. https://doi.org/10.1074/jbc.274.28.19509

Wu, G., Lu, Z.-H., Kulkarni, N., & Ledeen, R. W. (2012). Deficiency of ganglioside GM1 correlates with Parkinson's disease in mice and humans. *Journal of Neuroscience Research*, *90*(10), 1997-2008. https://doi.org/10.1002/jnr.23090

Wu, G., Lu, Z. H., Kulkarni, N., Amin, R., & Ledeen, R. W. (2011). Mice lacking major brain gangliosides develop Parkinsonism. *Neurochemical Research*, *36*(9), 1706-1714. https://doi.org/10.1007/s11064-011-0437-y

Wu, M., Neilson, A., Swift, A. L., Moran, R., Tamagnine, J., Parslow, D., … Ferrick, D. A. (2007). Multiparameter metabolic analysis reveals a close link between attenuated mitochondrial bioenergetic function and enhanced glycolysis dependency in human tumor cells. *American Journal of Physiology - Cell Physiology*,

292(1), 125-136. https://doi.org/10.1152/ajpcell.00247.2006

Yadava, N., & Nicholls, D. G. (2007). Spare respiratory capacity rather than oxidative stress regulates glutamate excitotoxicity after partial respiratory inhibition of mitochondrial complex I with rotenone. *Journal of Neuroscience*, *27*(27), 7310-7317. https://doi.org/10.1523/JNEUROSCI.0212-07.2007

Zeng, X. S., Geng, W. S., Jia, J. J., Chen, L., & Zhang, P. P. (2018). Cellular and molecular basis of neurodegeneration in Parkinson disease. *Frontiers in Aging Neuroscience*, *10*(109), 1-16. https://doi.org/10.3389/fnagi.2018.00109

Zhai, J., Ström, A. L., Kilty, R., Venkatakrishnan, P., White, J., Everson, W. V., … Zhu, H. (2009). Proteomic characterization of lipid raft proteins in amyotrophic lateral sclerosis mouse spinal cord. *FEBS Journal*, *276*(12), 3308-3323. https://doi.org/10.1111/j.1742-4658.2009.07057.x

Zhou, Y., & Danbolt, N. C. (2014). Glutamate as a neurotransmitter in the healthy brain. *Journal of Neural Transmission*, *121*(8), 799-817. https://doi.org/10.1007/s00702-014-1180-8

Zhu, M., & Fink, A. L. (2003). Lipid binding inhibits α-synuclein fibril formation. *Journal of Biological Chemistry*, *278*(19), 16873-16877. https://doi.org/10.1074/jbc.M210136200